9-1-2008

Elucidating the degree of selectivity for NLO surrogate attachment to model compounds and a co-polyimide using the Mitsunobu reaction

Timothy E. Woods

ELUCIDATING THE DEGREE OF SELECTIVITY FOR NLO SURROGATE ATTACHMENT TO MODEL COMPOUNDS AND A CO-POLYIMIDE USING THE MITSUNOBU REACTION

Timothy E. Woods

September 2008

A thesis submitted in partial fulfillment of the requirements
for the degree of

Master of Science

Department of Chemistry
Rochester Institute of Technology
Rochester, NY

ELUCIDATING THE DEGREE OF SELECTIVITY FOR NLO

SURROGATE ATTACHMENT TO MODEL COMPOUNDS

AND A CO-POLYIMIDE USING THE MITSUNOBU REACTION

Approved:

_____

Marvin L. Illingsworth
Professor of Chemistry
Thesis Advisor

_____

Paul Rosenberg
Department of Chemistry Head

COPYRIGHT STATEMENT

ELUCIDATING THE DEGREE OF SELECTIVITY FOR NLO

SURROGATE ATTACHMENT TO MODEL COMPOUNDS

AND A CO-POLYIMIDE USING THE MITSUNOBU REACTION

Signature:_____

Date:_____

ACKNOWLEDGEMENTS

This thesis represents not just my personal efforts, but combined efforts and participation of countless individuals too numerous to thank. Throughout my time at R.I.T. I have encountered many obstacles and challenges, and while it hasn't always been easy, without the contributions of the people below I would not have made it to this point.

First I wish to acknowledge my thesis advisor, Dr. M.L. Illingsworth. Even he would admit that I was not the strongest graduate student when I joined his research group, and there were doubts as to whether or not I had the abilities to make it through the M.S. program. Through his countless hours of teaching, patience, and dedication to myself and my research, I became a much stronger student and was able to gain an appreciation of chemistry which I previously lacked. His thoroughness in analyzing every aspect of research has taught me to take this same approach and resulted in this work.

I also wish to thank my graduate committee, Mr. Tom Allston, Dr. J. Cody, Dr. M. Miri, Dr. T.C. Morrill, and Dr. G. Takacs, for their valuable advice and time throughout this process. Tom deserves special thanks for greatly expanding my understanding of instrumentation and helping me analyze my products without blowing something up in the process. Also, without Dr. Morrill I would not be writing this, so thanks for giving me a chance.

As an individual who has had the good fortune of being in one of his courses, thanks to Dr. A. Langner, a man who has probably forgotten about more chemistry than I'll ever know.

I'd be in trouble if I forgot to thank my parents, whose encouragement (nagging) led to me going to graduate school in the first place. Thanks for your love and support over the years.

While at R.I.T. I have had the good fortune of meeting several individuals that helped me from going crazy along the way. Glen (Papa G) Labenski whom I had the unique experience of working with in my first quarter at R.I.T., has proven to be an invaluable resource of both chemistry-related and completely random facts which have helped me along the way. Glen's also taught me to watch out for the driplets when working in the lab, which really is a valuable piece of advice for everyone. I also have to thank Matt "New Guy" Brister, who has told me (and anyone else who would listen) more about his research than I believed was possible, to the point where my research seems like a vacation by comparison. Matt is also one of the kindest, most sincere people that I've ever known, and a true friend.

Lastly, thanks to Doo-Op (a.k.a. Erin) – you know you've met someone special when the story you're telling about giving your cat a bath is the ice-breaker. One day we'll look back on the (seemingly endless) time we've stayed with my mom and laugh about it (hopefully sooner rather than later). Remember that I always love you, and all of this is for you.

Dedicated to Jim Serach and

Jerry Wooding – two teachers whose devotion

to learning has inspired me to do

the same

TABLE OF CONTENTS

LIST OF FIGURES

LIST OF TABLES

LIST OF ABBREVIATIONS

^{1}H NMR	Proton Nuclear Magnetic Resonance
2-AP	2-aminophenol
$(2\text{-AP})_2$MADA Diimide	N,N'-bis(2-Hydroxyphenyl)-2,3,5,6-hexacarboxylic Acid Diimide
6FDA	4,4'-(Hexafluoroisopropylidene)-diphthalic anhydride
Ar	Argon
Bis-AP-AF	2,2-Bis(3-amino-4-hydroxyphenyl)hexafluoropropane
CaH_2	Calcium Hydride
co-PI[Bis-AP-AF/6FDA)$_{0.9}$(Bis-AP-AF/MADA)$_{0.1}$]$_n$	co-Poly[4,4'-((Hexafluoroisopropylidene)diphthalic anhydride / 2,2 Bis(3-amino-4-hydroxyphenyl)hexafluoropropane)$_{0.9}$ (Mellitic Acid Dianhydride / 2,2-Bis(3-amino-4-hydroxyphenyl)hexafluoropropane)$_{0.1}$]imide
COSY	H-H Correlation Spectroscopy
DCC	Dicyclohexylcarbodiimide
DEAD	Diethylazodicarboxylate
DFG	Difference Frequency Generation
DMAc	N,N-dimethylacetamide
DTA	Differential Thermal Analysis
EO	Electro Optic
Ethyl NLO Surrogate	2-(N-Ethylanilino)ethanol
EtOAc	Ethyl Acetate
EtOH	Ethanol
FTIR	Fourier Transform Infrared Spectroscopy
FWM	Four Wave Mixing
KOEt	Potassium Ethoxide
KOH	Potassium Hydroxide
N_2*(l)*	Liquid Nitrogen
MADA	Mellitic Acid Dianhydride
MAMA	Mellitic Acid Monoanhydride
MATA	Mellitic Acid Trianhydride
Mer	A Repeat Unit of a Polymer
Methyl NLO Surrogate	2-(methylphenylamino)ethanol
MS	Mass Spectroscopy
NLO	Nonlinear Optical
NLO-phore	Nonlinear Optical Chromophore
NMP	1-Methyl-2-pyrrolidinone
$OPPh_3$	Triphenylphosphine Oxide
PAA	Polyamic Acid
PPh_3	Triphenylphosphine
RBF	Round Bottom Flask
SFG	Sum Frequency Generation
SHG	Second Harmonic Generation
Simplified Model Compound	2'-Hydroxyphenyl-1,2-benzenedicarboxylic Acid Imide
T_g	Glass Transition Temperature
TGA	Thermogravimetric Analysis
THF	Tetrahydrofuran
THG	Third Harmonic Generation
TLC	Thin Layer Chromotography

ABSTRACT

The goals of this research are: to elucidate the degree of selectivity shown using the Mitsunobu reaction for pendent attachment to phenol and carboxylic acid functional groups, and to make progress towards the synthesis of a novel, UV-Crosslinkable, Mellitic Acid Dianhydride (MADA)-containing, low color, nonlinear optical (NLO) pendent co-polyimide (co-PI). Two of the three co-PI components lower the hydrophilicity and color of the product polymer by incorporating C-F bonds between their aromatic rings: the diamine, 2,2-bis(3-amino-4-hydroxyphenyl)hexafluoropropane (Bis-AP-AF), and the dianhydride, 4,4'-(hexafluoroisopropylidene)diphthalic anhydride (6FDA). MADA was synthesized using a previously established procedure, and its purity was verified by a 5.9% weight loss seen with thermogravimetric analysis (TGA). A novel organic compound containing MADA, N,N'-bis(2-hydroxyphenyl)-2,3,5,6-hexacarboxylic acid diimide [$(2\text{-AP})_2$MADA diimide], was synthesized to aid in selectivity determination.

Two model compound systems are presented in order to elucidate the degree of functional group selectivity. Using 3,5-dihydroxybenzoic acid, a stoichiometric amount of a pendant was attached exclusively at a carboxylic acid in the presence of two phenol functional groups under ambient conditions in freshly dried NMP. This conclusion was supported by the disappearance of the broad carboxylic acid proton signal, complete retention of both phenol proton signals, and the appearance of pendent group peaks in the ^{1}H NMR, and the appearance of a new spot in the thin layer chromatogram (TLC). Subsequent one-pot pendent attachment at the phenol groups was then shown, although an excess of fresh Mitsunobu reagents were required to achieve a modest yield. The $(2\text{-AP})_2$MADA diimide model compound was then synthesized in freshly dried NMP using a one-pot approach without the presence of a catalyst. Structural verification was provided by ^{1}H NMR, FTIR, and MS. Based on the presence of the carboxylic acid protons at ~ 8.20 ppm in the ^{1}H NMR and the presence of a weak, broad stretch at 3060 cm^{-1}

in the FTIR, the presence of a strongly H-bonded or zwitterionic structure was indicated. Exclusive pendent attachment at the phenol groups of $(2\text{-AP})_2$ MADA Diimide using a stoichiometric amount of Mitsunobu regents was verified by the disappearance of the phenol proton peak at ~10.0 ppm in the ^{1}H NMR and 3323 and 1095 cm^{-1} peaks in the FTIR, and the concurrent appearance of several peaks corresponding to ether linkages at 1244 and 1118 cm^{-1} in the FTIR. One-pot attachment of a second pendant at the unreacted functional group was then shown. A large excess of Mitsunobu reagents was required however to achieve a modest yield.

Finally, the co-PI[Bis-AP-AF/6FDA$)_{0.9}$(Bis-AP-AF/MADA$)_{0.1}]_n$ was synthesized using a one step imidization approach in freshly dried NMP. A high degree of imidization was achieved, demonstrated by the weak peak at 1653 cm^{-1} in the FTIR. Structural confirmation was provided by 1-D ^{1}H and 2-D COSY NMR and FTIR. TGA of the product polyimide showed initial major decomposition at 396 °C. Pendent attachment was carried out in a similar fashion to that used for $(2\text{-AP})_2$MADA diimide, and most likely takes place exclusively at the phenol groups on either mer, as indicated by a peak at 1139 cm^{-1} corresponding to ether linkages in the FTIR. Additional structural confirmation was provided by ^{1}H NMR and FTIR. A subsequent one-pot pendent attachment at the unreacted functional groups was also shown to be possible by ^{1}H NMR and FTIR. Only a modest yield was obtained however due to the use of a stoichiometric amount of Mitsunobu reagents.

1. INTRODUCTION

There is a growing trend in the telecommunications industry to switch from electrically driven to high bandwidth, optically driven devices. This switch offers both an increase in speed and the more efficient transfer of information. In the near future, intermediate devices will need to couple electrical components to optical components using electro-optic (EO) devices – a device that can act as a switch between an electrical and optical component. Nonlinear optical (NLO) materials are ideal for use in these devices and can be critical in spanning this technological gap.[1]

In NLO behavior, the dielectric polarization, P, responds nonlinearly to the electric field, E, of the light. This nonlinearity is typically only observed at very high intensities, such as light provided by a laser source. There are numerous varieties of optical phenomena that arise due to NLO, known as frequency mixing processes. These include but are not limited to: second harmonic generation (SHG), sum frequency generation (SFG), third harmonic generation (THG), difference frequency generation (DFG), parametric amplification, parametric oscillation, parametric generation, spontaneous parametric down conversion, optical rectification, and four wave mixing (FWM). There are also other nonlinear processes including the Kerr Effect, which is a change in the refractive index of a material in response to an electric field. It is distinct from the Pockell's Effect in that the induced index change is directly proportional to the square of the electric field instead of to the magnitude of the field.[1] Although the details of each of these effects are outside the scope of this thesis, the basic principles that govern many of these phenomena will be explored.

EO modulators are materials that exhibit different types of NLO behavior, and can serve as a useful example for elucidating the underlying physics of this branch of optics. EO modulators in short, convert an electrical signal to an optical signal and find primary use in the telecommunications industry to increase bandwidth over communication networks. While the ultimate competition to electro-optic modulation will come from all optical processing based on

the Kerr effect (this depends on third order optical nonlinearity, the magnitudes of which are not sufficient at the present), a macroscopic understanding of EO activity can be gained from examining the Pockell Effect. This effect is due to the electric field dependent index of refraction of a material. The velocity of light in a material is determined by the interaction of the electric field component of light with the charges (electronic and nuclear) of the material. This effect can be quantitatively defined by the index of refraction, *n*, of the material. By applying an electric field to the material significant enough to change the charge distribution within the material, the velocity of light and therefore the index of refraction of the material can be altered, which can be described by the following:

$$\Delta\Phi=\pi n^3 rVL/\lambda \;\&\; V_\pi=\lambda h/n^3 rL \qquad (1)$$

where $\Delta\Phi$ is the electric field dependent phase shift of light passing through an EO material, V is the applied electric field, *h* is the electrode spacing, *n* the field-independent index of refraction, *r* the electro-optic coefficient of the material, *L* the length of the material, λ the wavelength of light,, and V_π the voltage required to produce a phase shift. The importance of this property of the material is that it can be used to manipulate light in order to produce a controlled phase shift or to steer light. Mach Zehnder modulators and signal transducers both make use of this effect.[1]

Molecular optical non-linearity arises from induced polarization of a NLO molecule by application of an electric field, E_x, across a dielectric medium. This molecular polarization, P_i, can be represented mathematically as written below:

$$P_i = \alpha E_x + \beta E_x^2 + \gamma E_x^3 + \ldots \qquad (2)$$

where α is the linear polarizability, β is the first molecular hyperpolarizability (second order effect), and γ is the second hyperpolarizability (third order effect). In materials that exhibit linear optical response, the induced polarization is directly proportional to the strength of the electric field, whereas in materials that exhibit second order nonlinear optical response, the induced polarization is directly proportional to the second power of the electric field. Therefore, it is much easier to induce polarization in molecules that exhibit nonlinear optical response. In order for β to

be non-zero, a π-conjugated molecule having acentric or dipolar symmetry is required, i.e. it must be noncentrosymmetric. An excellent candidate is a charge transfer molecule of the general formula (electron donor)(π-electron bridge)(electron acceptor), outlined in *Figure 1.1*.

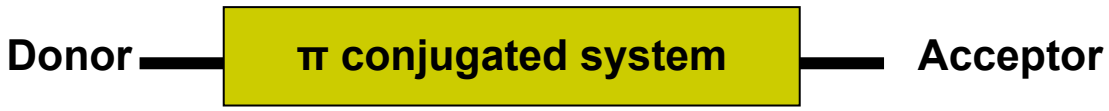

Figure 1.1 – General Formula for a Molecule that Exhibits a Large First Order Hyperpolarizability (second order nonlinearity).

Molecules of this nature are characterized by a neutral ground state and a charge-separated excited state, the mixing of which through the application of an electric field results in molecular polarization.[1,2] NLO-chromophores (NLO-phore) have been widely investigated in this capacity and will be a component of this study.[1]

Of the variety of NLO effects mentioned above, the one of primary interest in this research is SHG. As depicted in *Figure 1.2*, it arises from two photons of light with frequency f_1 passing though a NLO material, producing a single photon of light with frequency $2f_1$.

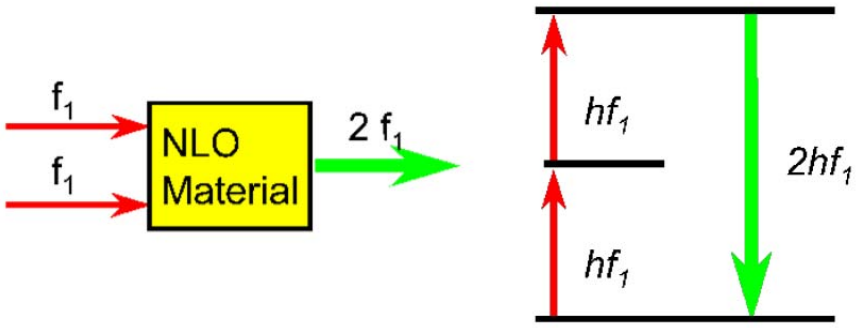

Figure 1.2– SHG Resulting from the Interaction of Light w/ NLO Material [3]

In other words, this "frequency mixing" of two photons results in a single photon of twice the frequency and half the wavelength of the original photons.[1,2]

Traditionally, inorganic materials have been the predominant material in modern EO modulator technology. Lithium niobate is the current material of choice due to several factors

including its availability, longevity on the market, and low signal insertion loss not currently matched by organic (polymer) materials. Inorganic materials however have a variety of drawbacks including high production cost, difficulty in processing, and poor cohesive strength and stability over a wide range of operating temperatures.[1,2] Organic NLO-functionalized polymers offer a variety of advantages and disadvantages over inorganic materials, outlined in *Table 1.1*.

Organic / NLO Material Characteristics	**Disadvantages of Organic / Polymer NLO Materials**
Fast Response Time	Poor Temporal Stability
Small dielectric constant	Mechanical Strength
Large NLO Coefficients (β)	Low NLO Activity
Non-toxic / Environmentally stable	Current Cost
High damage threshold	
Easy to engineer & synthesize	
Adjustable refractive indices	
High thermal stability	
Noncentrosymmetric	

Table 1.1 – Advantages and Disadvantages of Organic NLO-functionalized Polymers [1,2]

Over the past two decades, several factors have been elucidated which affect the degree of hyperpolarizability of organic-based NLO-phores. These factors are now used as general design criteria when synthesizing new NLO-phores. Molecular composition has been found to affect both hyperpolarizability coefficients and the region where UV absorption occurs.[2] One aspect of the molecule's composition that affects these NLO properties is the length of the π-conjugated system in the NLO-phore. The combination of electron-donor and acceptor groups has also been found to be a crucial aspect of the molecule's composition. Donor groups can provide additional electrons to the π-conjugated system causing a strong interaction between the donor – acceptor pair. The other key factor affecting the NLO coefficients of the material is the NLO-phore orientation within the polymer system. Shown in *Figure 1.3*, poling (application of a large,

external electric field) of the NLO-phores induces their alignment, resulting in high observed bulk hyperpolarizabilities. Loss or lack of shared orientation among the NLO-phores results in lower observed NLO coefficients of the material.

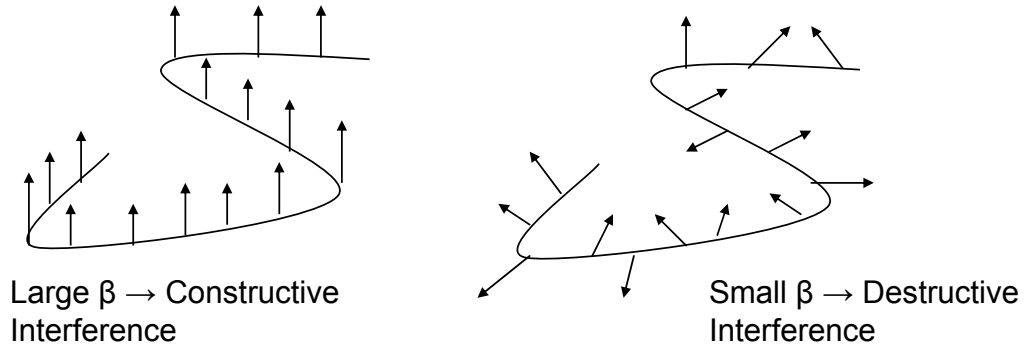

Figure 1.3 – Effect of NLO-phore Orientation on Observed First Order Hyperpolarizability (β)

While traditional approaches concentrated mainly on maximizing the strength of the π donor and acceptor groups as well as trying to increase the length of the π-conjugated system, recent approaches have concentrated on the development of NLO-phores with electron excessive/deficient heterocyclic bridges.[4,5] Electron-excessive/deficient heterocyclic bridges have been found to have a lesser/greater tendency to deplete the electron density from the donor/acceptor groups respectively, thereby increasing their donor/acceptor ability. As a result, a significant increase in NLO response is observed when electron excessive heterocyclic bridges act as auxiliary donors, while the electron-deficient heterocyclic bridges act as auxiliary acceptors.[5] All of these are important criteria to take into consideration when designing a potential NLO-phore, and have a large effect on the observed level of hyperpolarizability.[2]

Several methods have been developed to try and address the disadvantages posed by organic NLO materials. These include, the guest-host system, main chain incorporation, and grafting. In the guest-host system, the NLO material is incorporated into the host polymer matrix by solution casting. Second order nonlinearity is then induced by the application of an external electric field. While this approach allows for tailorable refractive indices, control of polymer

spatial ordering, and a wide range of host polymer choice, a significant loss of nonlinearity is seen following removal of the electric field due to relaxation of the NLO orientation.[6] In the main chain approach, the NLO-phore is incorporated into the backbone of the polymer. In many cases however where high temperatures are required to induce polymerization, NLO-phore degradation is seen resulting in low observed hyperpolarizabilities.[7,8] Finally in the grafted or pendent system, the NLO-phore is covalently bonded to the polymer backbone following polymerization. This system has several advantages including a large incorporation of NLO-phores onto the host polymer backbone, as well as reduced loss of poled NLO orientation over time. In addition, the grafted system offers the advantage of crosslinking the polymer chains together, thereby significantly reducing the amount of chain movement over time and preserving the poled NLO-phore orientation. This in turn results in an extended operational lifetime of the organic NLO-functionalized polymer, one of the main problems seen thus far with organic systems.[4,9]

One of the best and most widely researched class of NLO pendent polymers are polyimides. Several characteristics make them promising for NLO pendent systems, including high glass transition temperatures (T_g), good mechanical properties (low stress – high tensile modulus), availability of fluorinated varieties, low color, and the ability to incorporate crosslinking into the NLO pendent polyimide system.[10,11] A high T_g polymer is advantageous for NLO pendent attachment due to their ability to sustain the poled dipolar NLO orientation at high service operating temperatures, in excess of 200°C.[1] The thermal stability offered by polyimides is also beneficial, as a NLO pendent polymer must be able to survive the high temperatures associated with the manufacturing and operation of EO modulators without cracking. Furthermore, the ability to crosslink the individual NLO pendent polyimide chains together has been found to result in increased T_g and inhibit physical relaxation, thereby preserving NLO orientation.[12,13] Most importantly, the commercial availability of dianhydrides and diamines with hexafluoroisopropylidene groups positioned between their aromatic rings disrupts the π-conjugated system, resulting in a decrease of color in the resulting polyimide films.[14] This is

critical because using an intensely colored polyimide film could result in the absorbance of laser light, resulting in film decomposition. In addition, incorporation of C-F bonds into the polyimide backbone has been found to increase the T_g, while decreasing water absorption and the dielectric constant.[15,16]

In 1995, Dr. M.L. Illingsworth began investigating polyimides containing a MADA mer as a site for selective pendent attachment. Several previous graduate students working under Illingsworth have performed pendent attachment to polyimide backbones using MADA as a point of pendent attachment. In each case, dicyclohexylcarbodiimide (DCC) has been used as a dehydrating agent to facilitate pendent attachment to the polyimide backbone.[17,18]

The intent of this research is to focus on the synthesis and characterization of a MADA-containing 3-Component Polyimide, shown in *Figure 1.4*. A UV-Crosslinker pendent will then be attached selectively at the carboxylic acid functional groups using the Mitsunobu reaction, made possible by the incorporation of MADA in the polymer backbone. This will be followed by the attachment of a NLO-phore pendent at the unreacted phenol functional groups. The structure of this product is shown in *Figure 1.5*. This approach should result in the synthesis of a novel, crosslinkable, MADA-containing NLO pendent polyimide. The incorporation of a stoichiometric amount of MADA into the polymer backbone provides the unique opportunity to crosslink each polymer chain on either side of a rigid structure, previously not reported in the literature. After poling, UV-crosslinking should provide complete polymer chain immobilization and an increase in T_g, resulting in the retention of poled NLO configuration over an extended period of time. Furthermore, the incorporation of hexafluoroisopropylidene groups into the polyimide backbone should result in a relatively colorless polyimide, with absorption taking place outside the near UV-visible region.

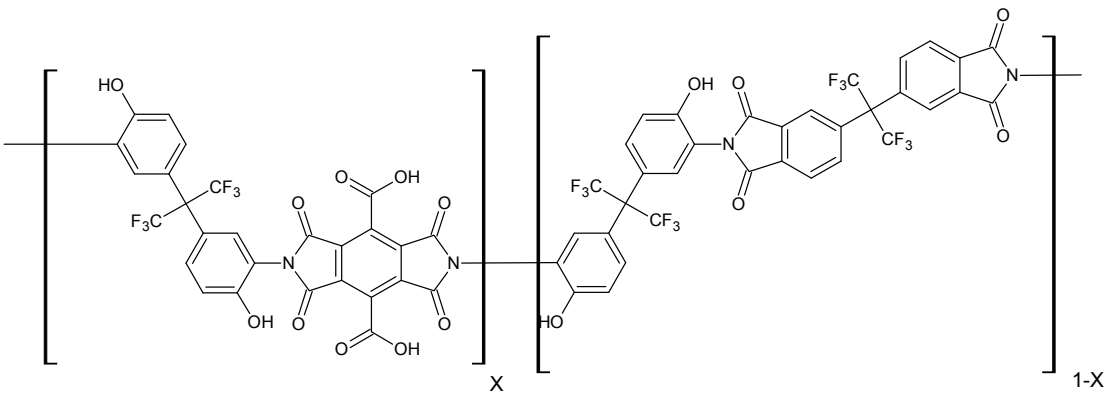

Figure 1.4 – Proposed Structure of a Novel, MADA-Containing, 3-Component Polyimide

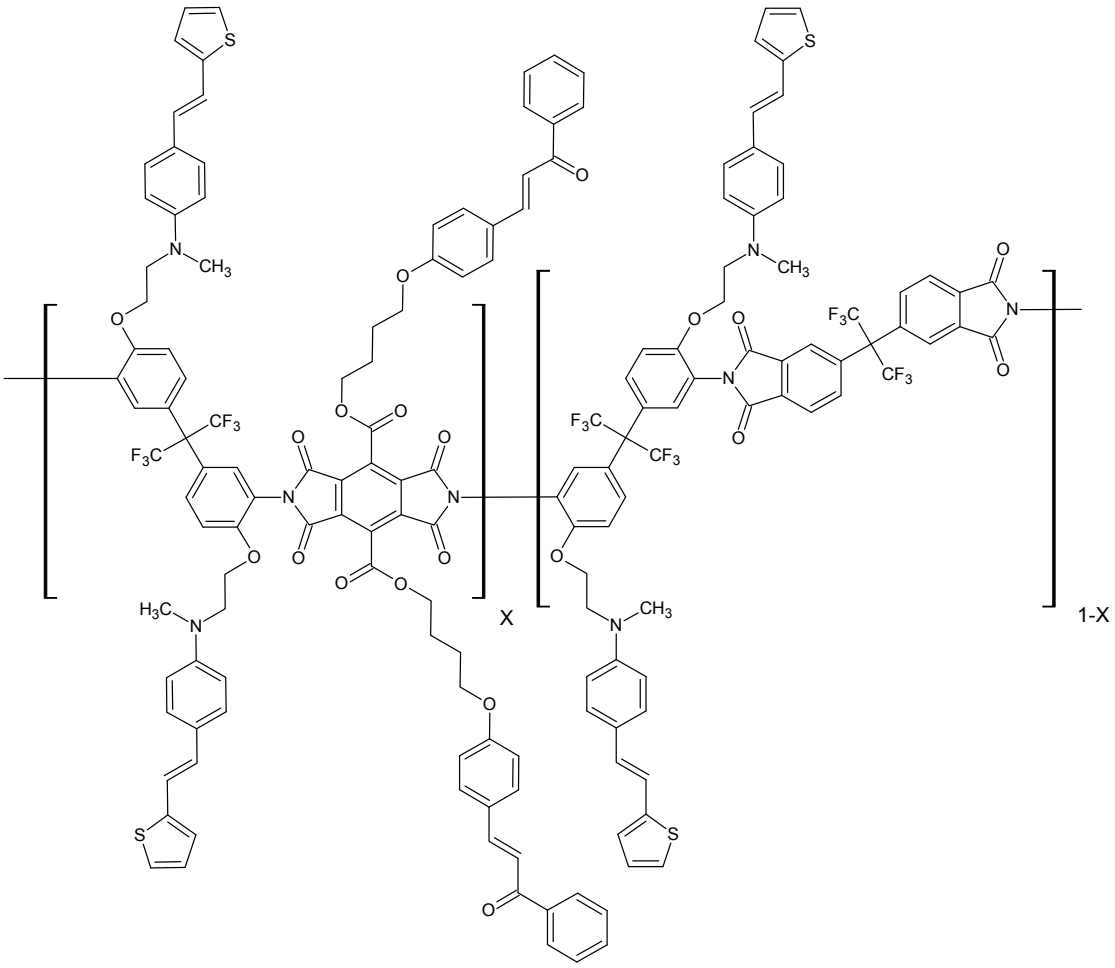

Figure 1.5 – Proposed Structure of a Novel, UV-Crosslinkable, MADA-Containing, NLO Pendent Polyimide

The specific focus of this research will be to elucidate the degree of site selectivity that takes place when a pendent is attached using the Mitsunobu reaction in the presence of carboxylic acid and phenol functional groups. While previous pendent attachments to polyimide backbones have taken advantage of dehydration reactions between two alcohols to yield an ether (plus H_2O), the extreme reaction conditions required (high temperatures) have been found to cause NLO-phore decomposition, resulting in low observed hyperpolarizabilities.[7] The Mitsunobu reaction has been previously utilized for NLO-phore pendent attachment to polyimide backbones due to the relatively mild reaction conditions required, as the reaction takes place at room temperature.[7,19] The selectivity shown between carboxylic acid and phenol functional groups for pendent attachment has not been established however. Through the synthesis of a model organic compound that resembles the MADA-containing 3-Component Polyimide, shown in *Figure 1.6*, functional group selectivity will be investigated to elucidate the amount of selectivity seen in a simple system. This knowledge will then be incorporated into the pendent attachment approach taken with the MADA-containing 3-Component Polyimide.

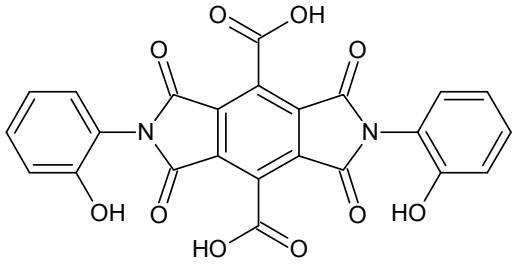

Figure 1.6 – Structure of the Desired MADA-Containing Model Compound

2. EXPERIMENTAL

2.1 Materials

The following were used as received. Mellitic acid was obtained from TCI America. Potassium iodide, 4-hydroxychalcone, and 4-chloro-1-butanol were obtained from Alfa Aesar. Sodium ethoxide, 2-chloroethanol, 2-thiophenemethanol, triphenylphosphine hydrobromide, N-methyl-N-(2-hydroxyethyl)-4-aminobenzaldehyde, 2-aminophenol (2-AP), 4-hydroxybenzoic acid, 3,5-dihydroxybenzoic acid, 2-(methylphenylamino)ethanol (Methyl NLO surrogate), 2-(N-ethylanilino)ethanol (Ethyl NLO Surrogate), diethylazodicarboxylate (DEAD), and triphenylphosphine were obtained from Sigma Aldrich. Dichloromethane, ethanol, ethyl acetate (EtOAc), hexanes, and methanol were obtained from J.T. Baker.

2,2-Bis(3-amino-4-hydroxyphenyl)hexafluoropropane (Bis-AP-AF) was obtained from TCI America and 4,4'-(hexafluoroisopropylidene)diphthalic anhydride (6FDA) was obtained from Sigma Aldrich or Alfa Aesar. Both Bis-AP-AF and 6FDA were purified by double sublimation under vacuum at 230-240 °C and 235-245 °C respectively using a liquid nitrogen [$N_2(l)$] trap, and stored in a desiccator with phosphorus pentoxide, P_2O_5, to prevent the absorption of moisture. Ice water was used in the cold finger of the sublimation apparatus.

N,N-dimethylacetamide (DMAc), 1-methyl-2-pyrrolidinone (NMP), and toluene were dried by heating at reflux with calcium hydride, CaH_2, under N_2 for at least 12 hours and distilled just prior to use. Tetrahydrofuran (THF) was dried by heating at reflux with sodium metal and benzophenone for at least 12 hours and distilled just prior to use. All glassware used was oven dried at ~90°C for at least 12 hours prior to use. All reactions performed under N_2 or Ar were performed with a minimum tank pressure of 500 psi.

Silica chromatography sheets with a fluorescent indicator, used for thin layer chromatography (TLC), were obtained from Fisher Scientific. Silica Gel (200-400 mesh, 60Å) used for UV-Crosslinker and NLO pendent isolation was obtained from Sigma Aldrich.

2.2 Synthesis of Mellitic Acid Dianhydride (MADA) [10]

MADA, a light grey powder, is prepared from mellitic acid by controlled cyclodehydration. Mellitic acid (~2.5 g, $7.3*10^{-3}$ mol) was finely ground using a mortar and pestle and evenly distributed on the bottom of a 500 mL filter flask via gentle shaking. A rubber stopper was inserted into the top of the flask and a thermocouple probe was inserted through a hole in a new stopper until it touched the bottom of the flask and the thermocouple plugged the hole. The flask was placed on a bed of sand inside a heating mantle, and any gaps between the side of the flask and the heating mantle were filled with sand. The flask was then placed under vacuum via its sidearm through use of a vacuum pump equipped with a $N_2(l)$ vacuum trap. The contents of the flask were then heated to 190-195 °C with a variable autotransformer (variac) for 12-13 hours, during which time the entire flask was wrapped in glass wool to prevent heat loss. After heating, the flask was allowed to cool to room temperature under vacuum before the MADA was removed. See *Figure 2.1*.

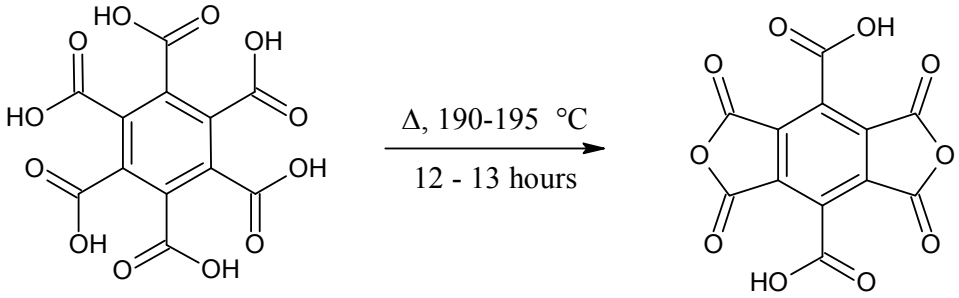

Figure 2.1 – Synthesis of MADA from Mellitic Acid

Using this method, it was found that a maximum of 2.5 g of MADA could be prepared at one time. Larger amounts of MADA proved to require multiple heating sessions for variable amounts of time that exceeded the 12-13 hour timeframe that was found to produce high purity MADA, using the amount of mellitic acid mentioned above.

The structure of synthesized MADA was confirmed by FTIR, and the purity was confirmed using thermogravimetric analysis (TGA). Pure MADA shows two weight losses, the

first equal to 5.88% of the sample mass attributed to the loss of one water molecule from the formation of the third anhydride ring, shown below in *Figure 2.2*:

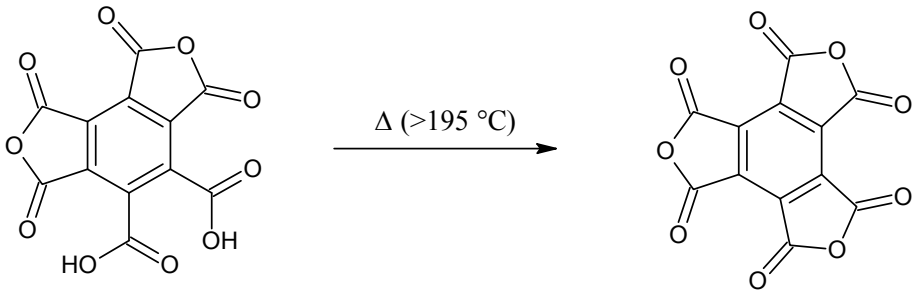

Figure 2.2 – Conversion of MADA to Mellitic Acid Trianhydride (MATA) During TGA [17]

2.3 Synthesis of UV-Crosslinker

The original UV-Crosslinker synthesis, shown in *Figure 2.3*, was taken from a paper by Hwang, et al[20] in the Japanese Journal of Applied Physics. In this synthesis, 4-hydroxychalcone (40.40 g, 0.1800 mol) is heated at reflux with potassium hydroxide (10.00 g, 0.1800 mol)(KOH), and KI (10 mg, 0.06 mol) in 500 mL of ethanol (EtOH), for 1 hour. 4-Chloro-1-butanol (20.10 g, 0.2000 mol) is then added and the resulting mixture is heated at reflux for 24 hours. The paper gives no method for product isolation and does not give any product characterization data.

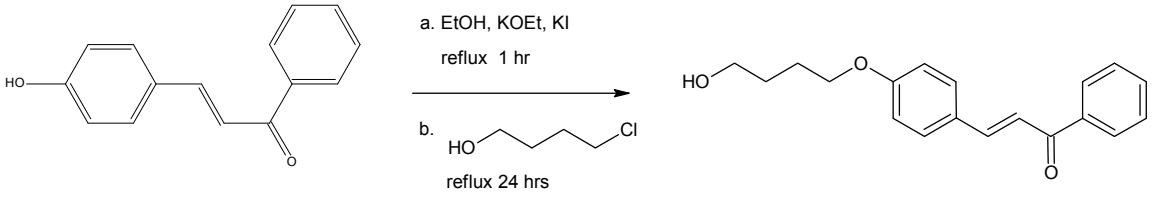

Figure 2.3 – Original Synthesis of UV-Crosslinker [20]

When the above synthesis was replicated on a 1/10 scale, a mixture of products was obtained, indicated by TLC (1:1 THF: hexanes and 1:1 EtOAc:hexanes). Product isolation was attempted by first filtering off the potassium chloride, KCl, byproduct and then rotoevaporating the bright orange reaction solution. TLC analysis on the resulting bright red oil indicated a mixture of products. Column chromatography was then attempted using silica gel with a 1:1 EtOAc:hexanes mobile phase. The separation observed with TLC was not observed when the

column fractions were analyzed; a mixture of products was still observed. Increasing the amount of time the KOH was allowed to react with the 4-hydroxychalcone from 1 to 24 hours produced a darker colored solution, but no increase in product was observed by TLC. Using a stronger base, potassium ethoxide (KOEt) also did not increase the amount of product.

A more reactive alkyl halide, 2-chloroethanol, was then selected to replace the 4-chloro-1-butanol, shown in *Figure 2.4*.

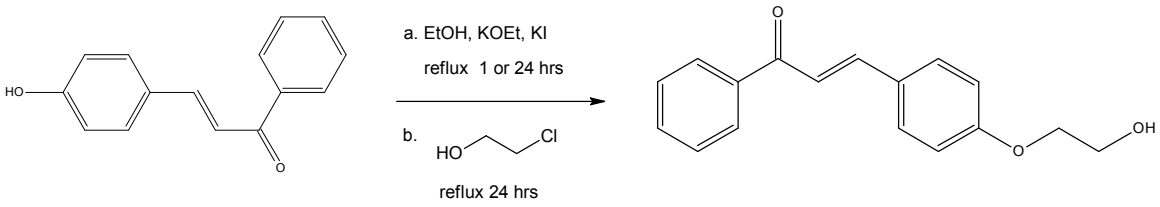

Figure 2.4 – Synthesis of Revised UV-Crosslinker with 4-Hydroxyclacone and 2-Chloroethanol

All reagent amounts and reaction conditions were kept the same as before. Using this revised synthesis, a larger ratio of product to starting material was observed via TLC, but as before, product isolation was unsuccessful.

Later work by L. Hawver continued to investigate different alkyl halides to attach to 4-hydroxychalcone. One alkyl halide, 6-chloro-hexanol has showed promising results in producing a predominantly single product, as indicated by TLC. Hawver has also been able to successfully recrystalize her crude product from an acetone:hexane solvent pair. This has generated a very small amount of what is possibly pure crosslinker as shown by NMR, however further experimentation is needed to verify this.[21]

2.4 Synthesis of 2-[N-Methyl-N-[4-[2-(2-thien)ethenyl]phenyl]amino]ethanol (NLO Pendent)[22]

2.4.1 Synthesis of 2-thienylmethylenetriphenylphosphonium bromide **1**

Triphenylphosphine hydrobromide (6.355 g, 0.08152 mol) was combined with 20 mL of acetonitrile in a 250 mL 2-neck round bottom flask (RBF) equipped with a magnetic stir bar. To this mixture, 2-thiophenemethanol (2.114 g, 0.08152 mol) was added, and the resulting mixture

was heated at reflux for 4 hours, then allowed to cool to room temp producing a copious amount of white precipitate in a pale yellow solution. The precipitate was then filtered off using a crucible filter with vacuum filtration and dried overnight in a vacuum oven at room temp. The product was used without further purification in the next step. See *Figure 2.5*.

Yield: 7.157 g (88.47 %)

2.4.2 Synthesis of Methyl NLO Pendent

N-methyl-N-(2-hydroxyethyl)-4-aminobenzaldehyde (2.920 g, $1.630*10^{-2}$ mol) and 7.157 g ($1.630*10^{-2}$ mol) of **1** were combined in a 250 mL 2-neck RBF with 35 mL of absolute ethanol and a magnetic stir bar, yielding a yellow liquid with some solid still remaining. To this, 3.0 mL ($4.5*10^{-3}$ mol) of a NaOEt solution (1.5M in ethanol) was added drop wise with stirring, yielding an olive drab solution with no undissolved solids. The RBF containing the reaction mixture was then purged with Ar and heated at reflux for 5 hours under Ar, resulting in a dark green solution with white solid. After cooling to r.t., the reaction mixture was poured onto 40 mL of ice water and the RBF rinsed with 5 mL of EtOH, yielding a brown liquid with red solid. The product was then extracted with 45 mL of dichloromethane, yielding a brown organic layer and a green aqueous layer. The organic layer was then washed with 40 mL of a saturated sodium bicarbonate, $NaHCO_3$ solution (light yellow aqueous layer with yellow/red organic layer) and dried over magnesium sulfate, $MgSO_4$. The resulting solution was rotoevaporated for 5 hours at 50 °C, yielding a brown viscous oil. See *Figure 2.5*.

The crude oil product from above was purified via column chromatography (silica gel; eluent: dichloromethane/EtOAc (90:10 v/v)). The product was identified as the first fraction off the column, which after solvent evaporation yielded a bright yellow sticky solid, a mix of *cis* and *trans* isomers. This solid was then recrystallized in a minimum amount of toluene in order to obtain the *trans* product only. The resulting light yellow crystals were obtained by vacuum

filtration with a crucible filter and were washed with chilled hexanes, then dried overnight in a vacuum oven at 50 °C.

Yield: 0.6985 g (17.23 %, amount of NaOEt not optimized), MP: 124.5-127 °C

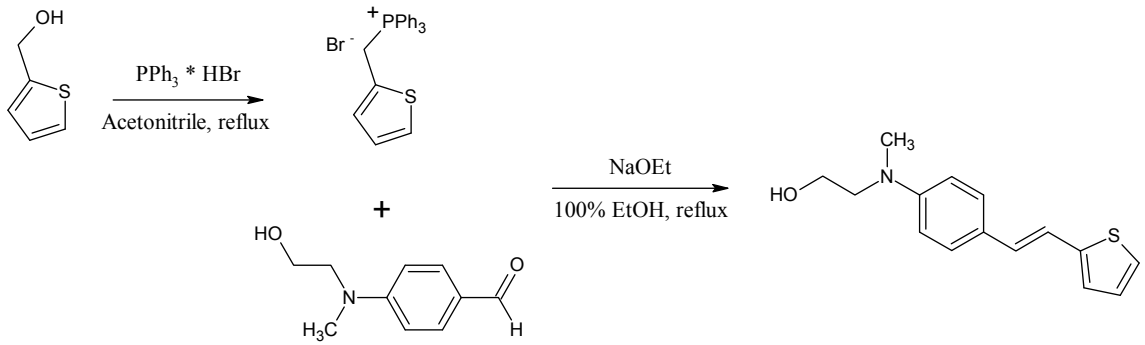

Figure 2.5 – Complete Synthesis of Methyl NLO Pendent

2.5 Synthesis of N,N'-bis(2-Hydroxyphenyl)-2,3,5,6-hexacarboxylic Acid Diimide [(2-AP)$_2$MADA Diimide] – Novel Compound

MADA (0.7551 g, 2.467*10^{-3} mol) and sublimed 2-AP (0.5415 g, 4.933*10^{-3} mol) were added sequentially to 30 mL of dried NMP in a 2-neck 250 mL RBF with a magnetic stir bar, resulting in a dark green homogeneous solution. The Dean Stark reaction apparatus shown in *Figure 2.6* was then assembled, and the apparatus purged with Ar. After stirring for ~15 minutes at room temperature, 10 mL of dried toluene was added (enough to fill the 5 mL trap), and the resulting mixture was heated to 170-180 °C, while the heat tape was heated to 110-120 °C (approximately the boiling point of toluene). Imidization was carried out at this temperature for 24-48 hrs under Ar, using toluene to azeotropically remove water via the Dean Stark Trap as shown in *Figure 2.7*, resulting in a dark brown reaction solution. This same procedure was repeated with DMAc at a lower imidization temperature, 160°C, again resulting in a dark brown reaction solution. Reaction progress was evaluated in each case by TLC (eluent: 1-propanol). The reaction was considered complete when a new light brown spot appeared near the solvent front (R_f = 0.93) and no other spots remained.

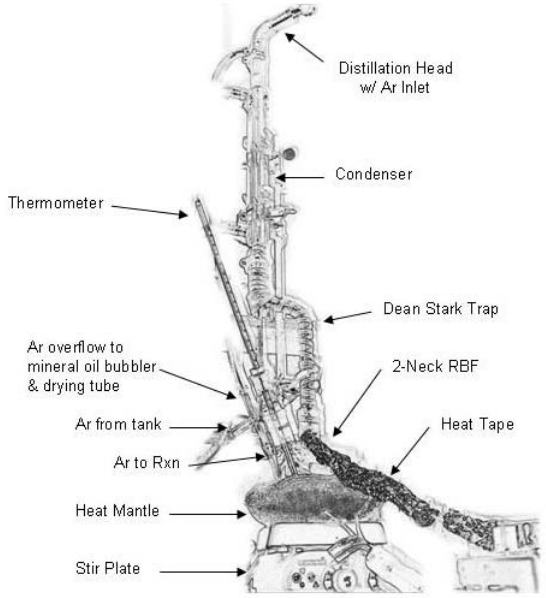

Figure 2.6 – (2-AP)$_2$MADA Diimide Synthesis Apparatus

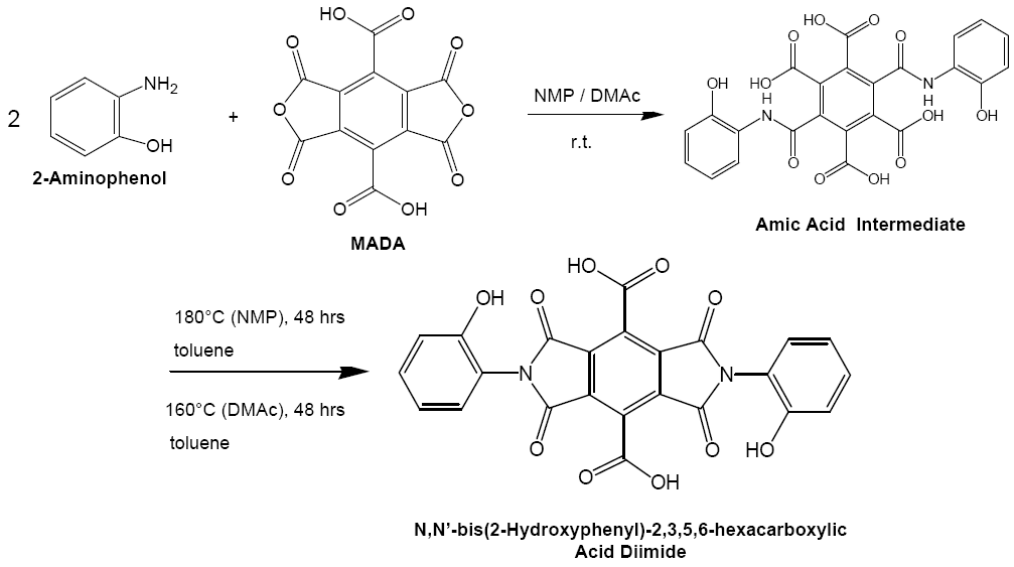

Figure 2.7 – Synthesis of (2-AP)$_2$MADA Diimide from 2-AP and MADA in both NMP and DMAc

Product isolation varied for each solvent system. With NMP, the reaction solution was diluted with 30 mL of additional NMP and poured into 250 mL of distilled water under vigorous stirring. This yielded a copious amount of light brown precipitate almost immediately. The precipitate was then collected via vacuum filtration with a crucible filter. A problem encountered

on numerous occasions was the incorporation of air into the reaction mixture after precipitation had been induced with water. This lead to a foamy, colloidal mix that was difficult to filter due to the fine precipitate particle size. Use of a larger capacity crucible filter with a finer pore frit and reduced vacuum pressure during filtering helped to alleviate this problem. Some product, however, was still lost through the filter frit. The light brown precipitate collected was air dried for ~5 minutes and then dried in a 100 °C vacuum oven equipped with a $N_2(l)$ vacuum trap for 18 hours.[6] A future improvement would be to use an explosion-resistant blender to precipitate the product, therefore providing increased agitation without the incorporation of air into the mixture, resulting in larger precipitate particle size.

Yield: 0.7809 g (65.32 %)

Due to DMAc's lower boiling point (164-166 °C), rotoevaporation followed by recrystallization was employed for product isolation. The crude reaction product was rotoevaporated for 4 hours at 40 °C, yielding a dark brown oil. This oil was then recrystallized from a methanol / water solvent pair. Methanol (10 mL) was added to the RBF containing the oil and the contents were brought to a boil with stirring. Decolorizing carbon (100 mg) was then added to the solution and boiling continued for 5 minutes, at which time an additional 15 mL of methanol was added to the solution. This solution was then vacuum filtered with a crucible filter containing a methanol / celite slurry, resulting in a brown filtrate. This decolorizing step was repeated with 200 mg of decolorizing carbon, producing a slightly lighter colored filtrate. The filtrate was then placed in a 25 mL Erlenmeyer flask and recrystallized from a 5:1 and 2:1 mix of methanol : water, respectively, yielding a light brown solid that was collected in both cases by vacuum filtration with a crucible filter. TLC of the isolated products from NMP and DMAc both showed a single, light brown spot near the solvent front ($R_f = 0.93$).

Yield: 0.3003 g (25.08 %, using a different isolation technique)

2.6 Synthesis of 2'-Hydroxyphenyl-1,2-benzenedicarboxylic Acid Imide (Simplified Model Compound)

In a 2-neck 250 mL RBF, phthalic anhydride (1.3688 g, $9.2411*10^{-3}$ mol) and sublimed 2-AP (1.0057 g, $9.2156*10^{-3}$ mol) were sequentially added to 30 mL of dried NMP with a magnetic stir bar, resulting in a yellow solution with some undissolved phthalic anhydride. The Dean Stark trap reaction apparatus (*Figure 2.6*) was then assembled and stirring was initiated under N_2, at which time almost all of the remaining phthalic anhydride dissolved. The reaction mixture was allowed to stir for 5 minutes at room temperature, at which time 10 mL of dried toluene was added. The reaction mixture was then heated to 180 °C, and imidized at this temperature for 48 hours under N_2, resulting in a brown solution. See *Figure 2.8*.

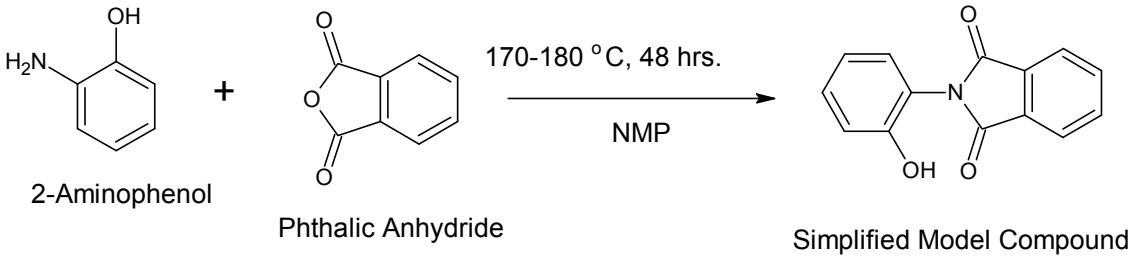

Figure 2.8 – Synthesis of Simplified Model Compound from 2-AP and phthalic anhydride

Product isolation was carried out identical to the manner employed for the MADA Model Compound in NMP. The crude reaction mixture was added to 120 mL of distilled water under vigorous stirring, yielding a very light brown clumpy precipitate. The precipitate was collected by vacuum filtration with a crucible filter and allowed to air dry for 5 minutes. It should be noted that a relatively transparent dark yellow filtrate was observed, suggesting that little if any solid passed through the filter. The collected solid was dried in a vacuum oven equipped with a $N_2(l)$ vacuum trap at 95 °C for 24 hours, resulting in a fine tan powder.[6]

Yield: 1.2589 g (57.16 %)

2.7 Synthesis of Simplified Model Compound with Methyl NLO Surrogate Pendent Group [Synthesis of 2-{2-[2-(Methylphenylamino)ethoxy]phenyl}indan-1,3-dione – Novel Compound]

Simplified Model Compound (0.1812 g, $7.574*10^{-4}$ mol) was combined with 15 mL of dried THF in a 250 mL 2-neck RBF with stirring, producing a homogenous dark yellow solution. To this solution, 0.7879g ($3.004*10^{-3}$ mol) of PPh_3, 0.1280 g ($8.466*10^{-4}$ mol) of Methyl NLO Surrogate, and DEAD (1.38 g, $3.00*10^{-3}$ mol) were added sequentially with stirring under Ar purge. No change in solution appearance was observed. The reaction solution was then stirred under Ar at room temperature for 48 hours. See *Figure 2.9*.

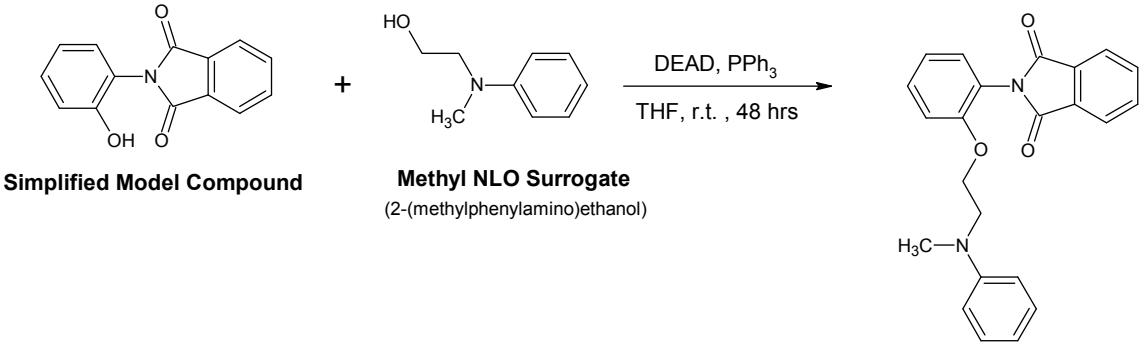

Figure 2.9 – Mitsunobu Reaction with Simplified Model Compound & Methyl Surrogate NLO in THF with DEAD

The crude Simplified Model Compound pendent product was isolated by rotoevaporation utilizing a $N_2(l)$ vacuum trap at room temperature for 2 hours, yielding a brown viscous oil. This crude oil product (1.5 mL) was purified via column chromatography (silica gel; eluent: THF/hexanes (50:50 v/v)). The product was identified as the third fraction off the column, and yielded a pale yellow solid after solvent evaporation. No yield was taken as the appearance of a significant amount of starting materials indicated that the DEAD used in previous work was of limited reactivity.

2.8 Synthesis of 3,5-Dihydroxybenzoic Acid with Methyl NLO and Ethyl NLO Surrogate Pendent Groups

2.8.1 Attachment of Methyl NLO Surrogate to Ar-COOH of 3,5-Dihydroxybenzoic Acid via Mitsunobu Reaction in NMP with DEAD [Synthesis of 3,5-Dihydroxybenzoic acid-2-(methylphenylamino)ethyl ester – Novel Compound]

3,5-Dihydroxybenzoic acid (0.617 g, $4.00*10^{-3}$ mol) was combined with 20 mL of dried NMP with stirring in a 2-neck 250 mL RBF, producing a translucent yellow solution. To this mixture, PPh_3 (1.0492 g, $4.0001*10^{-3}$ mol), Methyl NLO Surrogate (0.6048 g, $4.000*10^{-3}$ mol), and DEAD (2.61 g, $6.00*10^{-3}$ mol) were added sequentially with stirring under Ar purge, resulting in an orange colored solution. The reaction mixture was then stirred under Ar for 48 hours at room temperature. Reaction progress was tracked by TLC (eluent: 1:1 EtOAc:hexanes). This reaction was carried out in duplicate and one of the crude reaction products used in section *2.8.2* without further purification. See *Figure 2.10*.

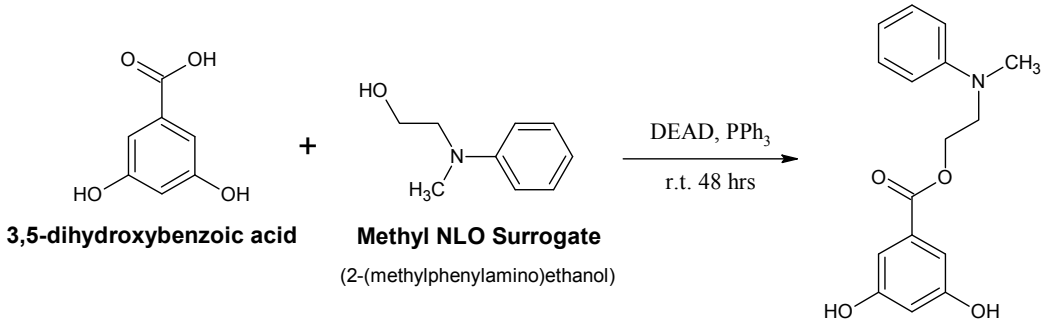

Figure 2.10 – Methyl NLO Surrogate Attachment to Ar-COOH on 3,5-Dihydroxybenzoic Acid via Mitsunobu Reaction in NMP with DEAD

The crude reaction product was isolated by pouring the reaction mixture into 150 mL of chilled distilled water in an explosion-resistant blender, followed by blending for approximately 10 minutes, yielding a brown oil. The blender container was then immersed in ice water for 20 minutes, resulting in the formation of more brown oil. The light brown mother liquor was then decanted off and the oil was collected for analysis. Due to the difficulty in collecting large quantities of the oil, no yield was obtained.

2.8.2 Attachment of Ethyl NLO Surrogate to Ar-OH of 3,5-Dihydroxybenzoic Acid via Mitsunobu Reaction in NMP with DEAD [Synthesis of 3,5-Bis[2-(ethylphenylamino)-ethoxy]benzoic acid 2-(methylphenylamino)ethyl ester – Novel Compound]

PPh_3 (2.0984 g, $8.0003*10^{-3}$ mol), Ethyl NLO Surrogate (1.3220 g, $8.0003*10^{-3}$ mol), and DEAD (3.83 g, $8.79*10^{-3}$ mol) were added sequentially with stirring to the crude reaction product from section *2.8.1* in a 2-neck 250 mL RBF under Ar purge. After the addition of DEAD, the reaction mixture changed from light to bright orange. The mixture was then stirred at room temperature for 48 hours under Ar. Reaction progress was evaluated by TLC (eluent: 1:1 EtOAc:hexanes). Based on these results, two more additions of DEAD (1.92 g, $4.40*10^{-3}$ mol) were made at 24 hour intervals, resulting in a complete reaction time of 96 hours. See *Figure 2.11*.

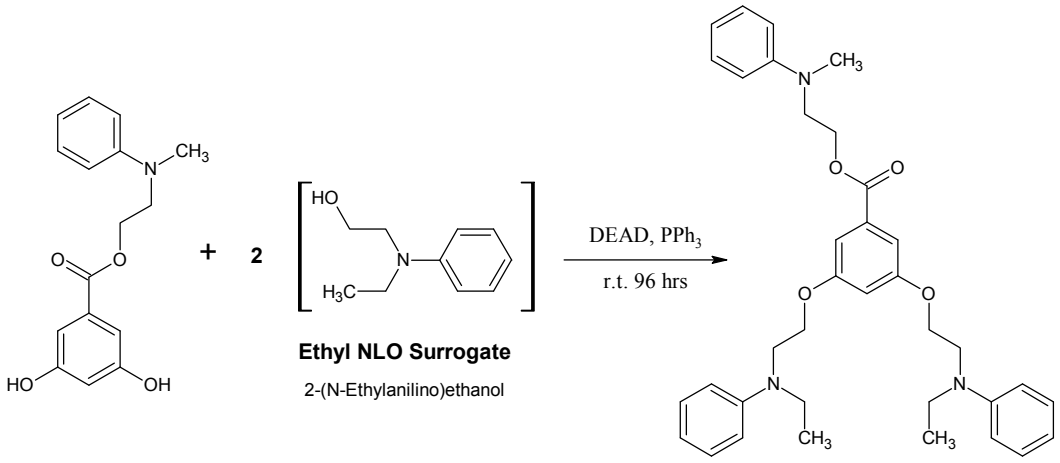

Figure 2.11 – Ethyl NLO Surrogate Pendent Attachment to Ar-OH on 3,5-Dihydroxybenzoic Acid via Mitsunobu Reaction in NMP with DEAD

The crude product was isolated by pouring the reaction mixture into 150 mL of iced water in an explosion-resistant blender, producing a brown oil. This was followed by blending for 20 minutes. Approximately every 5 minutes, 50 g of ice was added to the reaction mixture, with a final volume of 350 mL. Each addition of ice led to the formation of more oil. After blending, the light brown mother liquor was decanted off and the oil was collected for analysis. Due to the difficulty in collecting large quantities of the oil, no yield was obtained.

2.9 Synthesis of (2-AP)$_2$MADA Diimide with Methyl NLO and Ethyl NLO Surrogate Pendent Groups

2.9.1 Synthesis of (2-AP)$_2$MADA Diimide for Pendent Attachment – Novel Compound

Synthesis of the (2-AP)$_2$MADA Diimide followed the procedure outlined in section *2.5* with the following changes. MADA (1.0061 g, 3.2860*10^{-3} mol) was combined with sublimed 2-AP (0.7173 g, 6.573*10^{-3} mol) in a 250 mL 2-neck RBF. Due to the fact that the pendent attachments would take place in the same pot as the model compound synthesis, the Dean Stark Trap was charged with a piece of sodium metal in order to ensure the complete removal of water from the reaction product. All other conditions remained identical to section *2.5*, and imidization was carried out for 48 hours at 180 °C. The reaction was tracked by TLC (eluent: 1-propanol) and used without further purification in section *2.9.2.*

2.9.2 One – Pot Attachment of Methyl NLO Surrogate to Ar-COOH or Ar-OH of (2-AP)$_2$MADA Diimide via Mitsunobu Reaction in NMP with DEAD (No pendents attached) [Synthesis of 2,6-Bis(2-hydroxyphenyl)-1,3,5,7-tetraoxopyrrolo[3,4-f]isoindole-4,8-dicarboxylic acid bis[2-(methylphenylamino)ethyl] ester OR 2,6-Bis{2-[2-(methylphenylamino)ethoxy]phenyl}-1,3,5,7-tetraoxopyrrolo[3,4-f]isoindole-4,8-dicarboxylic acid – Novel Compound]

To the dark brown reaction mixture from section *2.9.1*, PPh_3 (1.7238 g, 6.5730*10^{-3} mol), Methyl NLO Surrogate (0.9937 g, 6.573*10^{-3} mol), and DEAD (3.5777 g, 8.2150*10^{-3} mol) were added sequentially with stirring under Ar purge. The mixture was then stirred for 48 hours at room temperature and the reaction progress was tracked by TLC (eluent: 1:1 EtOAc:hexanes). The reaction was terminated when TLC showed a new spot corresponding to product (R_f = 0.25) and the disappearance of all spots corresponding to starting materials. No change in reaction mixture appearance was noted. See *Figure 2.12*.

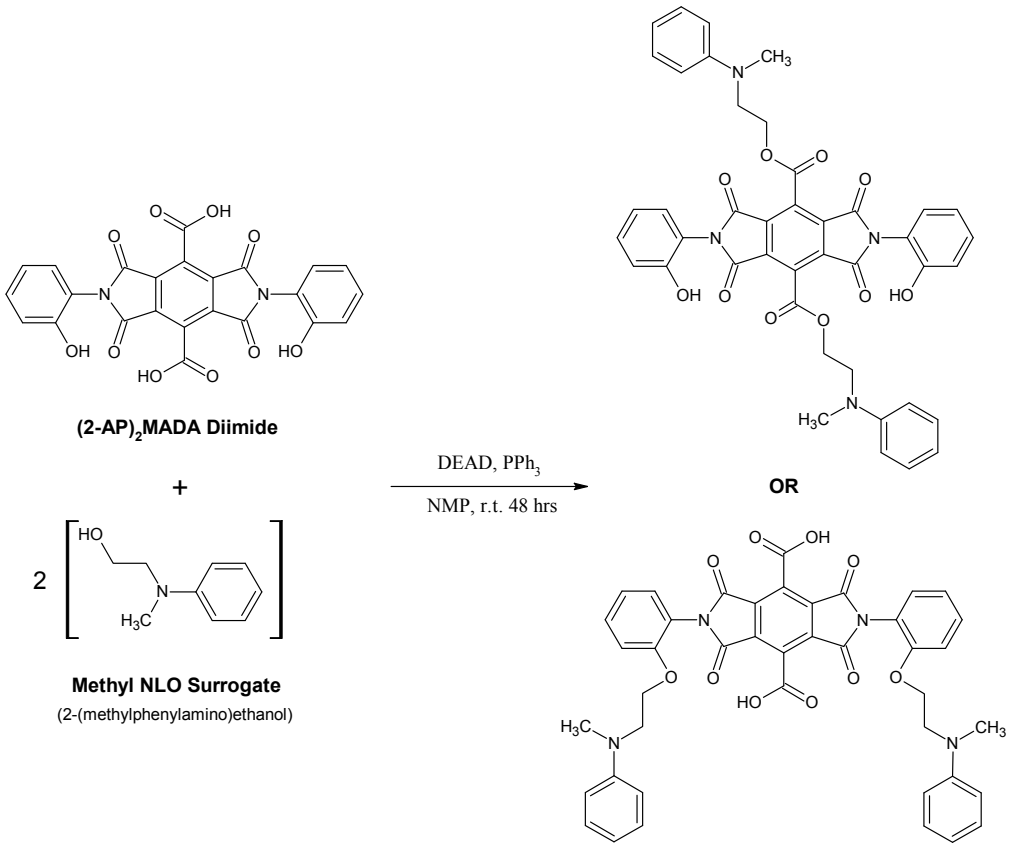

Figure 2.12 – Methyl NLO Surrogate Pendent Attachment to (2-AP)$_2$MADA Diimide at EITHER Ar-COOH OR Ar-OH

Product isolation was first attempted by flash column chromatography (silica gel; eluent: EtOAc/hexanes(50:50 v/v)). The crude reaction mixture was vacuum distilled at 70-80 °C to remove the NMP/toluene mixture, resulting in a dark brown viscous oil. The oil was then dissolved in 20 mL of eluent and 5 mL was loaded onto the column and eluted as follows: 1) 300 mL 1:1EtOAc:hexanes, 2) 200 mL 3:1EtOAc:hexanes, 3) 105 mL 6:1 EtOAc:hexanes. TLC analysis indicated that only by-product was obtained and that the desired product did not elute from the column. The remaining 15 mL of the crude reaction mixture was then rotoevaporated to remove the EtOAc:hexanes mixture and re-dissolved in 30 mL of NMP. This mixture was poured into 80 mL of chilled distilled water and blended for 20 minutes, producing a chocolate colored precipitate. The tan mother liquor was decanted off and the precipitate removed from the inside of

the blender container and air dried for approximately 1 hour, resulting in a light brown fine powder.

Yield: 1.215 g (49.34 %)

2.9.3 One – Pot Attachment of Methyl NLO Surrogate to Ar-COOH or Ar-OH of (2-AP)$_2$MADA Diimide via Mitsunobu Reaction in NMP with DEAD (Ethyl NLO Surrogate already attached) [Synthesis of 2,6-Bis-{2-[2-(ethylphenylamino)ethoxy]phenyl}-1,3,5,7-tetraoxo-pyrrolo[3,4-f]isoindole-4,8-dicarboxylic acid bis[2-(methylphenylamino)ethyl] ester OR 2,6-Bis-{2-[2-(methylphenylamino)ethoxy]phenyl}-1,3,5,7-tetraoxo-pyrrolo[3,4-f]isoindole-4,8-dicarboxylic acid bis[2-(ethylphenylamino)ethyl] ester – Novel Compound]

To the dark brown reaction mixture from section *2.9.1*, PPh_3 (1.4570 g, $5.5500*10^{-3}$ mol), Ethyl NLO Surrogate (0.9179 g, $5.550*10^{-3}$ mol), and DEAD (2.54 g, $5.83*10^{-3}$ mol) were added sequentially with stirring under Ar purge. The mixture was then stirred for 48 hours at room temperature and the reaction progress was tracked by TLC (eluent: 1:1 EtOAc:hexanes). Based on the TLC results, an additional 1.27 g ($2.92*10^{-3}$ mol) of DEAD was added to the reaction mixture and the mixture was stirred for an additional 48 hours. No change in reaction mixture appearance was noted.

Following the Ethyl NLO Surrogate pendent attachment, the Methyl NLO Surrogate pendent was attached in a similar manner in the same pot. PPh_3 (1.4570 g, $5.5500*10^{-3}$ mol), Methyl NLO Surrogate (0.8392 g, $5.550*10^{-3}$ mol), and DEAD (3.62 g, $8.33*10^{-3}$ mol) were added sequentially with stirring under Ar purge. The mixture was then stirred for 96 hours at room temperature and the reaction progress was tracked by TLC (eluent: 1:1 EtOAc:hexanes). TLC showed the formation of a new, light brown spot corresponding to product ($R_f = 0.27$) and the reduction in intensity of all spots corresponding to starting materials. See *Figure 2.13*.

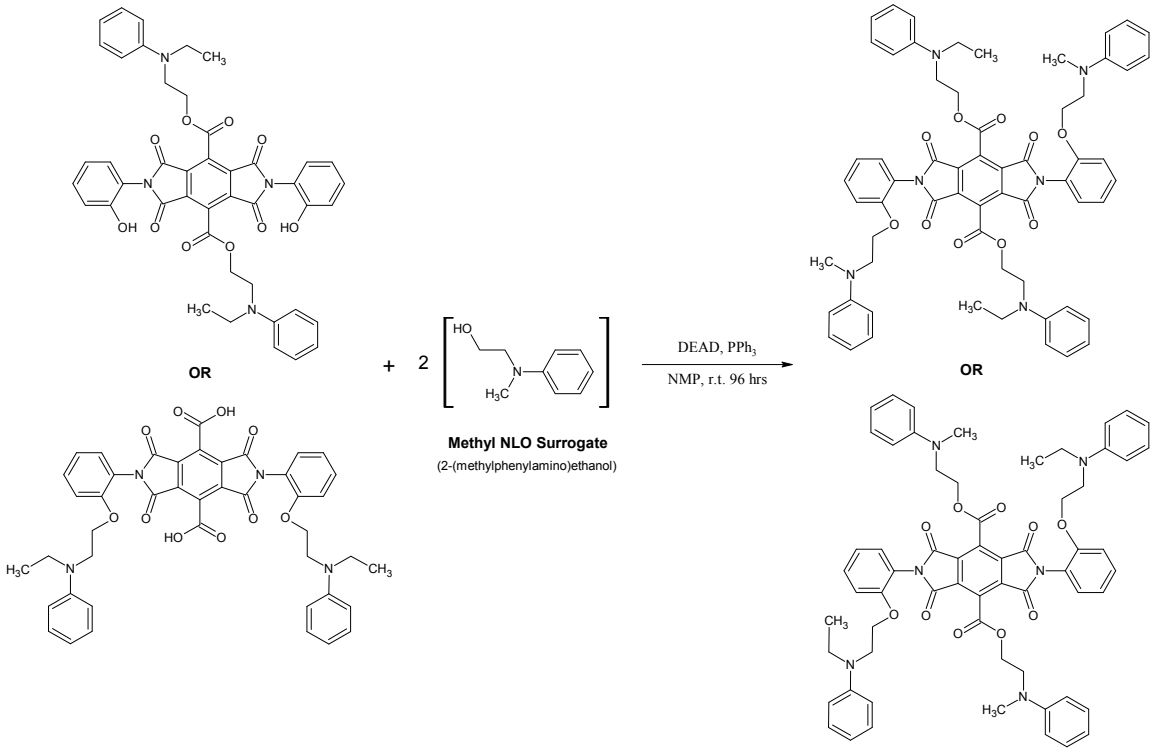

Figure 2.13 – Methyl NLO Surrogate Pendent Attachment to (2-AP)$_2$MADA Diimide Ar-COOH OR Ar-OH with Ethyl NLO Surrogate Pendent Already Attached at Alternate Location

The crude product was isolated by pouring the reaction mixture into 150 mL of iced water in an explosion-resistant blender, producing a dark brown oil. This step was followed by blending for 15 minutes. After 7 minutes, 50 g of ice was added to the reaction mixture so that the final volume was 200 mL. The addition of ice led to the formation of more oil. After blending, the chocolate colored mother liquor was decanted off and the oil product collected for analysis. Due to the difficulty in collecting large quantities of the oil, no yield was obtained.

2.10 Synthesis of co-Poly[4,4'-((Hexafluoroisopropylidene)diphthalic anhydride / 2,2 Bis(3-amino-4-hydroxyphenyl)hexafluoropropane)$_{0.9}$ (Mellitic Acid Dianhydride / 2,2-Bis(3-amino-4-hydroxyphenyl)hexafluoropropane)$_{0.1}$]imide, co-PI[(Bis-AP-AF/6FDA)$_{0.9}$(Bis-AP-AF/MADA)$_{0.1}$]$_n$ - Novel Compound

In a 2-neck 250 mL RBF an evenly distributed mixture of 2x sublimed 6FDA (1.6151 g, $3.6355*10^{-3}$ mol) and MADA (0.1237 g, $4.040*10^{-4}$ mol) was added under Ar purge with a magnetic stir bar. Dried NMP (17.55 mL) was then added to the RBF, and the mixture was stirred

under Ar at room temperature for 0.5 hours. While all of the 6FDA dissolved immediately, the MADA took an additional 2-4 minutes to completely dissolve, producing a dark green/brown solution. After 0.5 hours, the solution was cooled to 0-5 °C, followed by the addition of 2x sublimed Bis-AP-AF (1.4795 g, $4.0395*10^{-3}$ mol). The weigh container used in this step was rinsed using the reaction solution to ensure complete transfer of all diamine into the RBF. The resulting 15.5% weight solution was stirred at 0-5 °C for 2 hours upon which a noticeable increase in viscosity was observed. The solution was then warmed to room temperature and stirred under Ar for 72 hours.

After 72 hours, the Dean Stark Trap apparatus in *Figure 2.*6 was set up and purged with Ar for 15 minutes, followed by the addition of the reaction mixture from above. To this, 15 mL of dried toluene was added and the Dean Stark Trap was charged with a piece of sodium metal. The polyamic acid solution was then imidized at 170-180 °C for 6 hours under Ar. No change in solution appearance or viscosity was noted. See *Figure 2.14*.

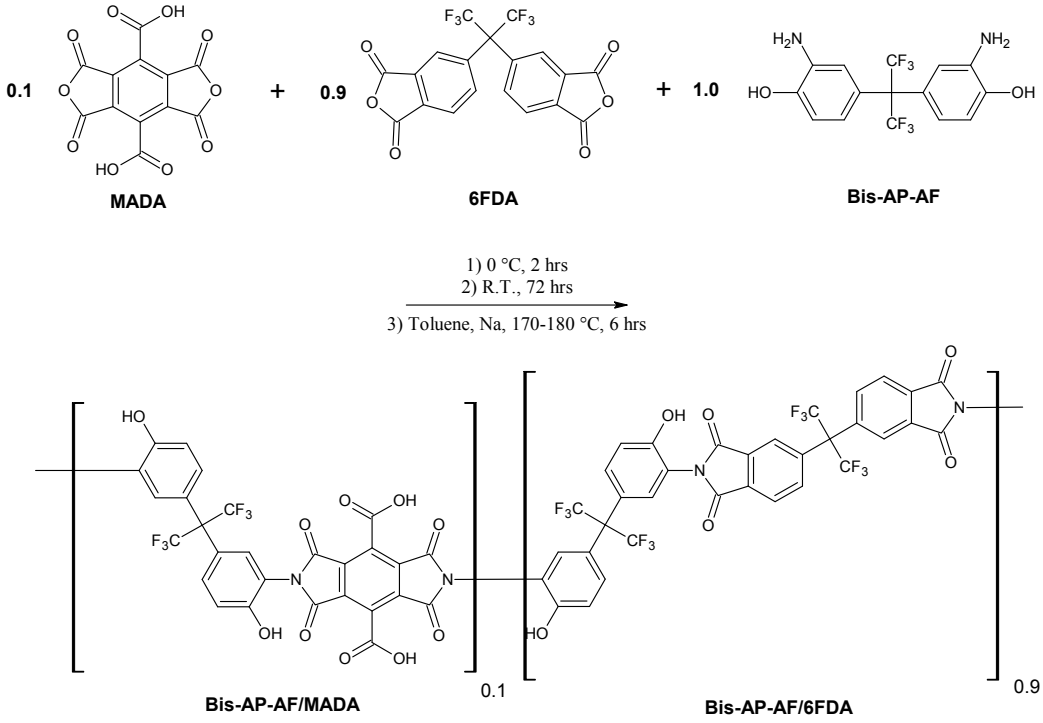

Figure 2.14 – Complete Synthesis of co-PI[Bis-AP-AF/6FDA)$_{0.9}$(Bis-AP-AF/MADA)$_{0.1}$]$_n$ from MADA, 6FDA, and Bis-AP-AF

Before the polyimide product was isolated, the reaction mixture was divided into two equal portions: one portion was isolated and the other used without further purification in section *2.11.1*. The polyimide product was isolated by pouring the reaction mixture into 200 mL of ice water in an explosion-resistant blender and blending for 30 minutes. Upon introduction into the iced water mixture, a tan clumpy precipitate appeared. Every 5-7 minutes, 50 mL of ice was added to the blender so that the final volume after 30 minutes was 450 mL. The tan precipitate became noticeably finer throughout the duration of agitation. After 30 minutes, the precipitate was collected by vacuum filtration with a crucible filter containing a fine frit. The coarse tan product was rinsed with distilled water and air dried for 5 minutes before being placed in a vacuum oven equipped with a N_2*(l)* vacuum trap at 100 °C for 24 hours. TLC of the isolated product (eluent: 3:1 EtOAC:hexanes) showed one spot corresponding to product and no spot corresponding to Bis-AP-AF.

Yield: 1.048 g (65.10 %)

2.11 Synthesis of co-PI[Bis-AP-AF/6FDA)$_{0.9}$(Bis-AP-AF/MADA)$_{0.1}$]$_n$ with Methyl NLO and Ethyl NLO Surrogate Pendent Groups

2.11.1 Attachment of Methyl NLO Surrogate to co-PI[Bis-AP-AF/6FDA)$_{0.9}$(Bis-AP-AF/MADA)$_{0.1}$]$_n$ at MADA Mer Ar-COOH OR Ar-OH Location via Mitsunobu Reaction in NMP with DEAD

PPh_3 (0.2119 g, 8.079*10^{-4} mol), Methyl NLO Surrogate (0.1222 g, 8.079*10^{-4} mol), and DEAD (0.38 g, 8.7*10^{-4} mol) were added sequentially to the remaining polyimide product from section *2.10* with stirring under Ar purge. No noticeable change in solution color or viscosity was observed. The resulting mixture was stirred at room temperature for 24 hours under Ar.

Before the pendent polyimide product was isolated, the reaction mixture was divided into two equal portions: one portion was isolated and the other used without further purification in section *2.11.2*. The pendent polyimide product was isolated by pouring the reaction mixture into 200 mL of iced water in an explosion-resistant blender and blending for 30 minutes. Upon introduction into the iced water mixture, a tan clumpy precipitate appeared. Every 5-7 minutes,

50 mL of ice was added to the blender so that the final volume after 30 minutes was 450 mL. The tan precipitate became noticeably finer throughout the duration of agitation. After 30 minutes, the precipitate was collected by vacuum filtration with a crucible filter containing a fine frit. The coarse tan product was rinsed with distilled water and air dried for 5 minutes before being placed in a vacuum oven equipped with a $N_2(l)$ vacuum trap at 50 °C for 24 hours. See *Figure 2.15*.

Yield: 0.5290g (61.60 %)

Percent Yield Calculation:

$$\text{Total Bis} - \text{AP} - \text{AF} = 1.4795\ \text{g} \times \frac{1\ \text{mol}}{366.26\ \text{g}} = 4.0395 * 10^{-3}\ \text{mol}$$

$$\text{First Pendent Attachment} = \frac{1}{4}\ \text{of original product} = 1.0099 * 10^{-3}\ \text{mol}$$

Product Molecular Weight:

$$[6\text{FDA} : \text{Bis - AP - AF}]_{0.9} + [\text{MADA} : \text{Bis - AP - AF}]_{0.1} = \text{Average MW / Mer}$$

$$\left[444.24\frac{\text{g}}{\text{mol}} + 366.26\frac{\text{g}}{\text{mol}}\right]_{0.9} + \left[306.14\frac{\text{g}}{\text{mol}} + 366.26\frac{\text{g}}{\text{mol}}\right]_{0.1}$$

$$\left[810.50\frac{\text{g}}{\text{mol}}\right]_{0.9} + \left[672.40\frac{\text{g}}{\text{mol}}\right]_{0.1} = 796.69\frac{\text{g}}{\text{mol}} = \text{Avg. MW / Mer}$$

$$\text{Avg. MW / Mer} + \left[\frac{\text{Amount of Methyl NLO Surrogate}}{\text{Total Phenol Sites}}(\text{Methyl NLO Surrogate}\right]$$

$$796.69\frac{\text{g}}{\text{mol}} + \left[0.4\left(134.20\frac{\text{g}}{\text{mol}}\right)\right] = 850.37\frac{\text{g}}{\text{mol}} = \text{Avg MW / Mer with Methyl NLO Pendent}$$

Percent Yield:

$$\text{Theoretical Yield} = 1..0099 * 10^{-3}\ \text{mol} \times \frac{850.37\ \text{g}}{1\ \text{mol}} = 0.8588\ \text{g}$$

$$\%\ \text{Yield} = \frac{\text{Actual Yield}}{\text{Theoretical Yield}} \times 100 = \frac{0.5290\ \text{g}}{0.8588\ \text{g}} \times 100 = 61.60\%$$

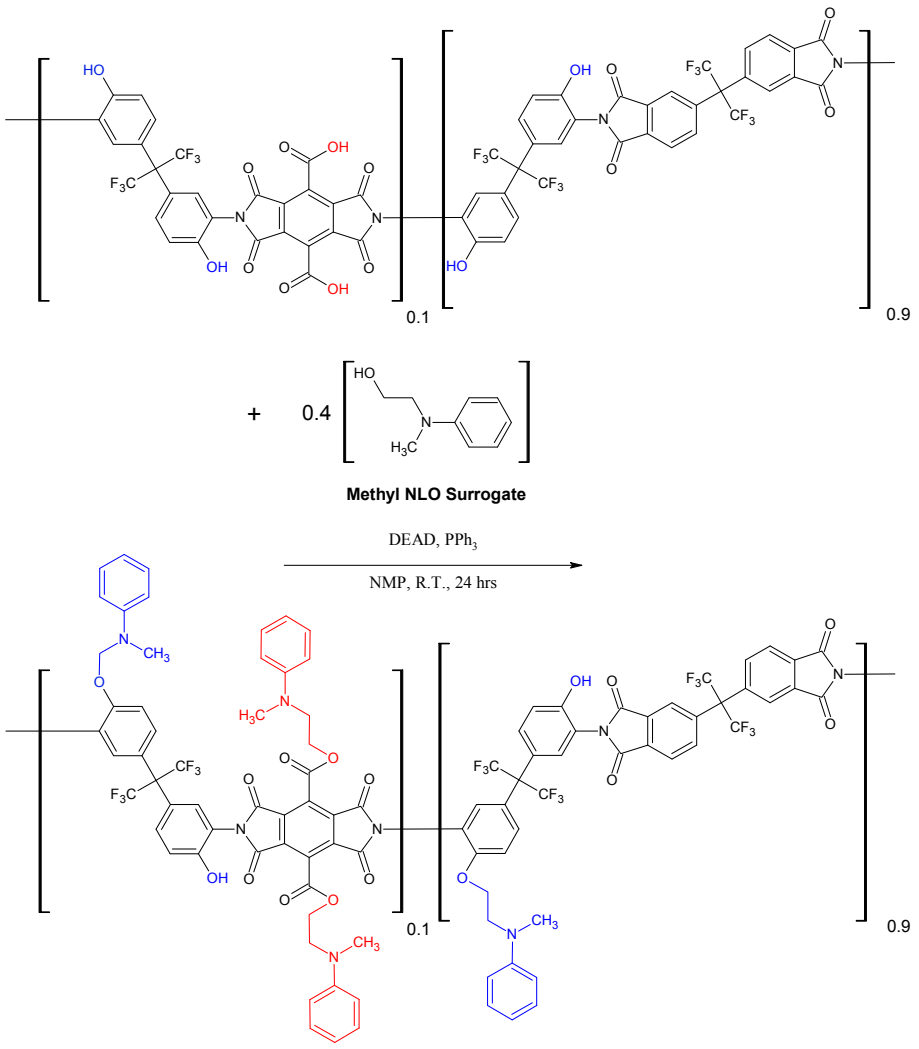

Figure 2.15 – Methyl NLO Surrogate Pendent Attachment to MADA Mer Ar-COOH AND/OR Both Mers at Ar-OH Locations

2.11.2 Attachment of Ethyl NLO Surrogate to co-PI[Bis-AP-AF/6FDA)$_{0.9}$(Bis-AP-AF/MADA)$_{0.1}$]$_n$ at Remaining Locations via Mitsunobu Reaction in NMP with DEAD

PPh_3 (0.5827 g, 2.220*10^{-3} mol), Ethyl NLO Surrogate (0.3671 g, 2.220*10^{-3} mol), and DEAD (1.45 g, 3.33*10^{-3} mol) were added to the pendent polyimide product from section *2.11.1* with stirring under Ar purge. A noticeable increase in viscosity was observed during the drop-wise addition of DEAD to the reaction mixture, to the point where the mixture appeared to congeal before decreasing in viscosity after several minutes of stirring. No change was noted in

the dark brown color of the solution. The resulting mixture was stirred at room temperature for 96 hours under Ar.

The pendent polyimide product was isolated by pouring the reaction mixture into 200 mL of ice water in an explosion-resistant blender and blending for 30 minutes. Upon introduction into the iced water mixture, a dark red precipitate began to adhere to the walls of the blender. Every 5-7 minutes, 50 mL of ice was added to the blender so that the final volume after 30 minutes was 450 mL. After each addition of ice, more of the dark red precipitate adhered to the blender walls. After 30 minutes, the mother liquor was decanted off, and the dark red precipitate was excised from the blender with a razor blade. The dark red tacky, film-like product was then dried in a vacuum oven equipped with a N_2*(l)* vacuum trap at 50 °C for 24 hours. See *Figure 2.16*.

Yield: 0.9058 g (77.75%)

Percent Yield Calculation:

$$\text{First Pendent Attachment} = \frac{1}{4}\text{ of original product} = 1.0099 * 10^{-3}\ \text{mol}$$

Product Molecular Weight:

$$\text{Avg. MW / Mer} + \left[\frac{\text{Amount of Ethyl NLO Surrogate}}{\text{Total Phenol Sites}}\left(\text{Ethyl NLO Surrogate}\right)\right]$$

$$850.37\frac{\text{g}}{\text{mol}} + \left[2.0\left(148.24\frac{\text{g}}{\text{mol}}\right)\right] = 1153.65\frac{\text{g}}{\text{mol}} = \text{Avg MW / Mer with Methyl and Ethyl NLO Surrogates}$$

Percent Yield:

$$\text{Theoretical Yield} = 1..0099 * 10^{-3}\ \text{mol} \times \frac{1153.65\ \text{g}}{1\ \text{mol}} = 1.1651\ \text{g}$$

$$\%\ \text{Yield} = \frac{\text{Actual Yield}}{\text{Theoretical Yield}} \times 100 = \frac{0.9058\ \text{g}}{1.165\ \text{g}} \times 100 = 77.75\%$$

Purification of the pendent polyimide product was attempted through the removal of the triphenylphosphine oxide, $OPPh_3$ byproduct with pentanes. A portion of the product (0.9058 g) was combined with 100 mL of chilled pentanes in an explosion resistant blender and blended for

3 – 1 minute pulses. During blending, the sheets of film were broken down by agitation, resulting in a medium size bronze colored powder. The product was collected by vacuum filtration with a crucible filter fitted with a fine frit. The pendent polyimide product was then oven dried in a vacuum oven equipped with a $N_2(l)$ vacuum trap at 50 °C for 18 hours.

Recovery: 0.6295 g (69.50%)

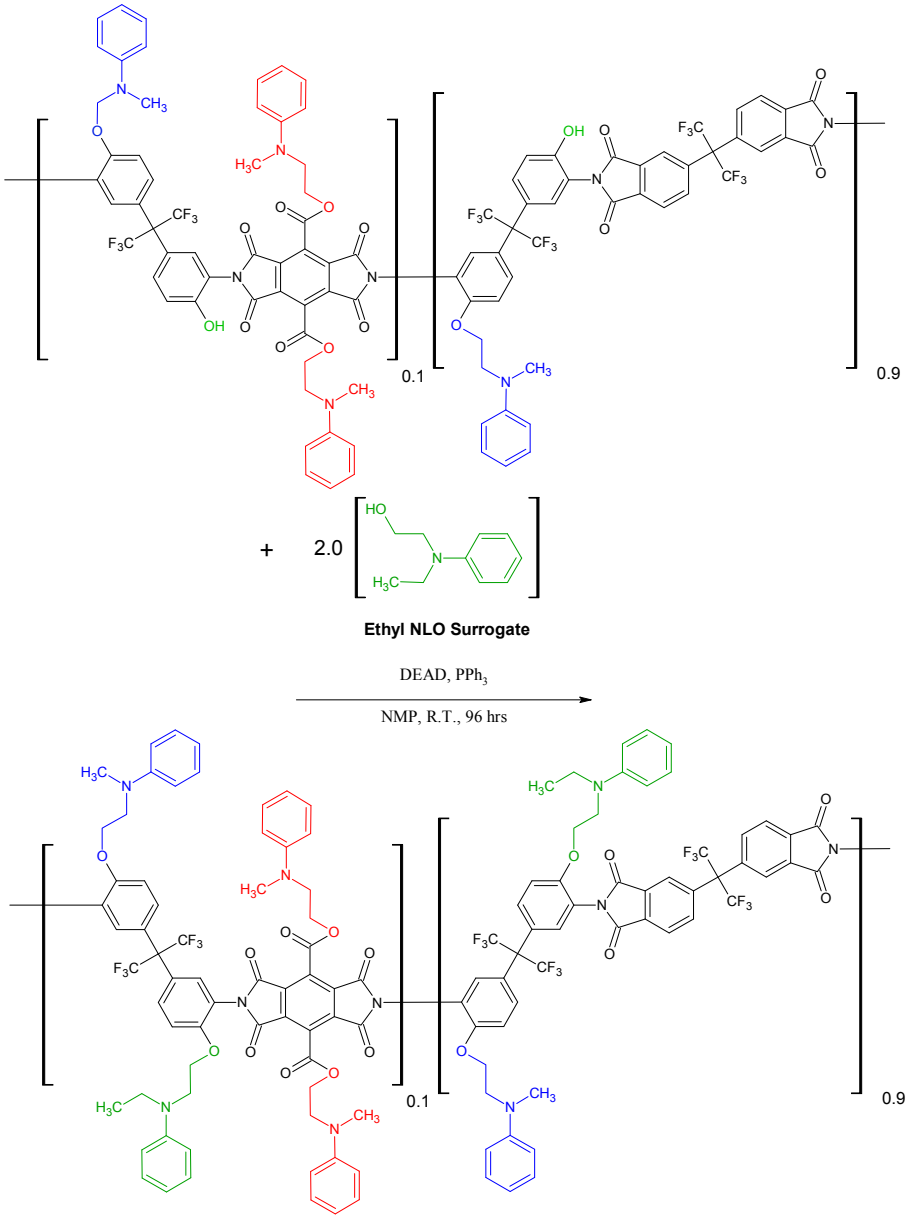

Figure 2.16 – Attachment of Ethyl NLO Surrogate to Unreacted co-PI[Bis-AP-AF/6FDA)$_{0.9}$(Bis-AP-AF/MADA)$_{0.1}$]$_n$ Ar-OH Locations with Attachment of Methyl NLO Surrogate to Ar-COOH of MADA Mer AND/OR Ar-OH of Both Mers.

2.12 Characterization Methods

2.12.1 Proton Nuclear Magnetic Resonance Spectroscopy (1-D ^{1}H NMR)

Proton NMR spectra were obtained for each product separately. Each product was dissolved in deuterated dimethylsulfoxide (d^6-DMSO) or deuterated chloroform (d^1-$CDCl_3$) (for synthesized NLO only) and mixed using a Vortex plate to ensure complete dissolution. One-dimensional NMR spectra were obtained at room temperature using a 300 MHz Bruker NMR Spectrometer using Bruker's Icon NMR software to obtain spectra and XWin NMR software to obtain integrations and analyze data.

2.12.2 Proton Nuclear Magnetic Resonance Spectroscopy (2-D ^{1}H NMR)

A 2-D ^{1}H NMR spectrum was obtained for the MADA 3-Component polyimide only. The polyimide was dissolved in deuterated dimethylsulfoxide (d^6-DMSO) and vortexed into solution. The two-dimensional NMR spectrum was obtained at room temperature using a 300 MHz Bruker NMR Spectrometer using Bruker's Icon NMR software to obtain spectra and XWin NMR software to analyze data.

2.12.3 Fourier Transform Infrared Spectroscopy (FTIR)

FTIR spectra were obtained for MADA, MADA Model Compound, Simplified Model Compound, MADA Model Compound with Methyl NLO Surrogate, MADA Model Compound with Methyl and Ethyl NLO Surrogate, MADA 3-Component Polyimide, and both 3-Component Pendent Polyimides. All spectra were obtained on a Shimadzu IR Prestige-21 with a Pike Miracle HATR Cell attachment from 4000 cm^{-1} to 500 cm^{-1}.

2.12.4 Mass Spectroscopy (MS)

Mass spectra were obtained for MADA, MADA Model Compound, and Simplified Model Compound. Spectra were obtained using an Applied Biosystems 3200 Q Trap LC/MS/MS. Methanol with a 1% acetic acid spike was used as the solvent for the MADA and MADA Model

Compound MS; 9:1 Methanol:THF v/v with a 1% acetic acid spike was used as the solvent for the Simplified Model Compound MS.

2.12.5 Thermogravimetric Analysis (TGA)

TGA thermograms were obtained for MADA and co-PI[Bis-AP-AF/6FDA)$_{0.9}$ (Bis-AP-AF/MADA)$_{0.1}$]$_n$. TGA were performed using a TA 2050 Thermogravimetric Analyzer (TA Instruments Inc.). Samples in the range of 10-20 mg were loaded into a flamed platinum TGA pan and purged under nitrogen in the TGA furnace for 15 minutes before analysis. MADA samples were heated from 30-150 °C at 10 °C / min, and from 150-500 °C at 1°C / min under nitrogen purge at 90 mL/min. co-PI[Bis-AP-AF/6FDA)$_{0.9}$ (Bis-AP-AF/MADA)$_{0.1}$]$_n$ samples were heated from 30-800 °C at 10 °C / min under nitrogen purge. The results were plotted as % weight loss vs. temperature. The midpoint of all observed decompositions was determined by plotting the 1st derivative of % weight loss vs. temperature.

2.12.6 Differential Thermal Analysis (DTA)

A DTA thermogram was obtained for the co-PI[Bis-AP-AF/6FDA)$_{0.9}$ (Bis-AP-AF/MADA)$_{0.1}$]$_n$. DTA was performed using a PerkinElmer STA 6000 (PerkinElmer Inc.). Samples in the range of 10-20 mg were loaded into a flamed ceramic DTA pan and purged under nitrogen in the STA furnace for 10 minutes before analysis. The polyimide sample was heated from 30-500 °C at 20 °C / min under nitrogen purge at 90 mL/min. The results were plotted as % weight loss vs. temperature. The T_g was determined by plotting the heat flow vs. temperature and calculating the inflection point of the exothermic event.

3. RESULTS

3.1 Mellitic Acid Dianhydride (MADA) Characterization

3.1.1 Thermogravimetric Analysis (TGA)

MADA purity was confirmed through TGA, shown in *Figure 3.1*. The thermogram is a plot of % weight loss versus temperature in °C. The first observed weight loss of 5.99% is close to the established 5.88% weight loss which corresponds to the loss of one water molecule upon mellitic acid trianhydride (MATA) formation.[17] Also, there is no evidence of the first weight loss in the thermogram of mellitic acid due to the loss of two water molecules upon the formation of the dianhydride, shown in *Figure 3.2*.

3.1.2 FourierTransform Infared Spectroscopy (FTIR)

MADA formation was confirmed through FTIR, shown in *Figure 3.3*. The major characteristic bands are at 3350, 1870, 1800, and 1211 cm^{-1} which correspond to O-H (carboxylic acid), C=O (anhydride, asymmetric), C=O (anhydride, symmetric), and C-O-C (anhydride) stretches, respectively. All assignments for FTIR peaks are summarized in section *3.11*, *Table 3.1*.

3.2 UV – Crosslinker Characterization

Replication of the original UV-Crosslinker synthesis by Hwang, et al[20] produced a bright red/orange oil that when analyzed by TLC produced three spots. The highest R_f value spot (0.84) most likely corresponded to a byproduct from the 4-chloro-1-butanol, while the middle spot (0.65) corresponded to 4-hydroxychalcone. The lowest R_F value spot (0.42) most likely corresponded to the crosslinker product. Purification via column chromatography failed to isolate the lowest R_f value spot for characterization. Varying the amount of time the base, KOH was allowed to react at reflux with the 4-hydroxychalcone from 1 to 24 hours produced a darker colored solution, but no increase in product was observed relative to the other spots in the TLC . Using a stronger base, potassium ethoxide, KOEt, also did not increase the amount of product

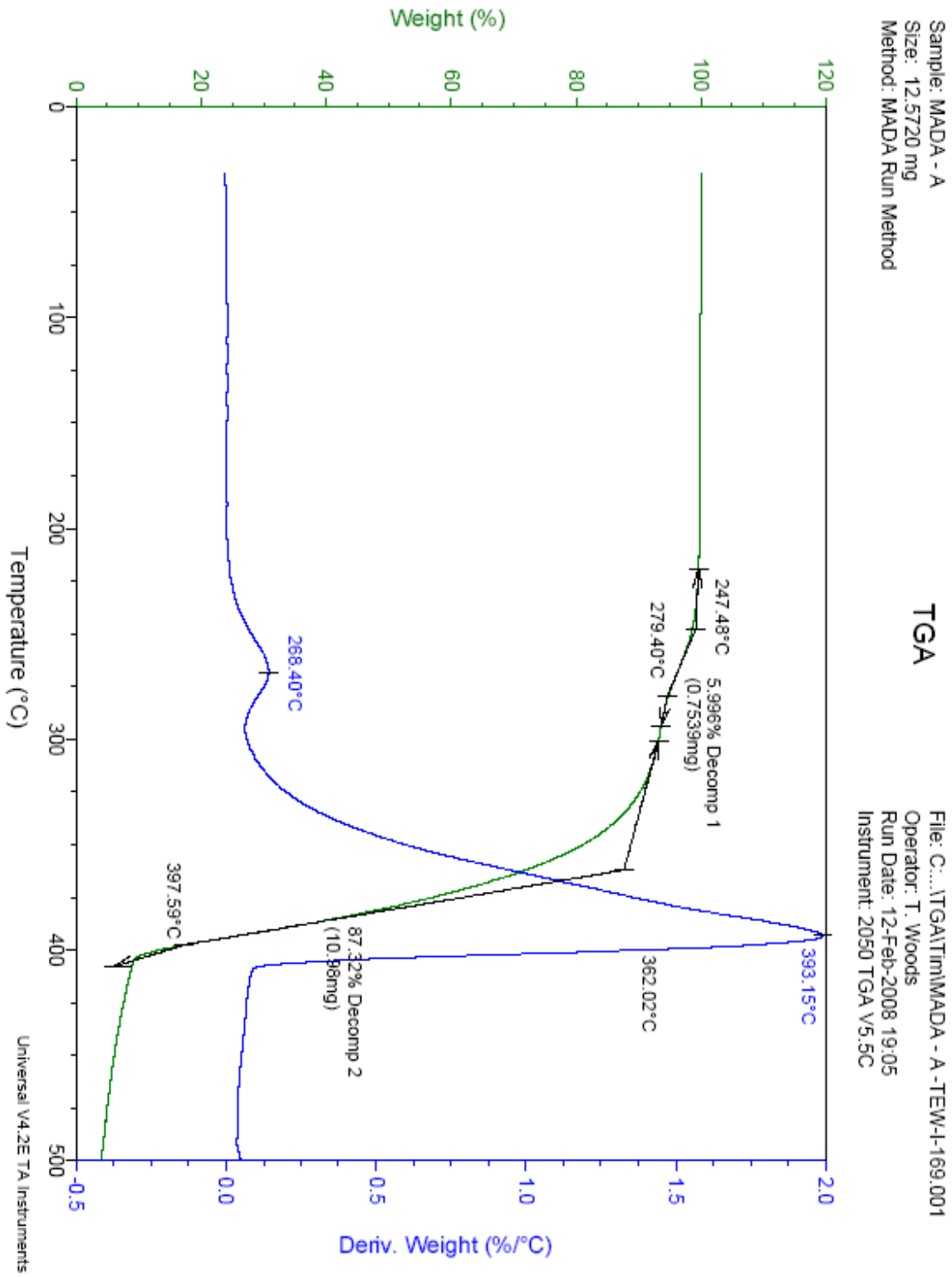

Figure 3.1 – TGA Thermogram of MADA

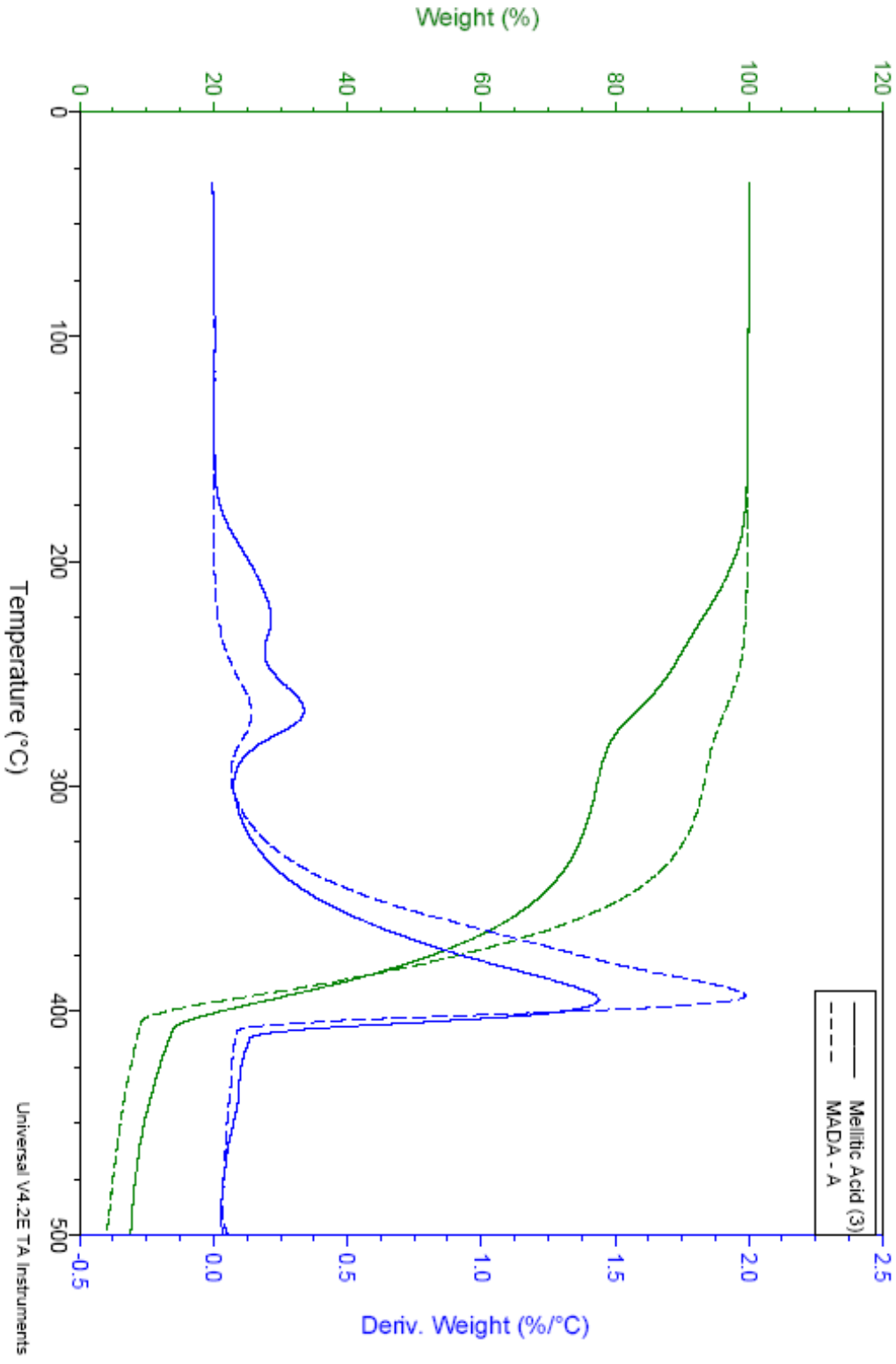

Figure 3.2 – Overlay of TGA Thermograms of Mellitic Acid and MADA, Showing Absence of First Weight Loss of Mellitic Acid in MADA Thermogram

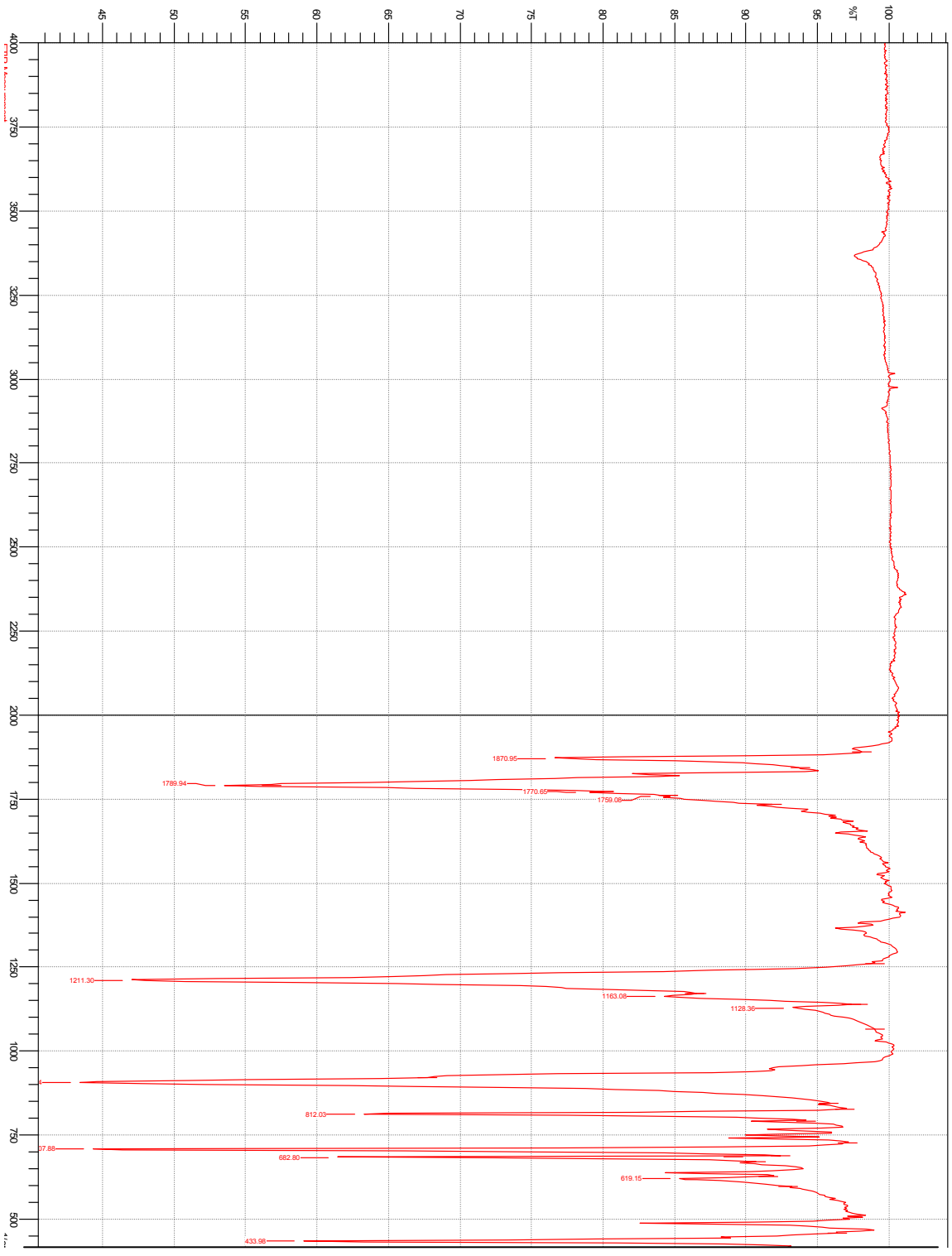

Figure 3.3 – FTIR of MADA

Changing the alkyl halide used from 4-chloro-1-butanol to 2-chloroethanol produced a noticeably greater amount of product was seen relative to the other spots in the TLC. While three spots were still observed at the end of the reaction, the lowest R_f value spot (0.38) became larger and more prominent while the middle R_f value spot (0.63) corresponding to 4-hydroxychalcone was less pronounced. Column chromatography again failed to demonstrate the separation displayed by TLC and yielded a mixture of products. The two-spot TLC verified that the mixture corresponded to crosslinker and 4-hydroxychacone.

Later work by L. Hawver using 6-chlorohexanol instead of 2-chloroethanol under the same reaction conditions generated a predominantly one-spot TLC corresponding to probable crosslinker product. Recrystallization with acetone:hexanes followed by washing with cold methanol produced a small amount of light yellow solid that yielded a one-spot TLC corresponding to probable product. NMR however was inconclusive on whether this was crosslinker product.[21]

3.3 2-[N-Methyl-N-[4-[2-(2-thien)ethenyl]phenyl]amino]ethanol (Synthesized NLO Pendent) Characterization

3.3.1 Melting Point

The melting point range of the light bright yellow product was 124.5-127 °C, which corresponds closely to the reported melting point of 132.8-137 °C, taking into account the water impurity in the final product.[22]

3.3.2 1-D Proton Nuclear Magnetic Resonance (^{1}H NMR)

The NMR obtained for the Synthesized NLO Pendent (*Figure 3.4*) was compared to the literature values reported by Samyn, et al.[22] and found to be in good agreement. A difference is seen in the experimental spectrum due to the presence of the methyl amino group (2.94 ppm (s; 3H)) versus the ethyl amino group (3.81 ppm (q; 2H), 1.17 ppm (t; 3H)) in the literature version. There is also a water impurity visible in the experimental spectrum at 1.51 ppm.[23] All

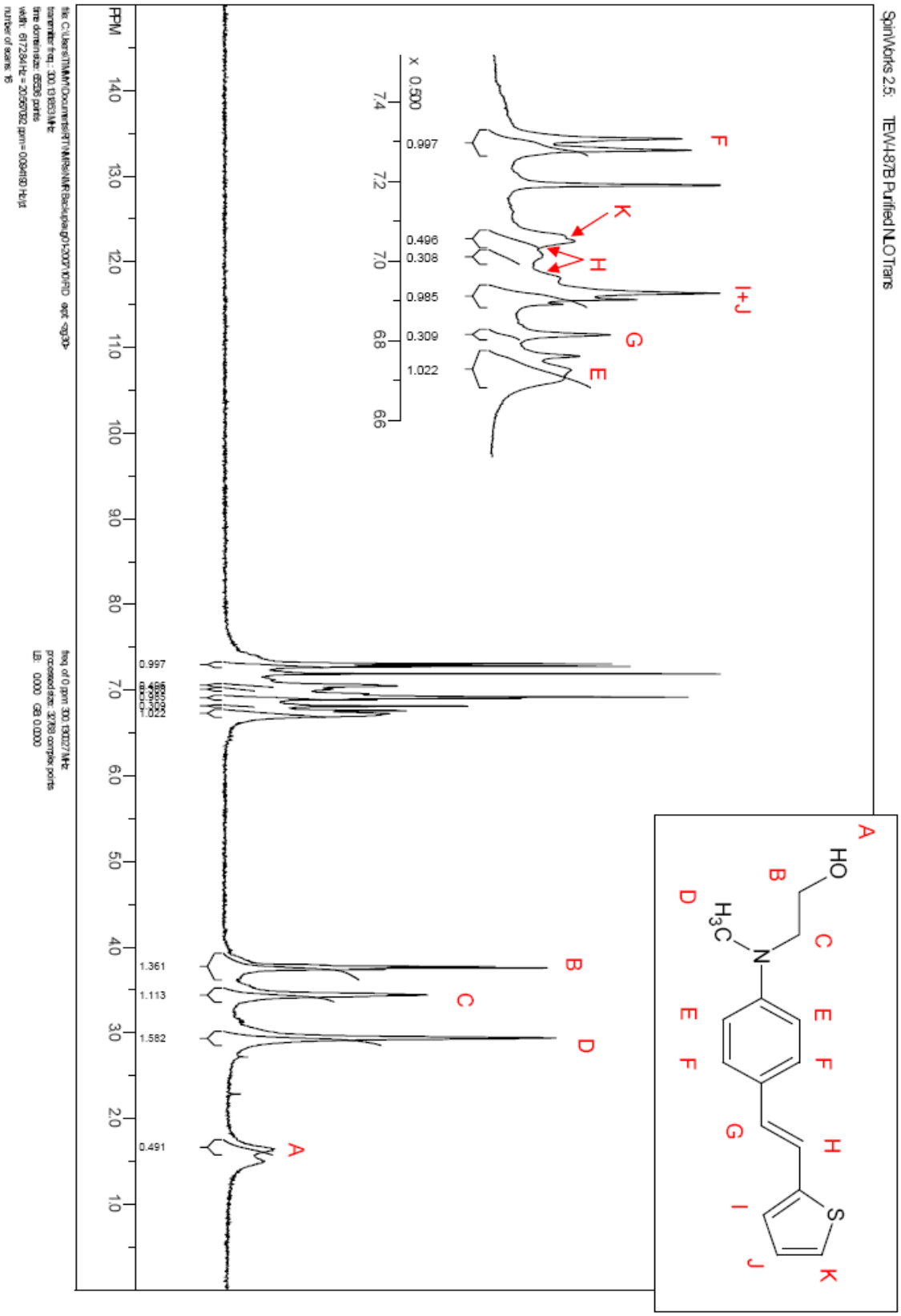

Figure 3.4 – ^{1}H NMR of Synthesized NLO

assignments for proton NMR peaks are summarized in section *3.11*, *Table 3.2*.

Lit ^{1}H NMR (ethyl): MP 132.8-137 °C; 1H NMR (CDCl3, ppm): *trans*: δ= 7.28 (d; 2H), 7.03 (m; 1H), 6.97(d; 1H), 6.88 (m; 2H), 6.79 (d; 1H), 6.70 (d; 2H), 3.65 (m; 2H), 3.45 (t; 2H), 2.95 (s; 3H), 1.55 (t; 1H)
Exp ^{1}H NMR (methyl): MP 124.5-127°C; 1H NMR (CDCl3, ppm): *trans*: δ= 7.30 (d; 2H), 7.05 (m; 1H), 7.03 (d; 1H), 6.95 (m; 2H), 6.85 (d; 1H), 6.74 (d; 2H), 3.81 (q; 2H), 3.45 (m; 2H), 2.94 (s; 3H), 1.65 (s; 1H) (H_2O impurity at 1.51)

3.4 (2-AP)$_2$MADA Diimide Characterization

3.4.1 TLC and Melting Point

The (2-AP)$_2$MADA diimide reaction progress was monitored by TLC. Starting materials (2-AP and MADA) were spotted alongside the reaction at various time points to determine the completion of compound synthesis. NMP was evaporated using a heat gun prior to plate elution. Both starting materials were retained at the baseline and an amic acid intermediate was visible almost immediately (R_f = 0.53). A new spot corresponding to product appeared near the solvent front (R_f = 0.93) at ~3 hours and was the only spot remaining at the end of imidization. All spots were light brown and visible with and without UV light. No melting point was observed prior to the onset of decomposition, observed at 300 °C.

3.4.2 1-D ^{1}H NMR

The ^{1}H NMR obtained for the (2-AP)$_2$MADA diimide is shown in *Figure 3.5*. Previous synthetic approaches were only able to isolate this compound as an isoquinoline salt, meaning that the carboxylic acid protons were not visible via NMR.[24] The current synthetic approach carried out imidization without the presence of an isoquinoline catalyst in order to facilitate viewing of the carboxylic acid protons. Both the phenol and carboxylic acid protons are visible at 9.88 ppm (s; 2H) and 8.32 ppm (s; 2H) although it has not been established which signal is due to which functional group. All aromatic protons are also visible as two sets of side-by-side triplet and doublet peaks at 7.26 ppm (m; 4H) and 6.90 ppm (m; 4H), respectively.

^{1}H NMR (d^6 DMSO, ppm): δ= 9.88 (s; 2H), 8.32 (s; 2H), 7.26 (m; 4H), 6.90 (m; 4H).

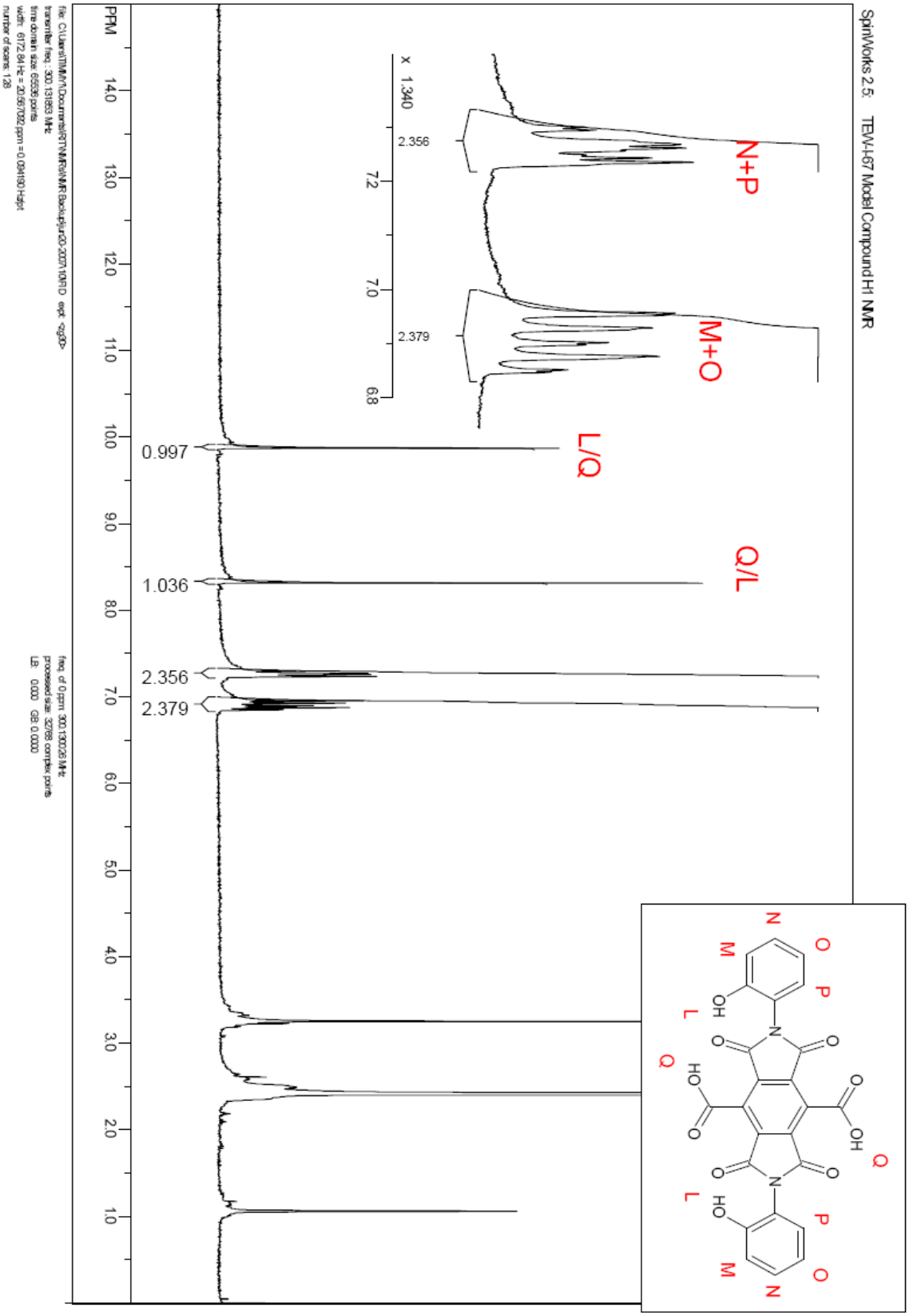

Figure 3.5 - ^{1}H NMR of (2-AP)$_2$MADA Diimide

3.4.3 FTIR

FTIR was used to confirm the structure of $(2\text{-AP})_2$MADA diimide and is shown in *Figure 3.6*. Imide peaks at 1776, 1724, 1377, and 727 cm^{-1} support the successful synthesis of the desired imide product.[7,17] The presence of the phenol groups is demonstrated by peaks at 3323 (O-H stretch) ,1095 (C-OH stretch), and 717 cm^{-1} (OH out of plane deformation), as well as the presence of the carboxylic acid groups by peaks at 1693 (C=O stretch), and 623 cm^{-1} (O-C=O bend). Furthermore, there are no indications of anhydride peaks at 1800 cm^{-1} nor amide peak at 1650 cm^{-1} in the FTIR spectrum, indicating that no intra- or intermolecular anhydride formation took place during imidization, and that a high degree of imidization had occurred, respectively.

3.4.4 Mass Spectroscopy (MS)

Figure 3.7 shows the mass spectrum obtained for the $(2\text{-AP})_2$MADA diimide. The large peak at 487.6 amu confirms the synthesis of the desired product with a molecular weight of 488.46. Peaks at 324.4 [N-(2-hydroxyphenyl)-2,3-tetracarboxylic acid imide], 161.3 (1,4-Dicarboxylic benzoic acid), 147.1 (*N*-formyl-*N*-phenylformamide), and 117.2 amu (benzoic acid) all correspond to $(2\text{-AP})_2$MADA Diimide fragments which further support the successful synthesis.

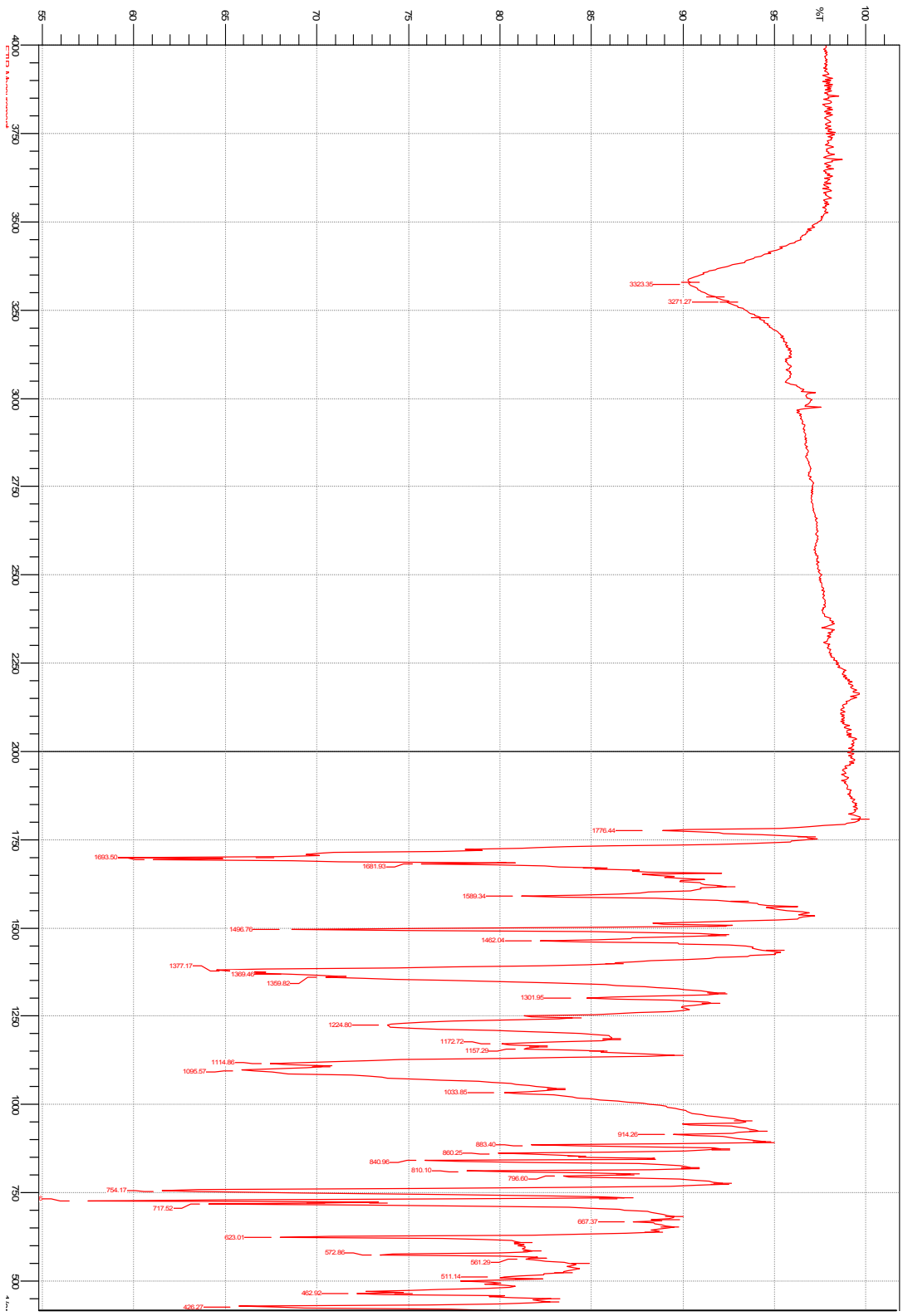

Figure 3.6 – $(2\text{-AP})_2$MADA Diimide FTIR

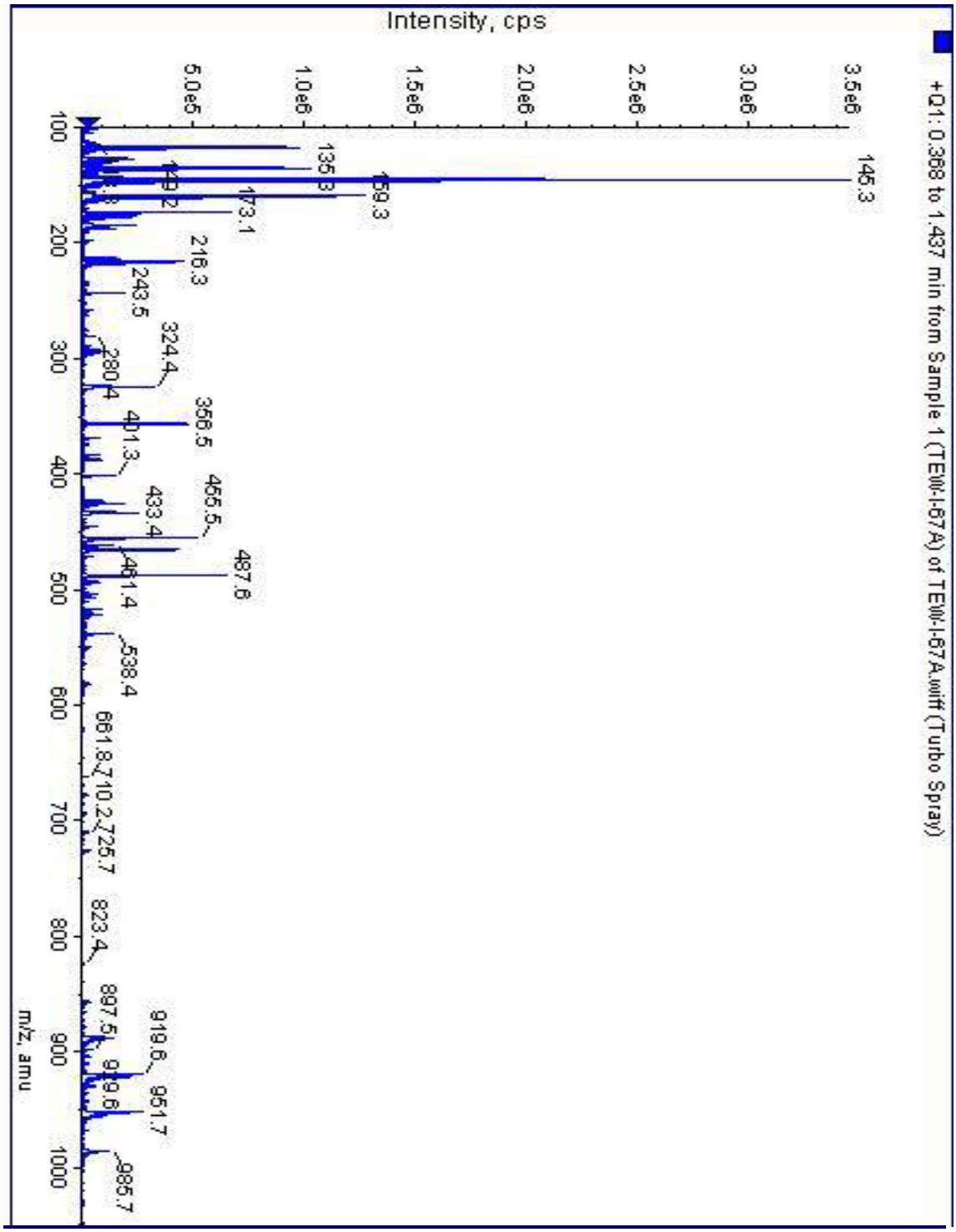

Figure 3.7 – MS of (2-AP)$_2$MADA Diimide

3.5 2'-Hydroxyphenyl-1,2-benzenedicarboxylic Acid Imide (Simplified Model Compound) Characterization

Since the objective of synthesizing the Simplified Model Compound was to test the effectiveness of old Mitsunobu reagents, no TLC system was used to monitor reaction progress. No melting point was observed due to decomposition before melting.

3.5.1 1-D ^{1}H NMR

Structural verification for the Simplified Model Compound was provided through ^{1}H NMR, shown in *Figure 3.8*. The phenol signal is visible at 9.76 ppm (s; 1H), along with the adjacent aromatic proton signals at 7.21 ppm (m; 2H) and 6.85 ppm (m; 2H). The splitting of these aromatic peaks strongly resembles the side-by-side triplet and doublet features seen in the $(2\text{-AP})_2$MADA diimide. Lastly, protons **F** + **G** are seen as 2 sets of overlapping triplets and doublets at 7.85 ppm (m; 4H).

^{1}H NMR (DMSO, ppm): δ= 9.76 (s; 1H), 7.85 (m; 4H), 7.21 (m; 2H), 6.85 (m; 2H).

3.5.2 FTIR

As with the $(2\text{-AP})_2$MADA diimide, FTIR was used to verify that imidization had taken place (*Figure 3.9*). The presence of characteristic imide peaks at 1786, 1721, 1388, & 720 cm^{-1} confirm the imide product was obtained. Also visible is a phenol peak at 3377 cm^{-1} (O-H stretch) and a carbonyl peak at 1681 cm^{-1} (C=O stretch), the former of which correspond to a similar peak seen with the $(2\text{-AP})_2$MADA diimide.

3.5.3 MS

Figure 3.10 shows the mass spectrum obtained for the Simplified Model Compound. The parent peak at 238.2 amu confirms the synthesis of the desired product with a molecular weight of 239.23. The peak at 210.2 corresponds to simplified model compound cleaving the fragment (C=O), supporting the above conclusion.

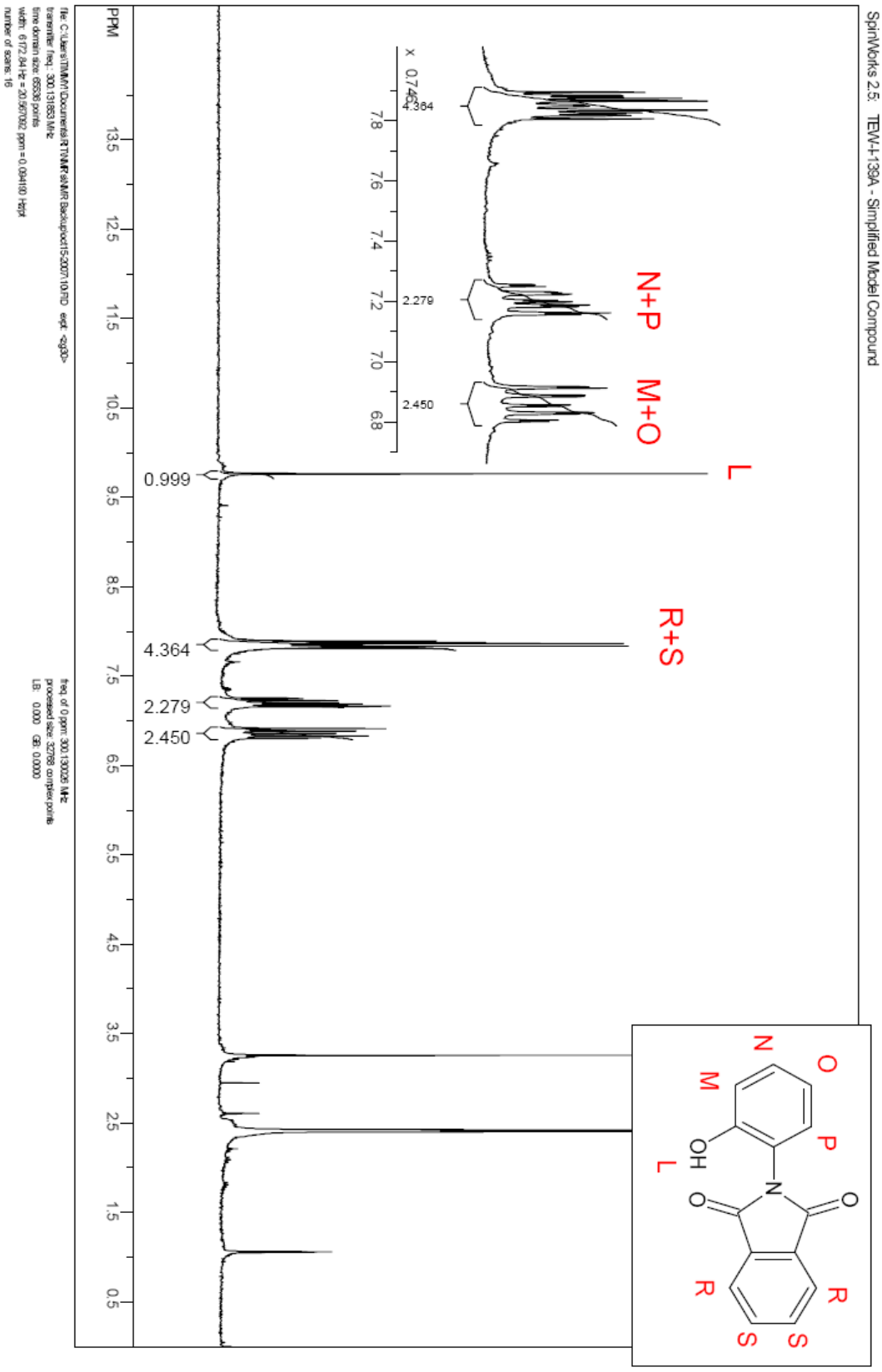

Figure 3.8 – ^{1}H NMR of Simplified Model Compound

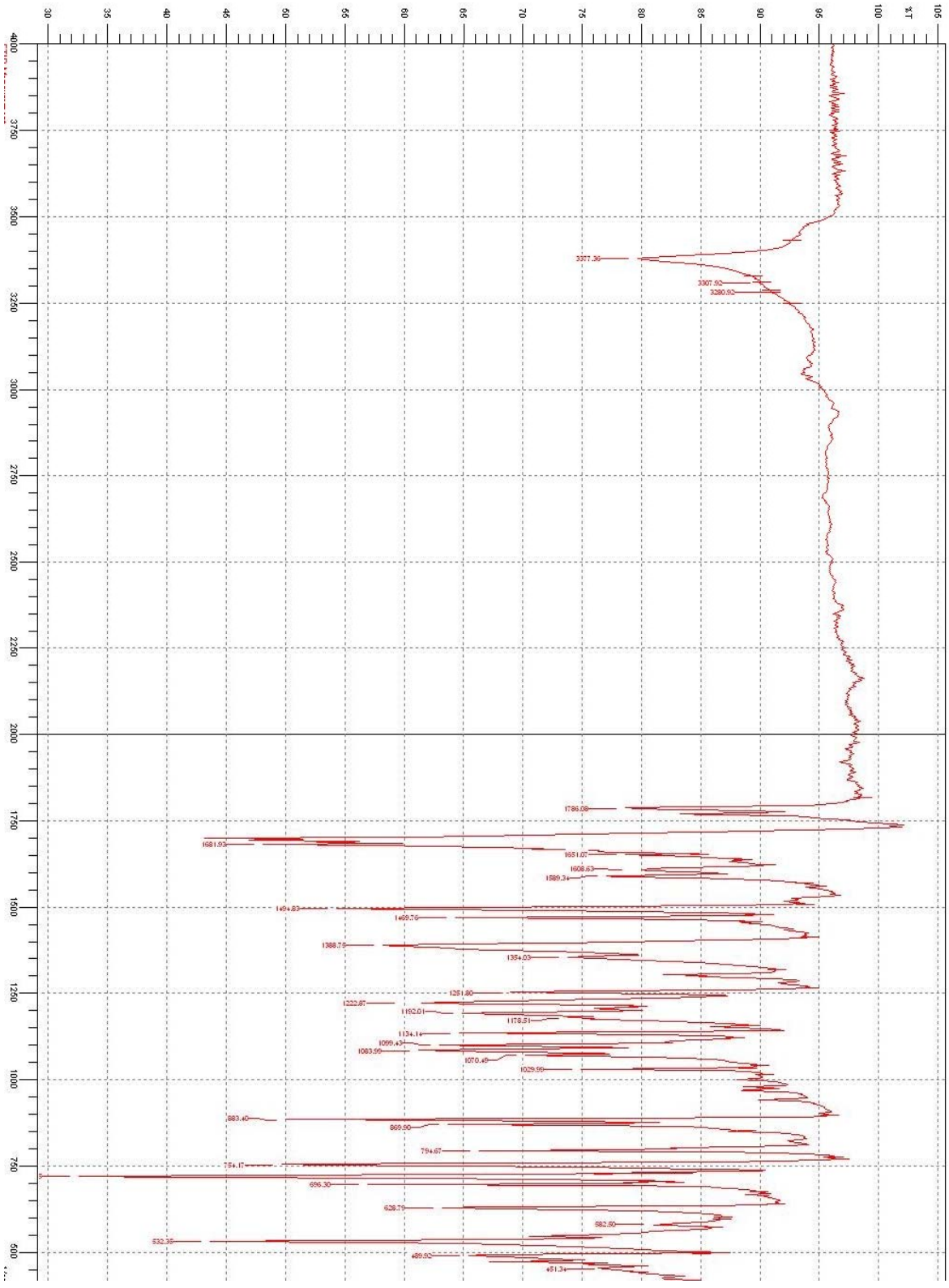

Figure 3.9 – Simplified Model Compound FTIR

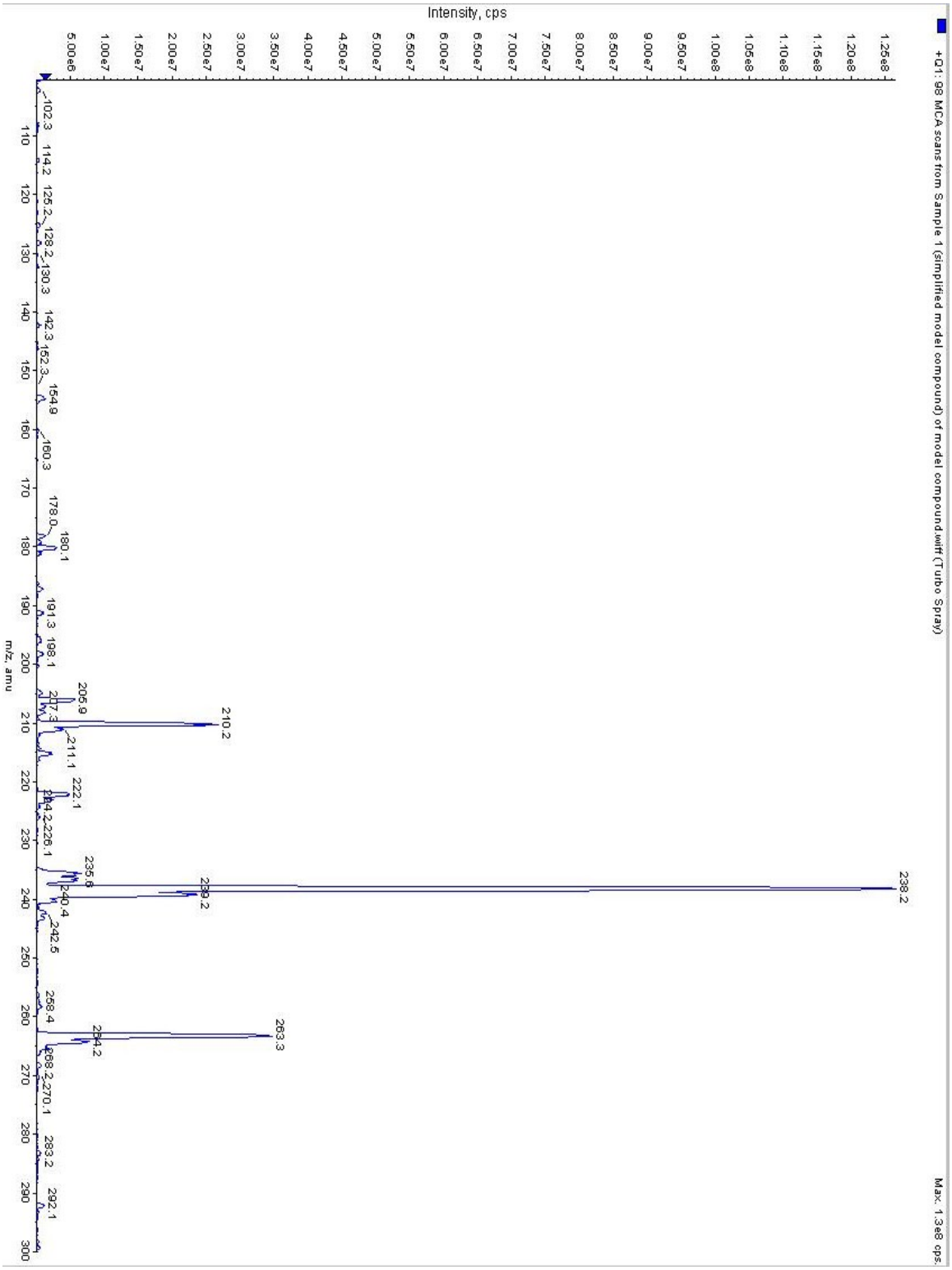

Figure 3.10 – Simplified Model Compound MS

3.6 Characterization of Simplified Model Compound with Methyl NLO Surrogate Pendent Group

3.6.1 TLC

The Mitsunobu reaction product to append the Methyl NLO Surrogate to the phenol on the Simplified Model Compound was evaluated by TLC. This was done both to gauge the reaction progress and also to qualitatively determine the quality of DEAD being used. A new spot (R_f = 0.59) not corresponding to starting material was noted at the conclusion of the reaction. Spots corresponding however to both Simplified Model Compound and Methyl NLO surrogate were still visible. The desired product isolated by column chromatography showed a one spot TLC, indicating that the sample consisted of mostly one substance.

3.6.2 1-D ^{1}H NMR

The ^{1}H NMR for the desired reaction product isolated by column chromatography is shown in *Figure 3.11*. The NMR confirms that some pendent attachment did take place, but that there is also greater than 50% of un-reacted Simplified Model Compound, based on the presence of the Simplified Model Compound phenol peak. New peaks at 6.46 ppm (m; 2H), 3.52 ppm (t; 1H), 3.34 ppm (t; 1H), and 3.19 ppm (s; 2H) all correspond to various protons associated with the Methyl NLO Surrogate. Absent is the alcohol proton signal from un-reacted Methyl NLO Surrogate observed under similar conditions, suggesting that the peaks seen can be attributed to attached pendent and not free pendent in solution. All signals corresponding to the Simplified Model Compound aromatic protons are also visible at 7.84 ppm (m; 4H), 7.20 ppm (m; 2H), and 6.84 ppm (m; 2H). The NMR also gives several indications that an incomplete reaction took place. First, the phenol peak at 9.77 ppm corresponding to the Simplified Model Compound phenol group is still present, which should disappear with complete pendent attachment to this functional group. Second, the phenol peak integrated for less than expected with respect to the other Simplified Model Compound peaks (expected 1:4 ratio; observed 0.38:2.2). Also, the NMR shows peaks corresponding to DEAD byproduct at 8.91 ppm (s), 3.95 ppm (q), and 1.09 ppm (t).

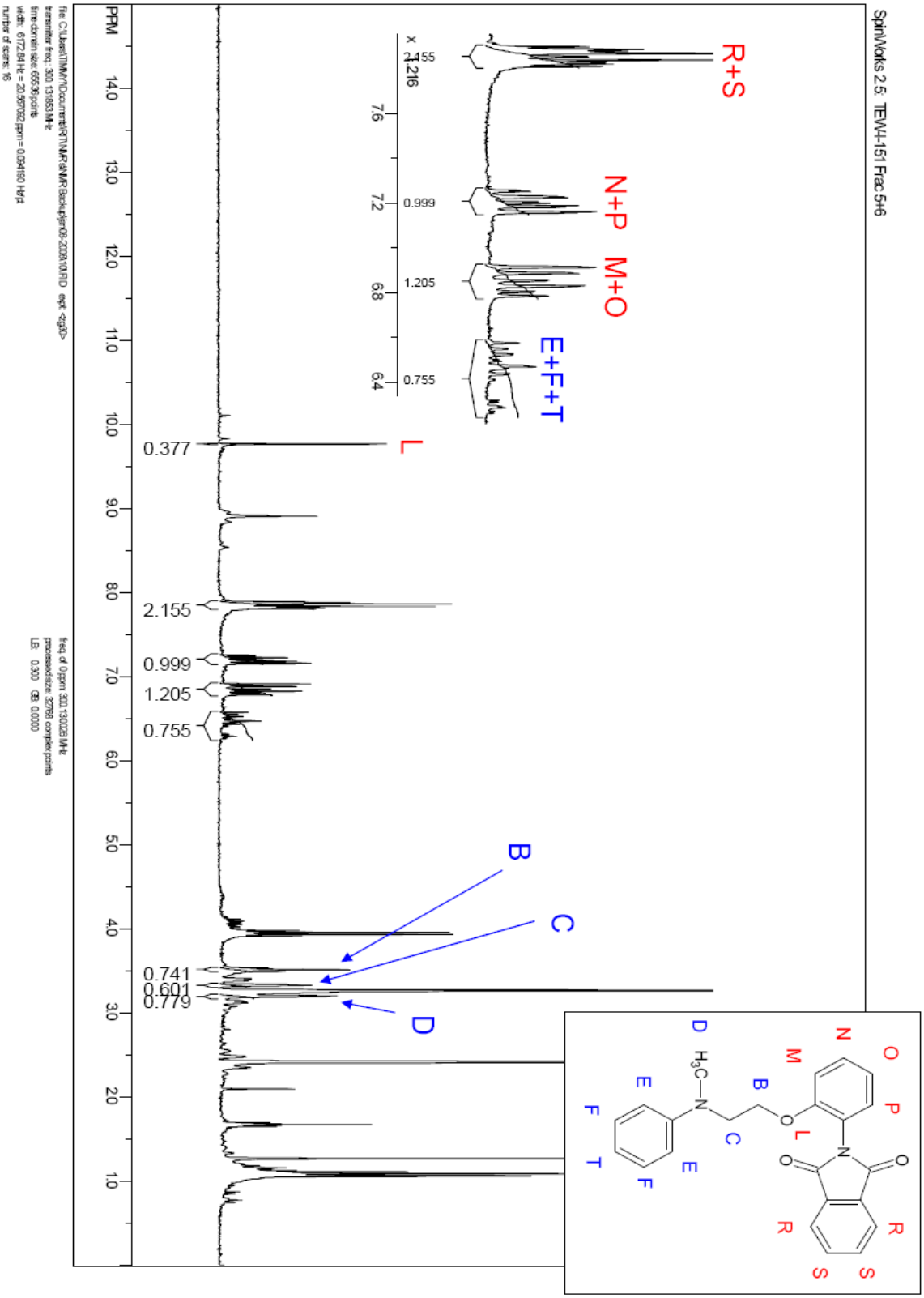

Figure 3.11 – Simplified Model Compound with Methyl NLO Surrogate ^{1}H NMR Showing That "Old" Dead Reagent is not Fully Potent

^{1}H NMR (DMSO, ppm): δ= 9.76 (s; 1H), 7.84 (m; 4H), 7.20 (m; 2H), 6.84 (m; 2H), 6.46 (m; 2H), 3.52 (t; 1H), 3.34 (t; 1H), 3.19 (s; 2H).

3.7 Characterization of 3,5-Dihydroxybenzoic Acid with Methyl NLO and Ethyl NLO Surrogate Pendent Groups

3.7.1 Methyl NLO Surrogate Attachment to Ar-COOH of 3,5-Dihydroxybenzoic Acid Characterization

3.7.1.1 TLC

The attachment of the Methyl NLO Surrogate to the Ar-COOH of 3,5-dihydroxybenzoic acid was monitored by TLC. All reagents were spotted adjacent to one another in order to determine rate and degree of product formation: 3,5-Dihydroxybenzoic acid (light brown, R_f = 0.08), Methyl NLO Surrogate (purple, R_f = 0.48), PPh_3 ((R_f = 0.92), DEAD (light yellow, R_f = 0.87), $OPPh_3$ (R_f = 0.08). Product formation was apparent by the formation of a new spot (light brown, R_f = 0.17) as soon as all Mitsunobu reagents were introduced, and confirmed by the subsequent disappearance of the spots corresponding to Methyl NLO Surrogate, PPh_3 and DEAD. TLC analysis at the conclusion of the reaction showed the spot due to product was much larger relative to the spot from 3,5-dihydroxybenzoic acid, and a spot corresponding to $OPPh_3$, a reaction by-product. No melting point was obtained due to the fact that the isolated product was an oil.

3.7.1.2 1-D ^{1}H NMR

Product structural confirmation was provided by ^{1}H NMR, shown in *Figure 3.12*. All observed peaks and their integrations are consistent with the expected structure. The presence of both phenol protons at 9.59 ppm (s: 2H) and the absence of the carboxylic acid proton at 12.60 ppm confirm that the pendent attachment occurred only at the latter location. This is crucial because it demonstrates that an equivalent amount of a pendent can be attached selectively at an aromatic carboxylic acid group in the presence of a phenol group using the Mitsunobu reaction. Both sets of aromatic protons of 3,5-dihydroxybenzoic acid are present at 6.73 ppm (d, ^{3}J = 3 Hz;

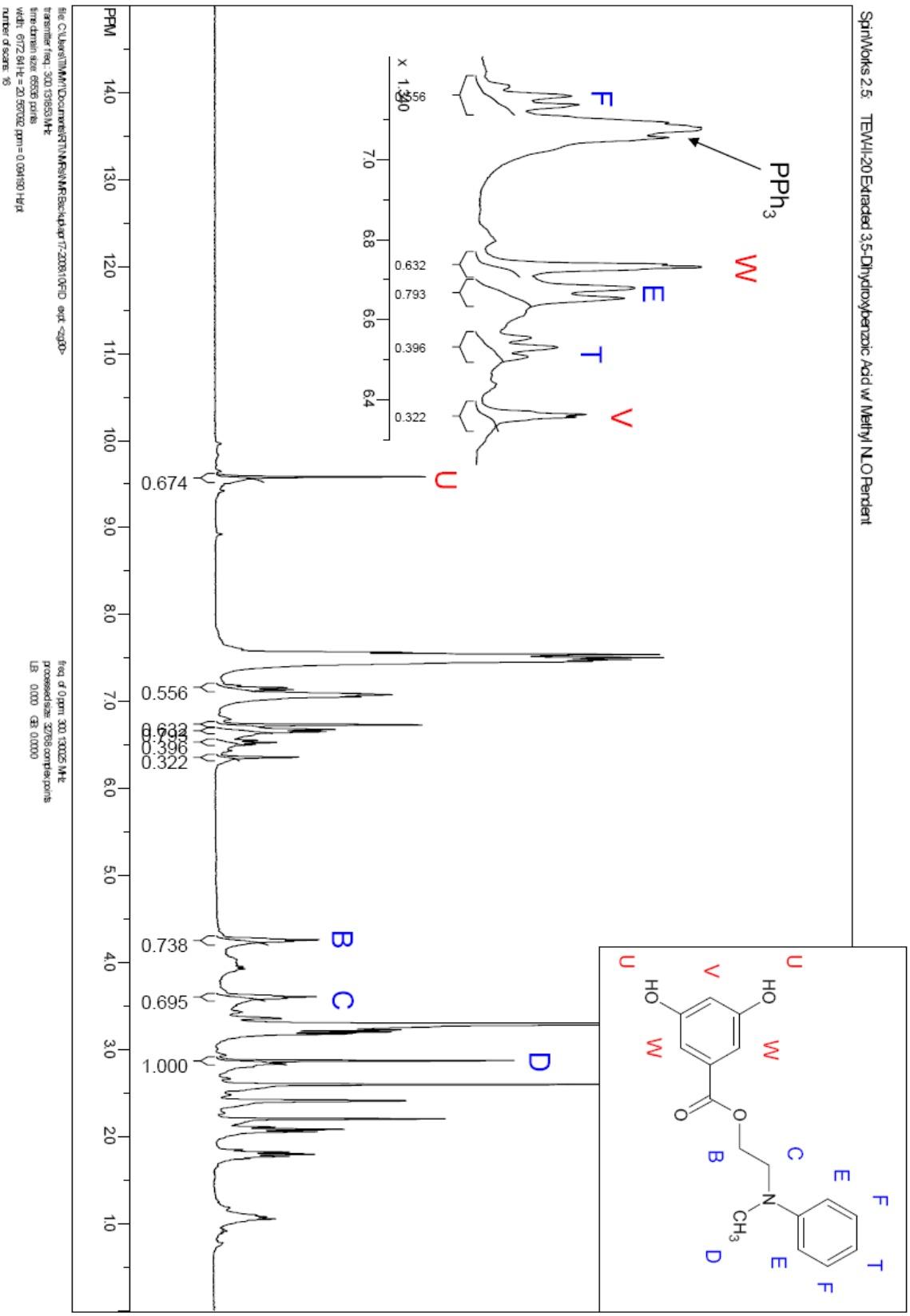

Figure 3.12 – 3,5-Dihydroxybenzoic Acid with Methyl NLO Surrogate ^{1}H NMR

2H) and 6.37 ppm (t, ^{3}J = 3 Hz; 1H). All four aromatic protons corresponding to Methyl NLO Surrogate are also present at 7.16 ppm (t; ~4H), 6.67 ppm (d; 2H) and 6.53 ppm (t; 1H), although the set at 7.08 ppm due not integrate as expected due to the overlap with the PPh_3 impurity. Both sets of methylene protons are visible at 4.26 ppm (t; 2H) and 3.61 ppm (t; 2H), along with the methyl protons at 2.88 ppm (s; 3H). Also evident is the presence of the $OPPh_3$ byproduct at 7.51 ppm (m), PPh_3 at 7.08 ppm (m), and NMP by signals at 3.21 ppm (t), 2.60 ppm (s), 2.09 ppm (t), and 1.80 ppm (m).

^{1}H NMR (DMSO, ppm): δ= 9.59 (s; 2H), 7.16 (t; 4H), 6.73 (d; 2H), 6.67 (d; 2H), 6.53 (t; 1H), 6.37 (t; 1H), 4.26 (t; 2H), 3.61 (t; 2H), 2.88 (s; 3H).

3.7.2 Ethyl NLO Surrogate Attachment to Ar-OH of 3,5-Dihydroxybenzoic Acid with Methyl NLO Surrogate on Ar-COOH Characterization

3.7.2.1 TLC

The attachment of the Ethyl NLO Surrogate to the phenol groups of 3,5-dihydroxybenzoic acid was monitored by TLC. All reagents were spotted adjacent to one another in order to determine rate and degree of product formation: 3,5-Dihydroxybenzoic acid w/ Methyl NLO Surrogate on Ar-COOH (light brown, R_f = 0.17), Ethyl NLO Surrogate (green, R_f = 0.60), PPh_3 ((R_f = 0.92), DEAD (light yellow, R_f = 0.87), $OPPh_3$ (R_f = 0.08). Product formation was apparent by the formation of a new spot (light brown, R_f = 0.75) as soon as all Mitsunobu reagents were introduced, and confirmed by the subsequent disappearance of the spots corresponding to 3,5-dihydroxybenzoic acid w/ Methyl Surrogate NLO on Ar-COOH, Ethyl NLO Surrogate, PPh_3 and DEAD. TLC analysis during the reaction indicated a much slower rate of reaction than with the first pendent attachment (48 hours vs. 132 hours), and a larger amount of DEAD to complete pendent attachment. At the conclusion of the reaction, TLC indicated a high degree of product formation with small spots corresponding to 3,5-dihydroxybenzoic acid with Methyl Surrogate NLO on Ar-COOH and Ethyl NLO Surrogate still evident, along with a spot

corresponding to $OPPh_3$, a reaction by-product. No melting point was obtained due to the fact that the isolated product was an oil.

3.7.2.2 1-D ^1H NMR

Product structural confirmation was provided by ^1H NMR, shown in *Figure 3.13*. All observed peaks are consistent with the expected structure. The peak at 9.59 ppm corresponding to the phenol protons seen previously in *3.7.1.1* is almost completely absent, implying that pendent attachment has taken place at both phenol groups as desired. In addition, the appearance of several new peaks in the NMR spectrum corresponding to the Ethyl NLO Surrogate also demonstrates pendent attachment. All three aromatic peaks are visible at 7.17 (t; 6H), 6.62 (d; 6H), and 6.49 ppm (t; 3H), closely resembling the chemical shifts seen previously with the attachment of the Methyl NLO Surrogate to the Ar-COOH location. Also present are all three sets of methylene protons from the Ethyl NLO Surrogate plus the ester methylene protons from the Methyl NLO Surrogate at 3.97 ppm (m; 14H), seen as a downfield set of overlapping triplets and an upfield set of an overlapping quartet and triplet. Lastly the methyl protons of the Ethyl NLO Surrogate are seen at 1.00 ppm (t; 6H). One interesting affect of the pendent attachment is the change in the chemical shift observed of the 3,5-dihydroxybenzoic acid proton **(V)** that is *ortho* to both phenol groups from 6.53 to 6.89 ppm due to its change in chemical environment, along with the change in splitting seen with the other two protons **(W)** from one doublet to two singlets at 6.81 ppm. The $OPPh_3$ reaction byproduct is seen at 7.51 (m) along with a small amount of unused PPh_3 at 7.08 ppm (m). Also evident is the presence of NMP in the product by signals at 3.21 ppm (t), 2.60 ppm (s), 2.09 ppm (t), and 1.80 ppm (m).

^1H NMR (DMSO, ppm): δ= 7.17 (t; 6H), 6.89 (s; 1H), 6.82 (s; 1H), 6.80 (s; 1H), 6.62 (d; 6H), 6.49 (t; 3H), 3.97 (m; 14H), 3.59 (t; 2H), 2.61 (s; 3H), 1.00 (t; 6H).

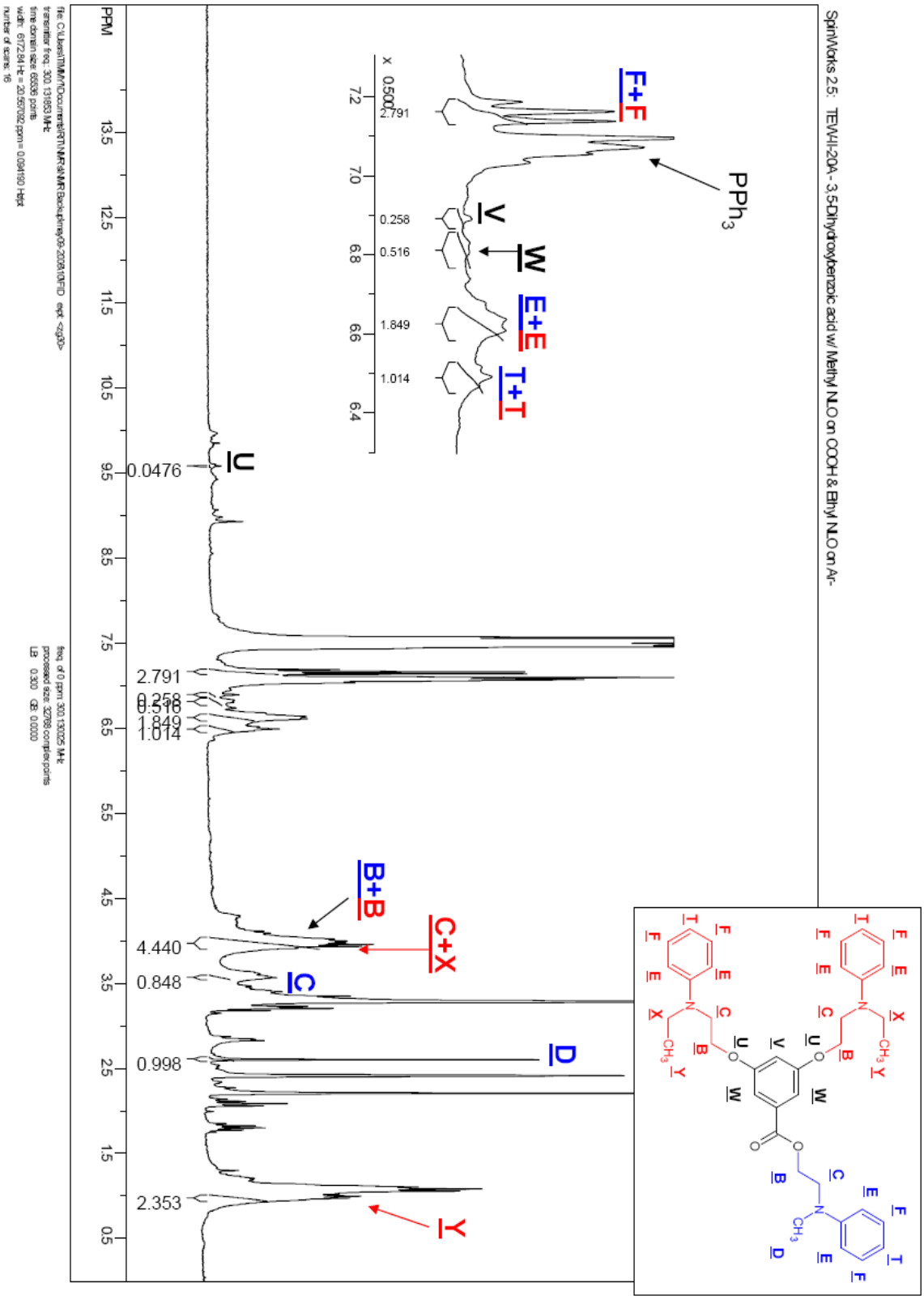

Figure 3.13 – 3,5-Dihydroxybenzoic Acid with Methyl NLO Surrogate on Ar-COOH and Ethyl NLO Surrogate on Ar-OH

3.8 Characterization of (2-AP)$_2$MADA Diimide with Methyl NLO and Ethyl NLO Surrogate Pendent Groups

3.8.1 Attachment of Methyl NLO Surrogate to Ar-COOH or Ar-OH of (2-AP)$_2$MADA Diimide Characterization

3.8.1.1 TLC

The attachment of the Methyl NLO Surrogate to the (2-AP)$_2$MADA diimide was monitored by TLC. All reagents were spotted against one another in order to determine rate and degree of product formation: (2-AP)$_2$MADA diimide (light brown, $R_f = 0.12$), Methyl NLO Surrogate (green, $R_f = 0.48$), PPh_3 (($R_f = 0.92$), DEAD (light yellow, $R_f = 0.87$), $OPPh_3$ ($R_f = 0.08$). Product formation was apparent by the formation of a new spot (light brown, $R_f = 0.25$) as soon as all Mitsunobu reagents were introduced, and confirmed by the subsequent disappearance of the spots corresponding to Methyl NLO Surrogate, PPh_3 and DEAD. TLC analysis at the conclusion of the reaction indicated a high degree of product formation with only small spots corresponding to (2-AP)$_2$MADA diimide and Methyl NLO Surrogate still evident, along with a spot corresponding to $OPPh_3$, a reaction by-product. No melting point was obtained due to the fact that the isolated product decomposed before it melted.

3.8.1.2 1-D ^{1}H NMR

Product structural confirmation was provided by ^{1}H NMR, shown in *Figure 3.14*. All observed peaks are consistent with the expected structure. Due to the fact that both the carboxylic acid and phenol functional groups are present in the same ratio, the spectra does not reveal where pendent attachment occurred. For simplification purposes, the structure in *Figure 3.14* shows pendent attachment at the phenol locations, even though this may not be the case. The spectrum does reveal that pendent attachment took place at either only the carboxylic acid or the phenol locations, as the peak at 8.13 ppm (d; 2H) corresponding to one of the above functional groups still integrates for two protons. Both sets of (2-AP)$_2$MADA diimide aromatic protons are seen at 7.06 ppm (m; 4H) and 6.44 ppm (m; 4H), being shifted slightly upfield by the pendent attachment

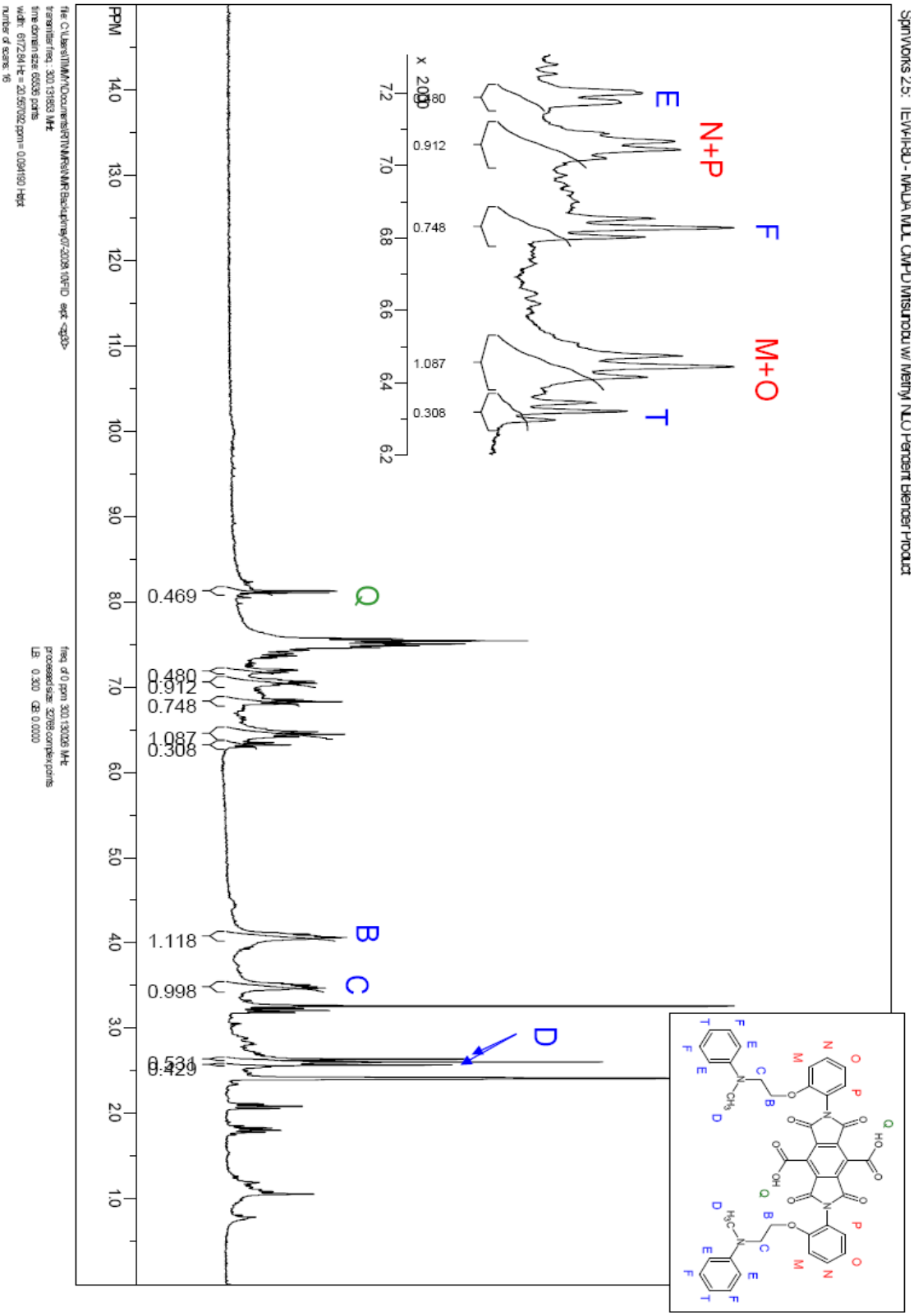

Figure 3.14 – [1]H NMR of (2-AP)$_2$MADA Diimide *with Methyl NLO Surrogate on either Ar-COOH or Ar-OH*

(0.2 ppm and 0.45 ppm respectively). All four aromatic protons corresponding to the Methyl NLO Surrogate are also present at 7.18 ppm (d; 4H), 6.82 ppm (t; 4H) and 6.34 ppm (t; 2H), with protons in the ortho position relative to the amine having been shifted downfield by 0.7 ppm. Both sets of methylene protons are also visible at 4.08 ppm (m; 4H) and 3.49 ppm (m; 4H), along with the two signals assigned to the methyl protons, at 2.65 ppm (s; 2H) and 2.57 ppm (s; 1H). Also evident is the presence of the $OPPh_3$ reaction byproduct at 7.51 ppm (m) and NMP by signals at 3.21 ppm (t), 2.60 ppm (s), 2.09 ppm (t), and 1.80 ppm (m).

^{1}H NMR (DMSO, ppm): δ= 8.13 (d; 2H), 7.18 (d; 4H), 7.06 (m; 4H), 6.82 (t; 4H), 6.44 (m; 4H), 6.34 (t; 2H), 4.08 (m; 4H), 3.49 (m; 4H), 2.65 (s; 2H), 2.57 (s; 1H).

3.8.1.3 FTIR

Structural verification of the single pendent $(2\text{-AP})_2$MADA diimide product was also provided through FTIR, shown in *Figure 3.15*. Characteristic imide peaks at 1778, 1720, 1375, and 721 cm^{-1} confirm the presence of the imide rings in the $(2\text{-AP})_2$MADA Diimide,[10,17] which is important because the one pot synthetic approach used did not isolate the imidized product prior to pendent attachment. Pendent attachment is confirmed by three new peaks at 745 and 692 (phenyl ring deformation) and 540 cm^{-1} (C-N-C bending). New peaks at 1244 (C-O-C stretch) and 1118 cm^{-1} (C-O-C stretch) are indicative of the pendent attachment taking place at the phenol functional groups, along with the absence of the phenol peaks at 1095 and 717 cm^{-1} previously seen in the $(2\text{-AP})_2$MADA diimide. This is also supported by the lack of a strong peak in the 645-575 cm^{-1} region, corresponding to an ester O-C-O bend. The presence of a new peak at 3061 cm^{-1} corresponding to the presence of a strongly hydrogen-bonded O-H stretch or a Zwitterion (N-H stretch) could also explain the change in chemical shift observed in the NMR spectrum for the protons corresponding to the un-reacted carboxylic acid group.

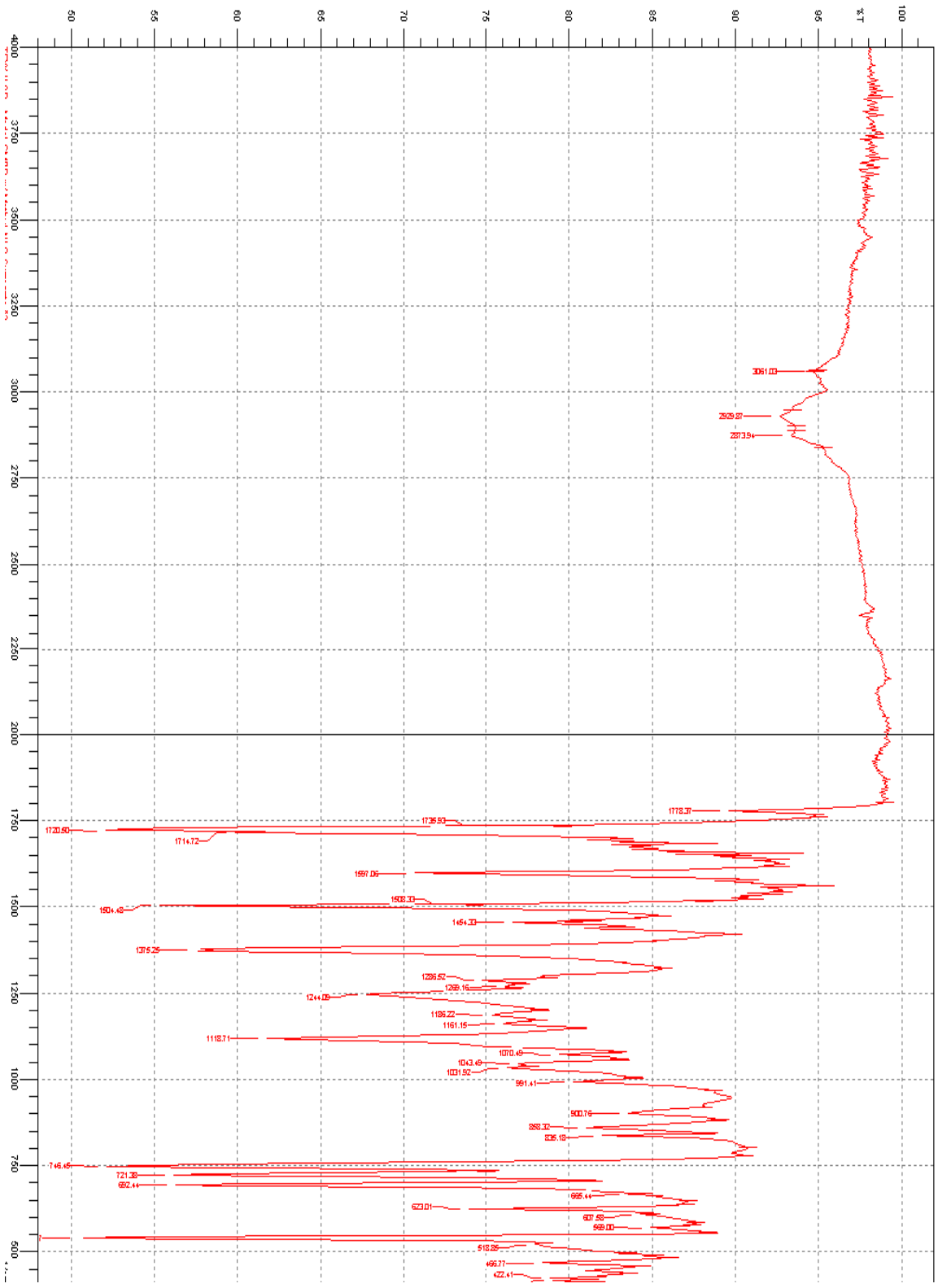

Figure 3.15 – FTIR of (2-AP)$_2$MADA Diimide with Methyl NLO Pendent on either Ar-COOH or Ar-OH

3.8.2 Attachment of Methyl NLO Surrogate to Ar-COOH or Ar-OH of (2-AP)$_2$MADA Diimide w/ Ethyl NLO on Ar-COOH or Ar-OH

3.8.2.1 TLC

The attachment of the Methyl NLO Surrogate to the (2-AP)$_2$MADA diimide with the Ethyl NLO Surrogate on Ar-COOH or Ar-OH was monitored by TLC. All reagents were spotted adjacent to one another in order to determine rate and degree of product formation: (2-AP)$_2$MADA diimide w/ Ethyl NLO Surrogate (light brown, $R_f = 0.17$), Methyl NLO Surrogate (green, $R_f = 0.54$), PPh_3 ($R_f = 0.92$), DEAD (light yellow, $R_f = 0.87$), $OPPh_3$ ($R_f = 0.11$). Product formation was apparent by the formation of a new spot (brown, $R_f = 0.27$) as soon as all Mitsunobu reagents were introduced, and confirmed by the subsequent lightening of the spots corresponding to Methyl NLO Surrogate, PPh_3 and DEAD. As was seen with the second pendent attachment to 3,5-dihydroxybenzoic acid, TLC analysis during the reaction indicated a much slower rate of reaction than with the first pendent attachment (48 hours vs. 132 hours), and a larger amount of DEAD to complete pendent attachment. TLC analysis at the conclusion of the reaction indicated a reasonable degree of product formation; however spots corresponding to the (2-AP)$_2$MADA diimide w/ Ethyl NLO Surrogate, PPh_3 and Methyl NLO Surrogate were still evident, along with a spot corresponding to $OPPh_3$, a reaction by-product. No melting point was obtained due to the fact that the isolated product was an oil.

3.8.2.2 1-D ^{1}H NMR

Product structural confirmation was provided by ^{1}H NMR, shown in *Figure 3.16.* Note that two equivalents of the Ethyl NLO Surrogate were attached first to the (2-AP)$_2$MADA diimide, followed by the attachment of the Methyl NLO Surrogate. The second pendent attachment was demonstrated by the weakening of the signal at 8.13 ppm (s; 1H) in the NMR spectrum, relative to the other (2-AP)$_2$MADA diimide peaks, which corresponds to either the unreacted carboxylic acid or phenol functional groups. Based on the decrease in integration, pendent attachment took place at between 45-50% of available sites. The appearance of several

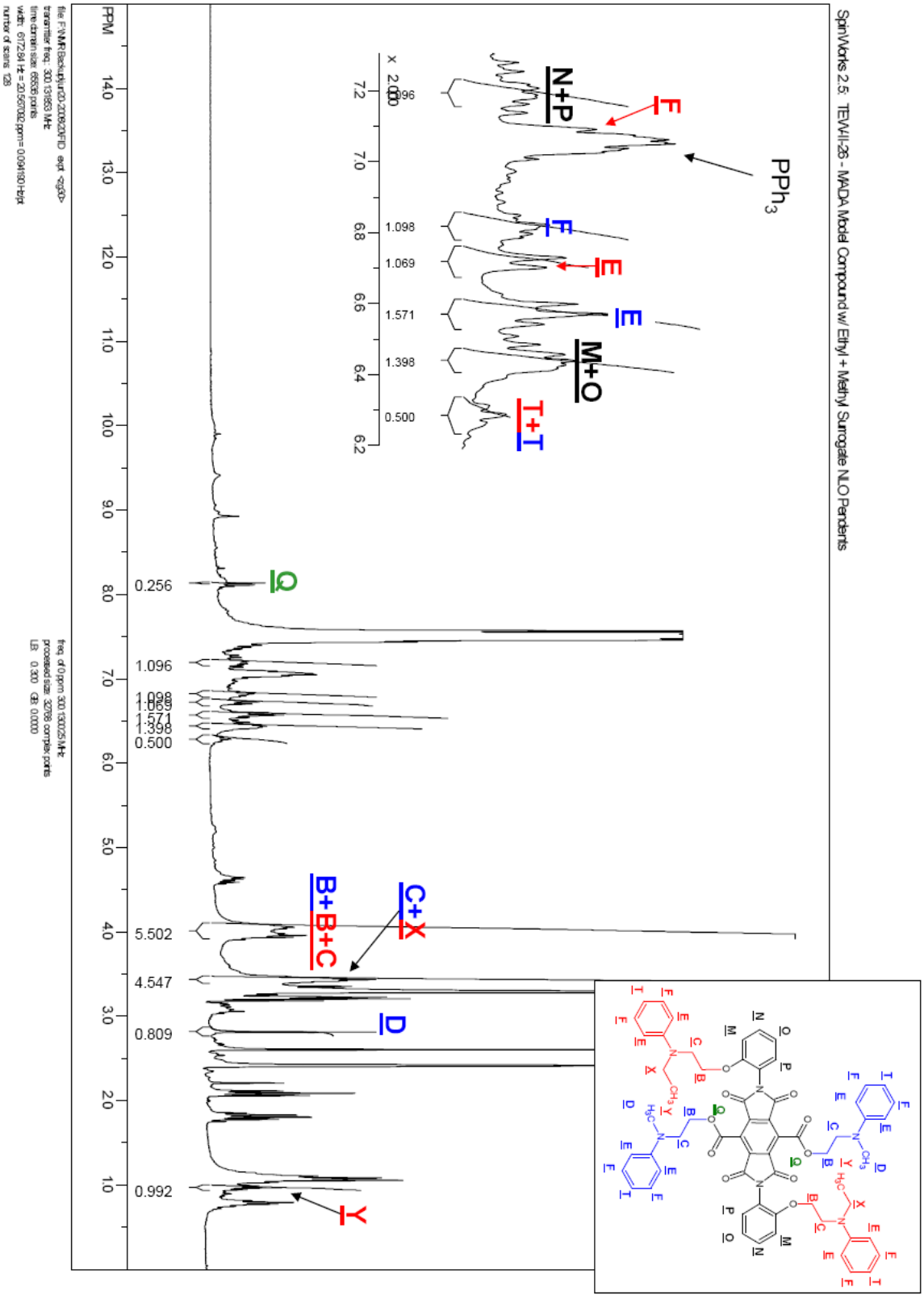

Figure 3.16 – ^{1}H NMR of $(2\text{-AP})_2$MADA Diimide with Ethyl NLO Surrogate on Ar-OH and Methyl NLO Surrogate on Ar-COOH

new peaks corresponding to Methyl NLO Surrogate (the second pendent group to be attached) also supports the pendent attachment to the $(2\text{-AP})_2$MADA diimide. All three aromatic peaks are visible at 6.81 (m; 4H), 6.57 (d; 4H), and 6.29 ppm (t; 2H), although one broad upfield at 6.57 ppm peak integrates incorrectly for unknown reasons. Note that the chemical shifts of the Ethyl NLO Surrogate aromatic protons are significantly different than those seen for the Methyl NLO Surrogate. Also present are two of the sets of methylene protons from the Ethyl NLO Surrogate plus the ester methylene protons from the Methyl NLO Surrogate at 4.00 ppm (m; overlapped), seen as a downfield set of overlapping triplets and an upfield triplet. The other set of methylene protons from the Ethyl and Methyl NLO Surrogates are seen at 3.43 ppm (m; overlapped) as a overlapping triplet and quartet. Once again, both peaks attributed to the methylene NLO Surrogate protons do not integrate correctly for unknown reasons. Lastly the methyl protons of the Methyl NLO Surrogate are seen at 2.81 ppm (s; 3H). This integration also alludes to the fact that pendent attachment has not taken place at all available locations, since the Ethyl NLO Surrogate methyl protons were used as the landmark peak when integrating. The interpretation of results is complicated by the presence of several Mitsunobu reaction byproducts in the NMR spectrum. Spent DEAD is evident by peaks at 8.11 ppm (d), 4.60 ppm (m), and 1.09 ppm (t), along with $OPPh_3$ at 7.50 ppm (m), and a small amount of unused PPh_3 at 7.06 ppm (m). Also evident is the presence of NMP by signals at 3.21 ppm (t), 2.60 ppm (s), 2.09 ppm (t), and 1.80 ppm (m).

^{1}H NMR (DMSO, ppm): δ= 8.13 (s; 1H), 7.18 (m; 4H), 6.81 (m; 4H), 6.72 (d; 4H), 6.57 (d; 4H), 6.44 (m; 4H), 6.29 (t; 2H), 4.00 (m; 33H), 3.43 (m; 27H), 2.81 (s; 3H), 0.97 (t; 3H).

3.9 co-PI[Bis-AP-AF/6FDA)$_{0.9}$ (Bis-AP-AF/MADA)$_{0.1}$]$_n$ Characterization

3.9.1 TLC

TLC analysis was performed on the polyimide product in order to confirm incorporation of all three components into the product. Each of the three components was spotted adjacent to one another along with the polyimide product: MADA (R_f = 0.00), Bis-AP-AF (green, R_f = 0.69), 6FDA (R_f = 0.00), Polyimide (v. light yellow, R_f = 0.05). The absence of any spot corresponding to Bis-AP-AF in the ***co***-PI[Bis-AP-AF/6FDA)$_{0.9}$ (Bis-AP-AF/MADA)$_{0.1}$]$_n$ Characterization product suggested the incorporation of all three components into the copolymer.

3.9.2 1-D ^{1}H NMR

Product structural confirmation was provided by ^{1}H NMR, shown in *Figure 3.17*. All observed peaks are consistent with the expected structure. Due to the fact that there are two phenol groups in every mer regardless of composition, this peak at 10.34 ppm (s; 2H) was chosen as the landmark for all integrations. The three aromatic protons of the 6FDA anhydride component are visible at 8.05 ppm (d; 1.8H), 7.85 ppm (d; 1.8H), and 7.64 ppm (s; 1.8H). Also visible are the three aromatic protons of the diamine component at 7.42 ppm (s; 2H), 7.13 ppm (m; 2.2H), and 6.99 ppm (d; 1.8H). The multiplet at 7.13 ppm is due to three overlapping doublets, the biggest of which is due to protons **GG** of the diamine, and is flanked on either side by smaller doublets. The downfield doublet is a shadow of protons **GG** of the diamine (**GG'**), while the upfield doublet (**FF'**) is a shadow of protons **FF** of the diamine. This was expected due to the different influence of neighboring MADA (0.1x) versus 6FDA (0.9x) residues. Also evident is the presence of NMP in the product by signals at 3.21 ppm (t), 2.60 ppm (s), 2.09 ppm (t), and 1.80 ppm (m).

^{1}H NMR (DMSO, ppm): δ= 10.34 (s; 2H), 8.05 (d; 1.8H), 7.85 (d; 1.8H), 7.64 (s; 1.8H), 7.42 (s; 2H), 7.13 (m; 2.2H), 6.99 (d; 1.8H).

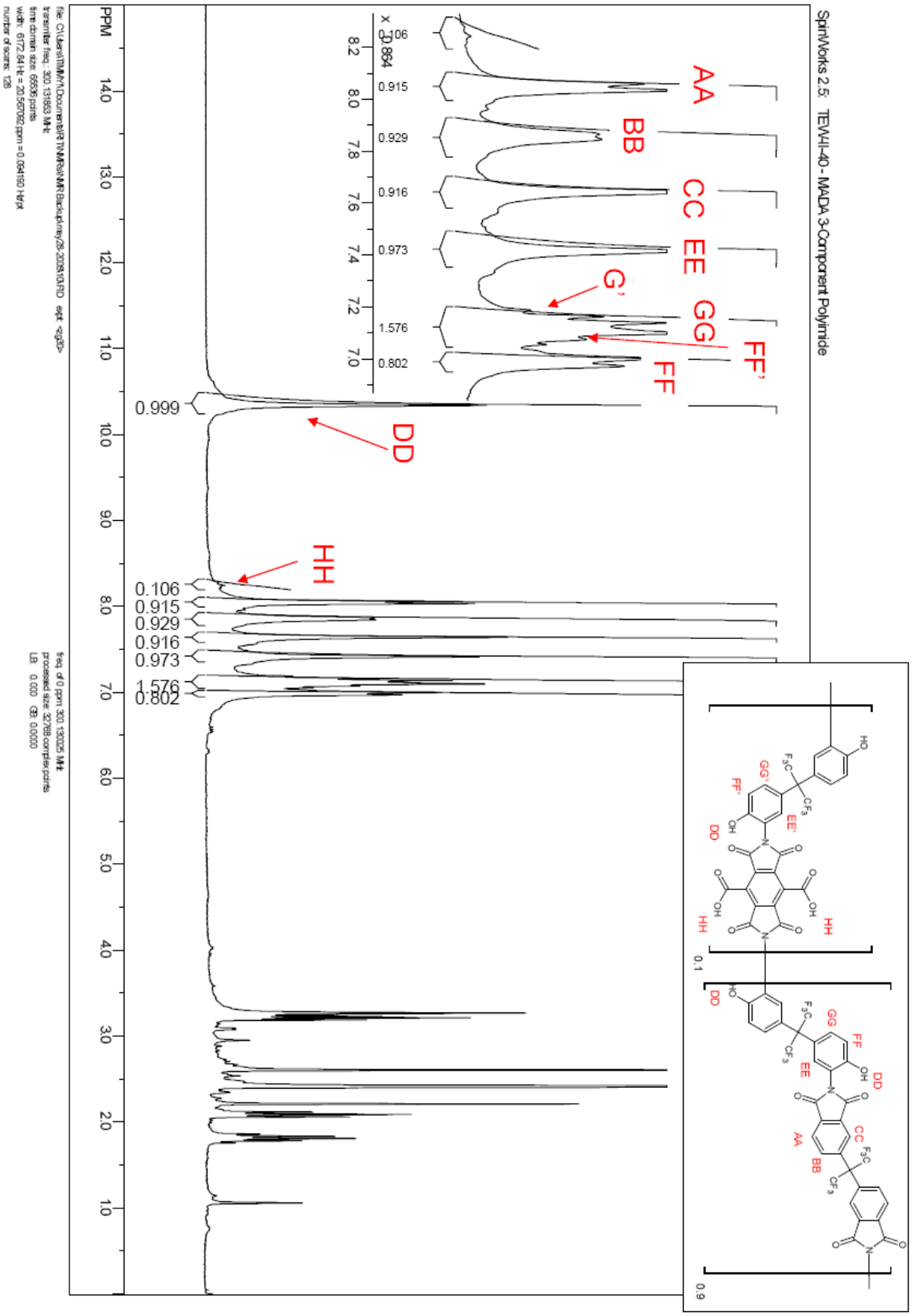

Figure 3.17 – 1-D ^{1}H NMR of co-PI[Bis-AP-AF/6FDA)$_{0.9}$ (Bis-AP-AF/MADA)$_{0.1}$]$_n$

3.9.3 2-D ^{1}H NMR

2-D ^{1}H NMR was performed to determine the assignments for the diamine multiplet and doublet, shown in *Figure 3.18*. The NMR experiment utilized is called 2-D cosy90sw, which applies two 90 degree pulses to a spin system and after Fourier transform gives proton assignments. Proton coupling is indicated by the three red squares. Coupling is seen with the downfield and upfield doublets which is part of the multiplet at 7.13 ppm. This coupling is consistent with the **GG'** and **FF'** assignments made in the 1-D ^{1}H NMR in *Figure 3.17*, suggesting that peaks **GG** and **FF** both have shadows.

3.9.4 FTIR

Structural verification of the co-PI[Bis-AP-AF/6FDA)$_{0.9}$ (Bis-AP-AF/MADA)$_{0.1}$]$_n$ was also provided through FTIR, shown in *Figure 3.19*. Imide peaks at 1786, 1724, 1375, and 723 cm^{-1} support the successful synthesis of the desired polyimide.[10,17] In addition, only a small peak is seen at 1653 cm^{-1}, (C=O stretch) corresponding the polyamic acid intermediate, signifying a high degree of imidization.[8] The presence of the phenol groups is demonstrated by a broad peak at 3500-3250 (O-H stretch), 1107 (C-OH stretch), and 642 cm^{-1} (OH out of plane deformation), as well as the presence of the carboxylic acid groups by peaks at 1693 (C=O stretch), and 623 cm^{-1} (O-C=O bend) for the MADA residues. Peaks corresponding to the hexafluoroisopropylidene groups are also present at 1205 and 1174 cm^{-1} (C-F stretch). Furthermore, there are no indications of anhydride peaks in the FTIR spectrum, indicating that no intra- or intermolecular anhydride formation took place during imidization.

3.9.5 TGA

The TGA thermogram of the co-PI[Bis-AP-AF/6FDA)$_{0.9}$ (Bis-AP-AF/MADA)$_{0.1}$]$_n$ is shown in *Figure 3.20*. The first weight loss that is evident occurs at just below 200 °C, most likely due to intra- or intermolecular anhydride formation and the evolution of occluded NMP.

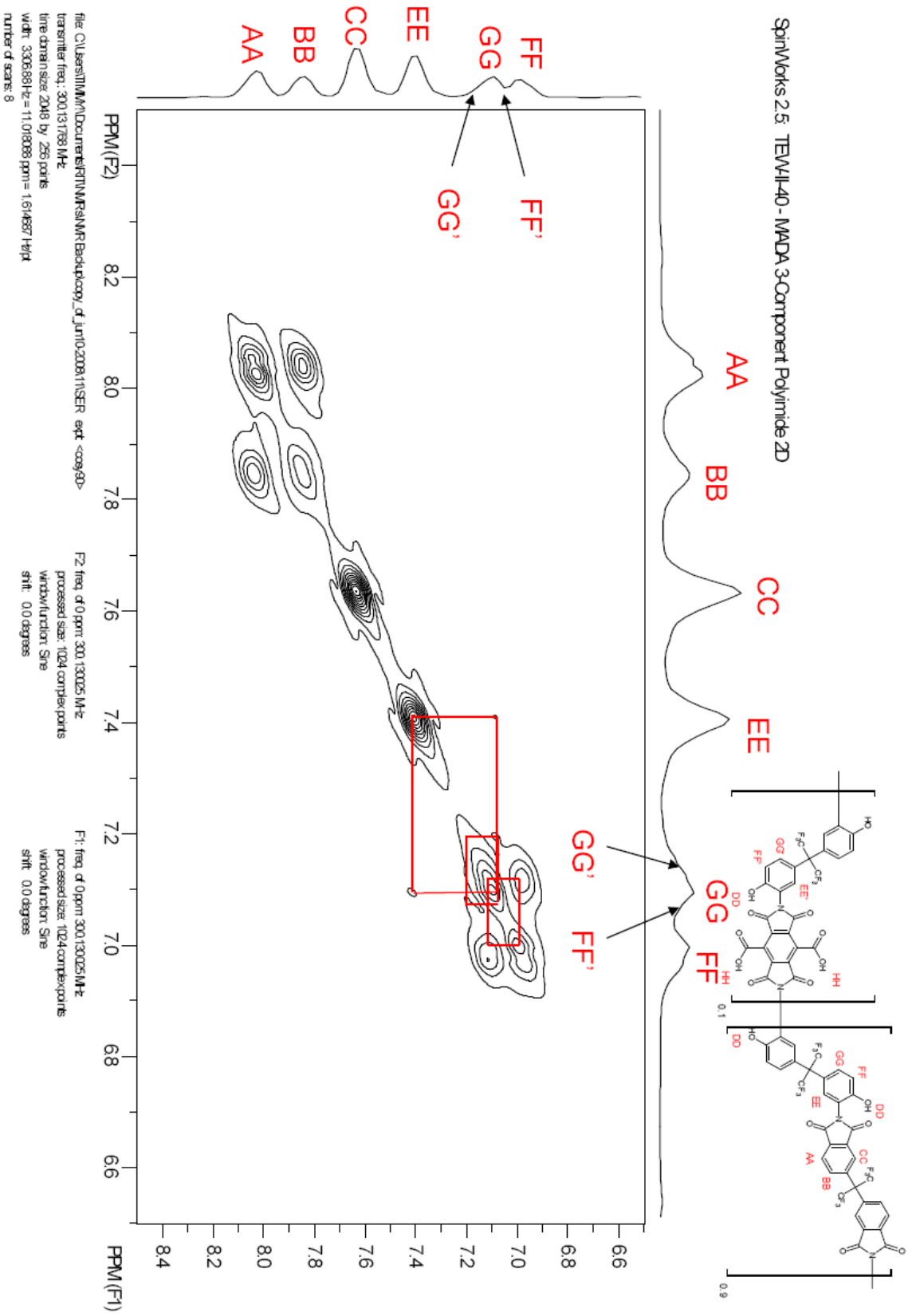

Figure 3.18 – co-PI[Bis-AP-AF/6FDA)$_{0.9}$ (Bis-AP-AF/MADA)$_{0.1}$]$_n$ 2-D ^{1}H NMR

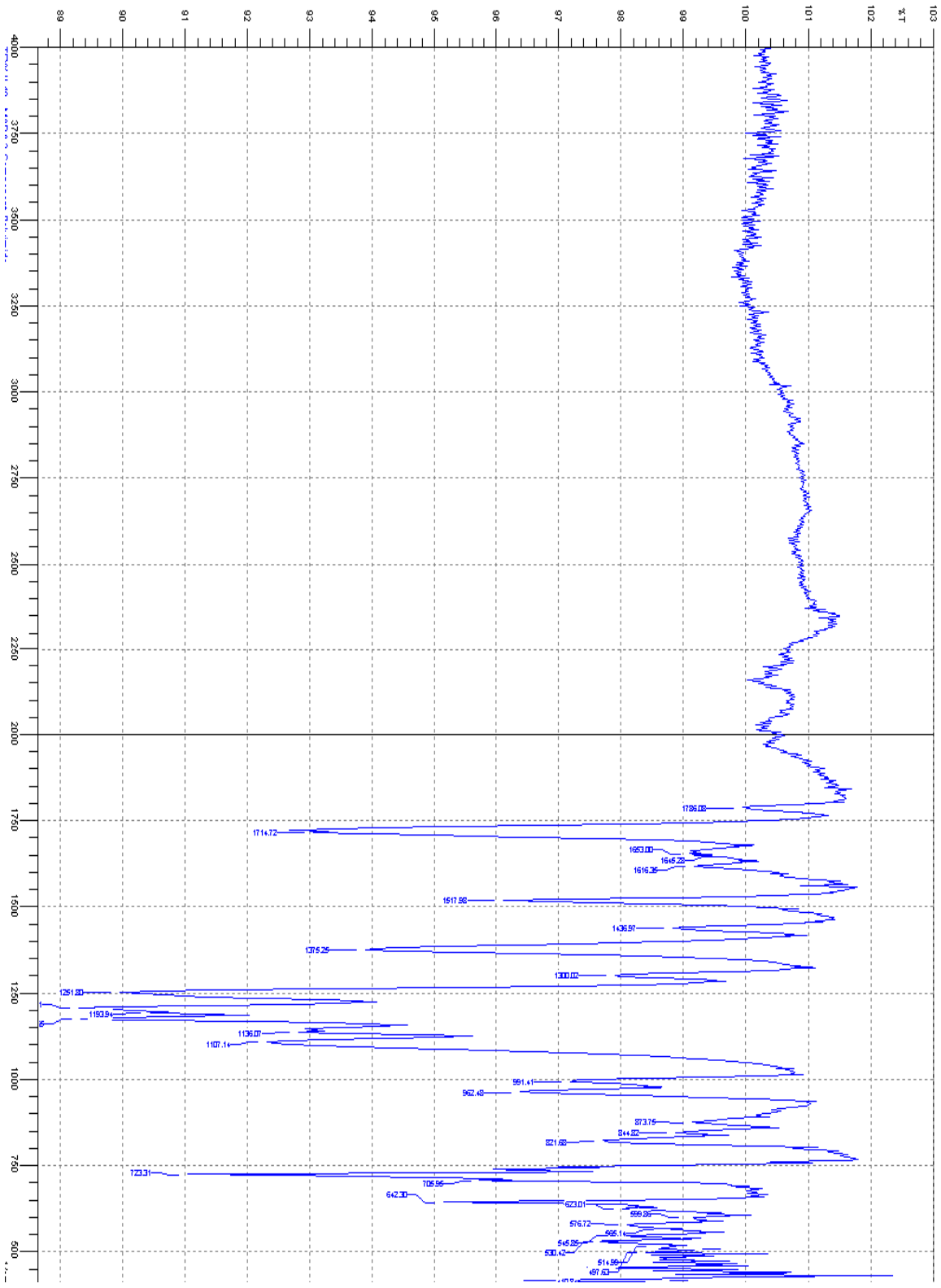

Figure 3.19 – FTIR of co-PI[Bis-AP-AF/6FDA)$_{0.9}$ (Bis-AP-AF/MADA)$_{0.1}$]$_n$

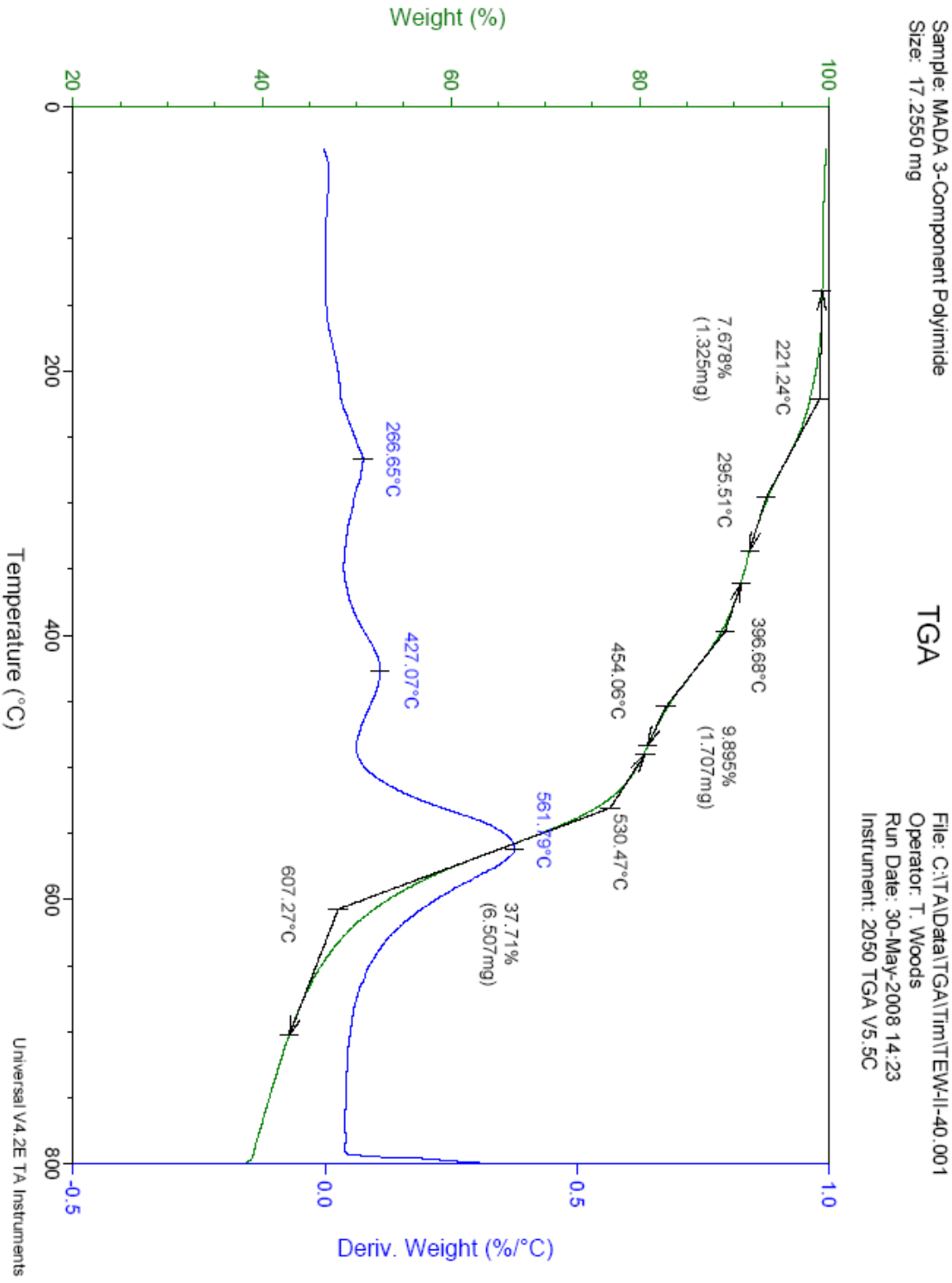

Figure 3.20 – TGA thermogram of co-PI[Bis-AP-AF/6FDA)$_{0.9}$ (Bis-AP-AF/MADA)$_{0.1}$]$_n$

The high decomposition temperature (396 °C) confirms the thermal stability that is displayed with most polyimides.[1]

3.9.6 Differential Thermal Analysis (DTA)

DTA was utilized to observe the glass transition (T_g) of the co-PI[Bis-AP-AF/6FDA)$_{0.9}$ (Bis-AP-AF/MADA)$_{0.1}$]$_n$. Due to the fact that no T_g was visible below 200°C, Differential Scanning Calorimetry (DSC) could not be utilized because of permissible equipment temperature ranges. The DTA thermogram in *Figure 3.21* shows a T_g at 265 ° C. It should be noted however that because the observed T_g is occurring during a significant weight loss event, a chemical change is occurring in addition to a kinetic change.

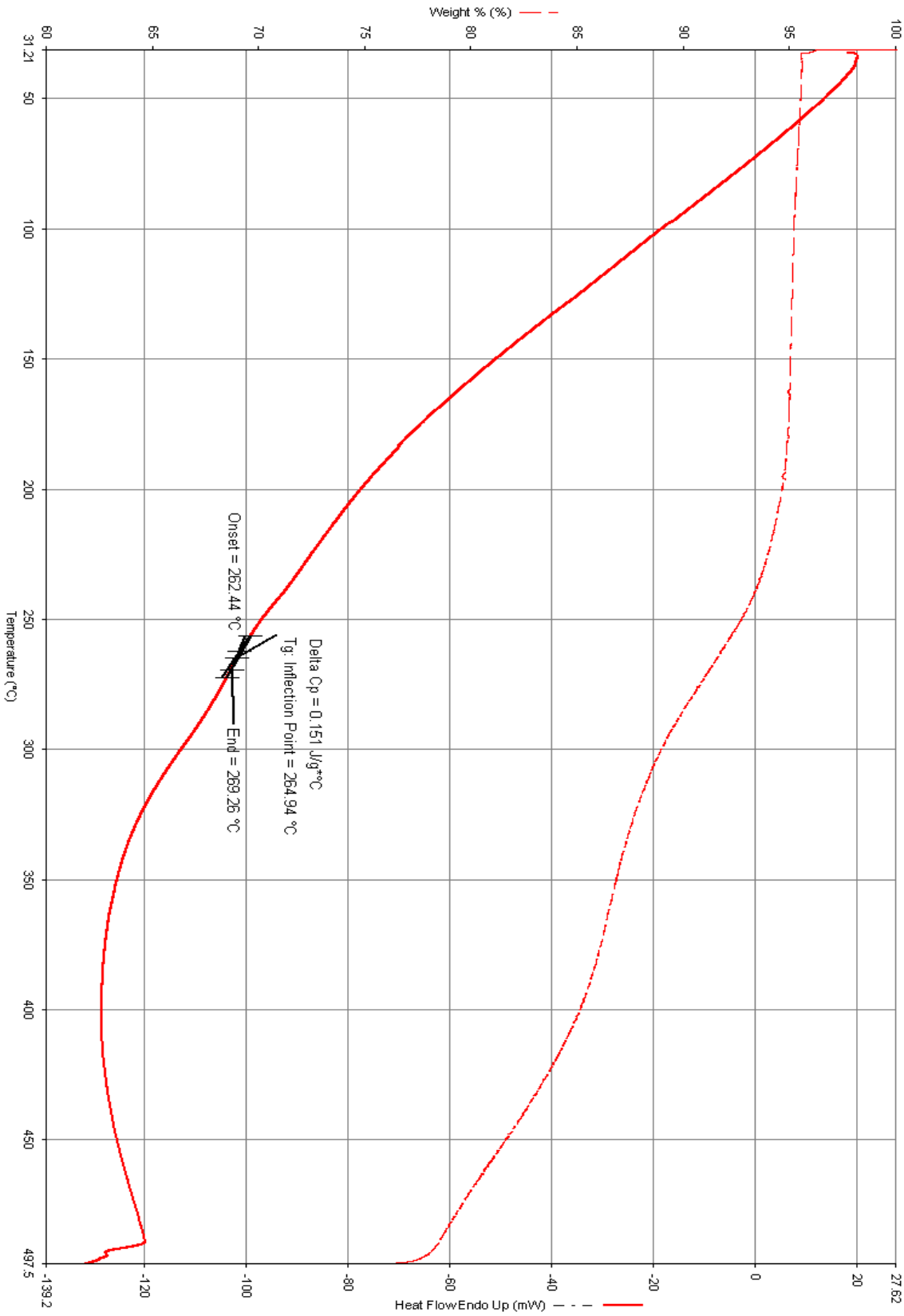

Figure 3.21 – DTA Thermogram of co-PI[Bis-AP-AF/6FDA)$_{0.9}$ (Bis-AP-AF/MADA)$_{0.1}$]$_n$

3.10 Characterization of co-PI[Bis-AP-AF/6FDA]$_{0.9}$ (Bis-AP-AF/MADA)$_{0.1}$]$_n$ w/ Methyl NLO and Ethyl NLO Surrogate Pendent Groups

3.10.1 Attachment of Methyl NLO Surrogate to co-PI[Bis-AP-AF/6FDA]$_{0.9}$ (Bis-AP-AF/MADA)$_{0.1}$]$_n$ at Ar-COOH of MADA Mer OR Ar-OH of Either Mer Characterization

3.10.1.1 TLC

TLC was performed on the pendent polyimide product in order to confirm attachment of the Methyl NLO Surrogate to the copolymer. Each of the three copolymer components was spotted adjacent to one another along with the Mitsunobu reagents: MADA (R_f = 0.00), Bis-AP-AF (green, R_f = 0.69), 6FDA (R_f = 0.00), $OPPh_3$ (R_f = 0.31), Methyl NLO Surrogate (purple, R_f = 0.73). The appearance of only one spot corresponding to the pendent polyimide product (v. light yellow, R_f = 0.05) and the absence of all Mitsunobu reagents confirmed the pendent attachment to the polyimide backbone.

3.10.1.2 1-D ^{1}H NMR

Structural verification of the single pendent polyimide product was provided through 1-D ^{1}H NMR in *Figure 3.22*. All polyimide signals seen previously in *Figure 3.17* remained unchanged. Pendent attachment is demonstrated by the appearance of four Methyl NLO Surrogate signals in the spectrum. Due to the copolymer composition (1 Bis-AP-AF-MADA : 9 Bis-AP-AF-6FDA), however, the location of the pendent attachment cannot be absolutely confirmed. However, a weakening of the phenol signal was observed consistent with pendent attachment taking place at this location. Two of the three aromatic proton signals are visible at 6.59 ppm (d; 2H) and 6.49 ppm (t; 1H), while the third signal is obscured by the aromatic proton signals on the polyimide backbone. Both sets of methylene protons are also visible at 3.95 ppm (t; 2H) and 3.45 ppm (t; 3H), although the upfield signal does not integrate for the expected value (which is 2H). The upfield signal integration is higher than expected due to its proximity to the DMSO peak at 3.26 ppm,. Lastly, the methyl protons of the Methyl NLO Surrogate are visible at 2.81 ppm (s; 2H) and integrate as expected. Also evident is the presence of the $OPPh_3$ byproduct.

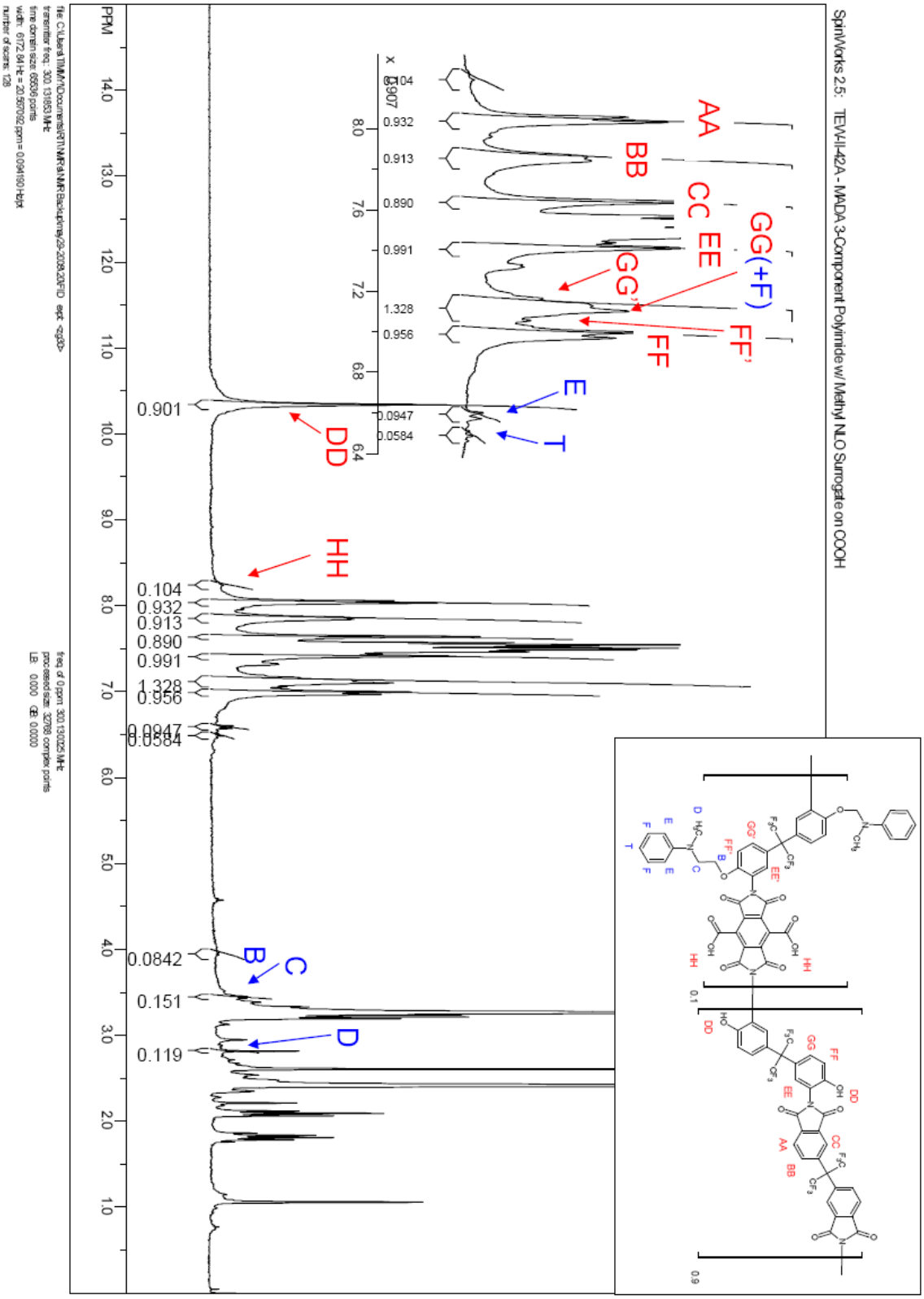

Figure 3.22 – 1-D ^{1}H NMR of co-PI[Bis-AP-AF/6FDA)$_{0.9}$ (Bis-AP-AF/MADA)$_{0.1}$]$_n$ with Methyl NLO Surrogate on Ar-OH

at 7.51(m) and NMP in the product by signals at 3.21 ppm (t), 2.60 ppm (s), 2.09 ppm (t), and 1.80 ppm (m).

^{1}H NMR (DMSO, ppm): δ= 10.34 (s; 1.8H), 8.05 (d; 1.8H), 7.85 (d; 1.8H), 7.64 (s; 1.8H), 7.42 (s; 2H), 7.13 (m; 2.2H), 6.99 (d; 1.8H), 6.59 (d; 2H), 6.49 (t; 1H), 3.95 (t; 2H), 3.45 (t; 3H), 2.81 (s; 3H)

3.10.1.3 FTIR

Pendent attachment was also confirmed by FTIR, shown in *Figure 3.23*. Pendent attachment to the polyimide backbone was confirmed by the appearance of a new signal at 540 cm^{-1} (C-N-C bending) previously seen with the first pendent attachment to the MADA Model Compound. The increase in intensity of the peak at 1139 cm^{-1} (C-C-N bending or C-O-C antisymmetric stretch) also implies pendent attachment, while suggesting the phenol groups as the possible location. The decrease in intensity of the signals attributed to the polyimide phenol groups at 3500-3250 (O-H stretch), 1109 (C-OH stretch) and 642 cm^{-1} (O-H out of plane deformation) also suggests that the pendent attachment took place at the phenol locations on either or both of the two different mers that comprise the copolymer.

3.10.2 Attachment of Ethyl NLO Surrogate to co-PI[Bis-AP-AF/6FDA)$_{0.9}$ (Bis-AP-AF/MADA)$_{0.1}$]$_n$ at Ar-OH Locations Characterization

3.10.2.1 TLC

TLC was performed on the pendent polyimide product in order to confirm attachment of the Ethyl NLO Surrogate to the polyimide. Each of the three copolymer components was spotted against one another along with the Mitsunobu reagents: MADA (R_f = 0.00), Bis-AP-AF (green, R_f = 0.69), 6FDA (R_f = 0.00), $OPPh_3$ (R_f = 0.31), Ethyl NLO Surrogate (green, R_f = 0.76). The appearance of one predominant spot corresponding to the pendent polyimide product (v. light yellow, R_f = 0.05) confirmed the pendent attachment to the polyimide backbone, along with small spots corresponding to the $OPPh_3$ and DEAD byproducts .

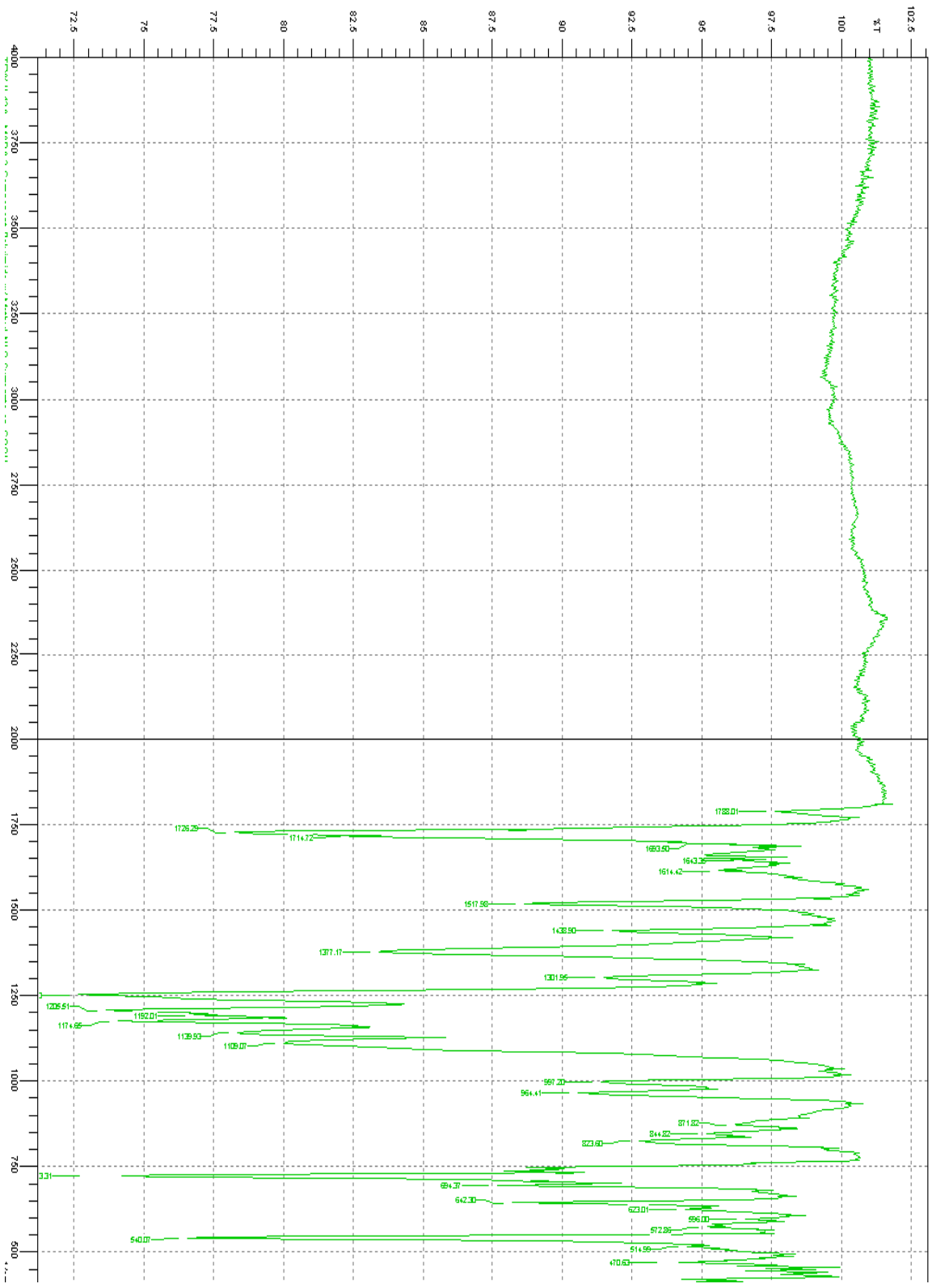

Figure 3.23 – FTIR of co-PI[Bis-AP-AF/6FDA)$_{0.9}$ (Bis-AP-AF/MADA)$_{0.1}$]$_n$ with Methyl NLO Surrogate on Ar-OH

3.10.2.2 1-D ^{1}H NMR

Structural verification of the dual pendent polyimide product was provided through 1-D ^{1}H NMR in *Figure 3.24*. One of the prime indicators of pendent attachment is the reduction in signal intensity of the phenol protons at 10.35 ppm (s; 0.5H). The integration implies that pendent attachment has taken place at roughly 63% of the phenol locations on both mers of the copolymer. The appearance of signals unique to the Ethyl NLO Surrogate in the NMR spectrum also supports pendent attachment. All three sets of aromatic protons are seen at 7.06 ppm (t; 2H), 6.43 ppm (d; 2H), and 6.27 ppm (t; 1H). All three sets of methylene protons are also seen at 4.02 ppm (m; 4H) and 3.43 ppm (t; 2H). Lastly, the methyl protons are seen at 0.97 ppm (t; 3H). The small signal at 4.60 ppm (s; 0.31H) corresponding to the alkyl OH on free Ethyl NLO Surrogate also confirms that most of the protons being seen can be attributed to pendents on the polyimide backbone. All polyimide signals remained unchanged except for one set of aromatic protons on the Bis-AP-AF portion of each mer (**FF)**, which were shifted from 6.99 to 6.77 ppm due to the attachment of the Ethyl NLO Pendent to the phenol locations. This mimics the same behavior seen with the pendent attachment to the phenol groups of 3,5-dihydroxybenzoic acid, where the aromatic proton that was *ortho* to each phenol group saw a significant shift when pendent attachment took place. A similar upfield chemical shift was also observed with the (2-AP)$_2$MADA Diimide aromatic protons that were *ortho- para* to the phenol when pendent attachment occurred. One important change from the previous two polyimides is the lack of NMP signals in the NMR spectrum, due to trituration of the dual pendent polyimide in chilled pentanes after isolation and vacuum oven drying. Still evident is the presence of the $OPPh_3$ byproduct at 7.51(m) and a small amount of unreacted PPh_3 at 7.00 ppm (m).

^{1}H NMR (DMSO, ppm): δ= 10.35 (s; 0.5H), 8.05 (d; 1.8H), 7.85 (d; 1.8H), 7.62 (s), 7.42 (s), 7.22 (m; 2.2H), 7.06 (t; 2H), 6.77 (d; 2H), 6.55 (m; 3H), 6.43 (d; 2H), 6.28 (t; 1H), 4.03 (m; 5H) 3.44 (t; 2H), 2.82 (s; 3H), 0.97 (t; 3H).

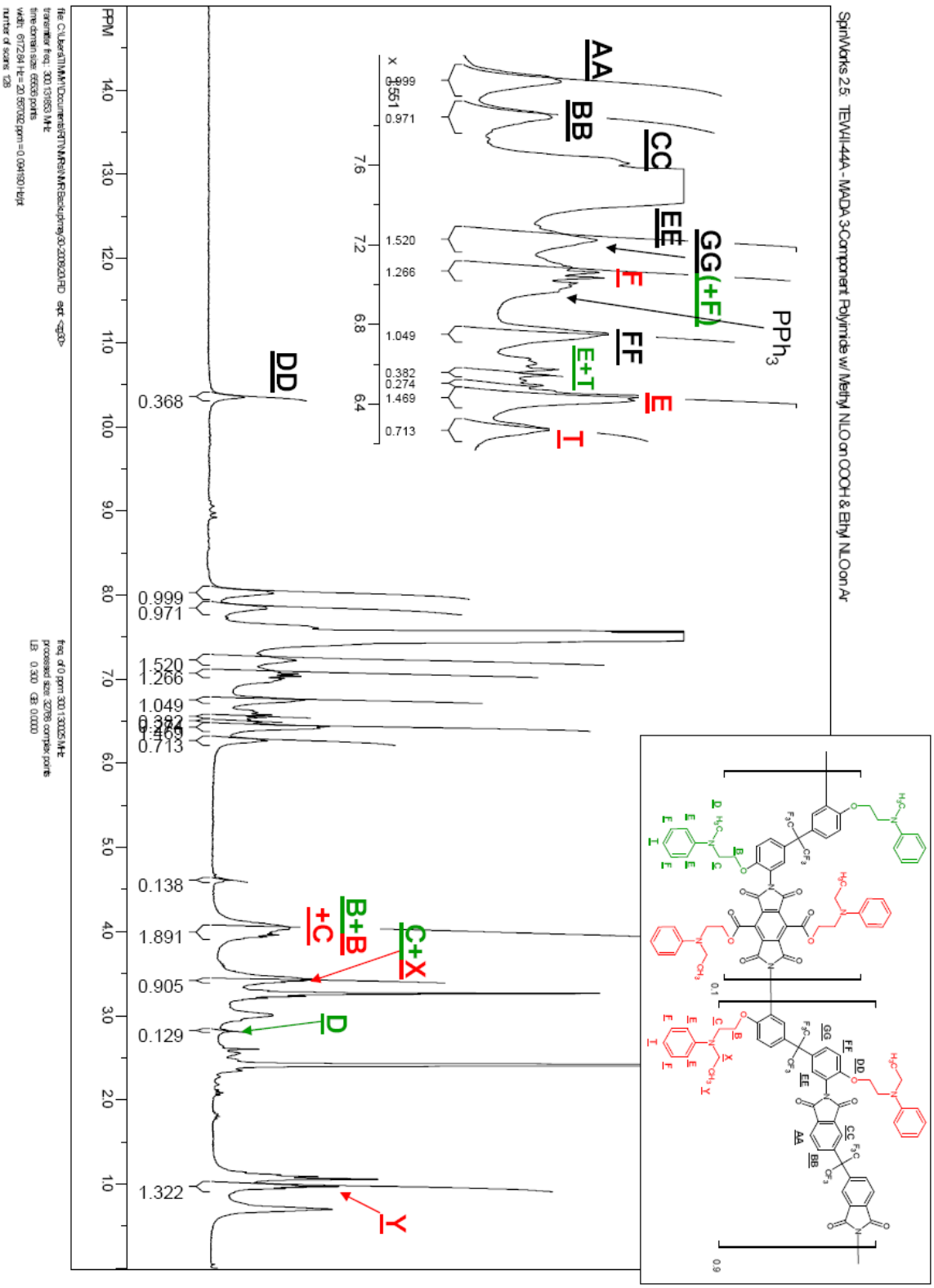

Figure 3.24 – 1-D ^{1}H NMR of co-PI[Bis-AP-AF/6FDA)$_{0.9}$ (Bis-AP-AF/MADA)$_{0.1}$]$_n$ with Methyl NLO Surrogate on MADA Mer and Ethyl NLO Surrogate on Both Mers

3.10.2.3 FTIR

Pendent attachment was also confirmed by FTIR, shown in *Figure 3.25.* Pendent attachment to the polyimide backbone was confirmed by the increase in intensity of the peak at 540 cm^{-1} (C-N-C bending) previously seen with the pendent attachment to the MADA Model Compound. The increase in intensity of the peak at 1116 cm^{-1} (C-C-N bending or C-O-C antisymmetric stretch) also implies pendent attachment, while suggesting the phenol groups as the possible location. New signals at 2968 (CH_2 antisymmetric and symmetric stretching), 1597 (Ethyl NLO Surrogate ring stretch), and 746 and 692 cm^{-1} (monosubstituted benzenes CH out of plane deformation – 2 bands) all correspond to attachment of the Ethyl NLO Surrogate to the polyimide backbone. The decrease in intensity of the signals attributed to the polyimide phenol groups at 1109 (C-OH stretch) and 640 cm^{-1} (O-H out of plane deformation) also suggests that the pendent attachment took place at the phenol locations on either or both of the two different mers that comprise the copolymer. Lastly, the disappearance of the peak at 1653 cm^{-1} (C=O) attributed to the polyamic acid intermediate seen with the last two polyimides, suggests that the Mitsunobu reaction could have caused further imidization of any remaining PAA.

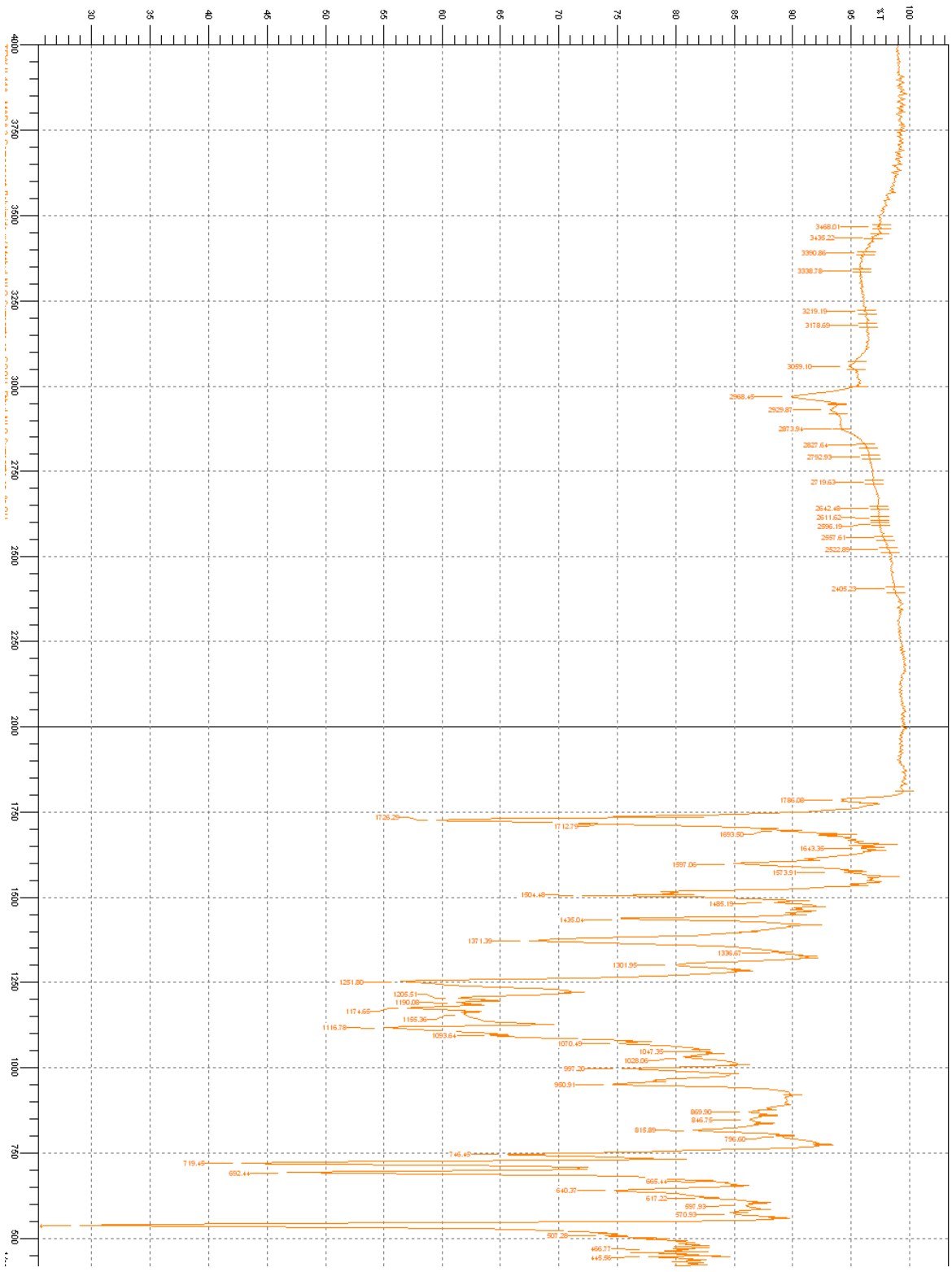

Figure 3.25 – FTIR of co-PI[Bis-AP-AF/6FDA)$_{0.9}$ (Bis-AP-AF/MADA)$_{0.1}$]$_n$ with Methyl NLO Surrogate on MADA Mer and Ethyl NLO Surrogate on Both Mers

3.11 Spectral Assignments

To facilitate in the comparison of spectral data, see *Tables 3.1* and *3.2*.

Table 3.1 – Summary of FTIR Assignments (cm^{-1})

FTIR Stretch/Bend	MADA	$(2\text{-}AP)_2$ MADA Diimide	Simplified Model Compound	$(2\text{-}AP)_2$MADA Diimide w/ Methyl NLO Surrogate	Polyimide	Polyimide w/ Methyl NLO on Ar-OH (Either Mer)	Polyimide w/ Both NLO Pendents
O-H (Carboxylic Acid)	3350 (w)	-	-	-	-	-	
O-H (Phenol)	-	3323 (m, br)	3377 (m, br)	-	3500-3250 (w, br)	3500-3250 (w, br)	-
NH^{4+} (Zwitterion)	-	3060 (w, br)	-	3061 (w, br)	3060 (w, br)	-	-
CH_2 (Methylene, NLO)	-	-	-	-	-	-	2968 (w)
C=O (Anhydride)	1870 (m)	-	-	-	-	-	-
C=O (Anhydride)	1800 (s)	-	-	-	-	-	-
C=O (Imide)	-	1776 (s)	1786 (s)	1778 (w)	1786 (w)	1788 (w)	1786 (w)
C=O (Imide)	-	1724 (s)	1721 (s)	1720 (s)	1724 (s)	1726 (s)	1726 (s)
C=O (Carbonyl)	-	1693 (sh)	1681 (sh)	-	1693 (sh)	1693 (sh)	1693 (sh)
C=O (PAA)	-	-	-	-	1653 (w)	1653 (w)	-
C-H ring stretch (NLO)	-	-	-	-	-	-	1597 (m)
C-N (Imide)	-	1377 (s)	1388 (s)	1375 (s)	1375 (s)	1377 (s)	1371 (s)
C-O-C (Ether, NLO)	-	-	-	1244 (m)	-	-	-
C-O-C (Anhydride)	1211 (s)	-	-	-	-	-	-
C-F (CF_3)	-	-	-	-	1205 (s)	1205 (s)	1205 (s)
	-	-	-	-	1174 (s)	1174 (s)	1174 (s)
C-O-C (Ether, NLO)	-	-	-	1118 (s)	-	1139 (s)	1116 (s)
C-OH (Phenol)	-	1095 (s)	1099 (s)	-	1107 (s)	1109 (s)	1109 (w)
C-H ring bend (Imide)	-	727 (s)	720 (s)	721 (s)	723 (s)	723 (s)	719 (s)
C-H Out of Plane Def. (Monosub. Benzene)	-	-	-	745 (s)	-	-	746 (m)
	-	-	-	692 (s)	-	-	692 (s)
O-H Out of Plane Deformation (phenol)	-	717 (m)	638 (m)	-	642 (m)	642 (m)	640 (w)
O-C=O (Carboxylic Acid)	682 (m)	623 (m)	-	623 (m)	623 (w)	623 (w)	-
C-N-C (Amine, NLO)	-	-	-	540 (s)	-	540 (s)	540 (vs)

Key: s = strong; m = medium; w = weak; v = very; br = broad; sh = shoulder.

Table 3.2 – Summary of Proton NMR Assignments (ppm)

Proton	Letter	Synthesized NLO	$(2\text{-AP})_2$ MADA Diimide	Simplified Model Cmpd	Simplified Model Cmpd w/ Methyl NLO	3,5-Dihydroxybenzoic Acid Single Pendent	3,5-Dihydroxybenzoic Acid Dual Pendent	$(2\text{-AP})_2$ MADA Diimide Single Pendent	$(2\text{-AP})_2$ MADA Diimide Dual Pendent	Polyimide	Single Pendent Polyimide	Dual Pendent Polyimide
Carboxylic Acid	**Q**	-	8.32	-	-	-	-	8.13	8.13	-	-	-
	HH	-	-	-	-	-	-	-	-	8.24	8.24	-
Phenol	**L**	-	9.88	9.76	9.76	-	-	-	-	-	-	-
	U	-	-	-	-	9.59	-	-	-	-	-	-
	DD	-	-	-	-	-	-	-	-	10.34	10.34	10.35
Imide	**M**	-	6.90	6.85	6.84	-	-	6.44	6.44	-	-	-
	N	-	7.26	7.21	7.20	-	-	7.06	7.18	-	-	-
	O	-	6.90	6.85	6.84	-	-	6.44	6.44	-	-	-
	P	-	7.26	7.21	7.20	-	-	7.06	7.18	-	-	-
	AA	-	-	-	-	-	-	-	-	8.05	8.05	8.05
	BB	-	-	-	-	-	-	-	-	7.85	7.85	7.85
	CC	-	-	-	-	-	-	-	-	7.64	7.64	7.62
	EE	-	-	-	-	-	-	-	-	7.42	7.42	7.42
	FF	-	-	-	-	-	-	-	-	6.99	6.99	6.77
	FF'	-	-	-	-	-	-	-	-	7.13	7.13	-
	GG	-	-	-	-	-	-	-	-	7.13	7.13	7.22
	GG'	-	-	-	-	-	-	-	-	7.13	7.13	-
Olefin	**G**	6.85	-	-	-	-	-	-	-	-	-	-
	H	7.03	-	-	-	-	-	-	-	-	-	-
Aromatic	**E**(*Me*)	6.74	-	-	6.46	6.67	6.62	7.18	6.57	-	6.59	6.55
	E(*Et*)	-	-	-	-	-	6.62	-	6.72	-	-	6.43
	F(*Me*)	7.30	-	-	6.46	7.16	7.17	6.82	6.81	-	7.13	7.22
	F(*Et*)	-	-	-	-	-	7.17	-	7.12	-	-	7.06
	I	6.95	-	-	-	-	-	-	-	-	-	-
	J	6.95	-	-	-	-	-	-	-	-	-	-
	K	7.05	-	-	-	-	-	-	-	-	-	-
	R	-	-	7.85	7.84	-	-	-	-	-	-	-
	S	-	-	7.85	7.84	-	-	-	-	-	-	-
	T(*Me*)	-	-	-	6.46	6.53	6.49	6.34	6.29	-	6.49	6.55
	T(*Et*)	-	-	-	-	-	6.49	-	6.29	-	-	6.28
	V	-	-	-	-	6.37	6.89	-	-	-	-	-
	W	-	-	-	-	6.73	6.82, 6.80	-	-	-	-	-
Methylene	**B**(*Me*)	3.81	-	-	3.52	4.26	3.97	4.08	4.00	-	3.95	4.03
	B(*Et*)	-	-	-	-	-	3.97	-	4.00	-	-	4.03
	C(*Me*)	3.45	-	-	3.34	3.61	3.59	3.49	3.43	-	3.45	3.44
	C(*Et*)	-	-	-	-	-	3.97	-	4.00	-	-	4.03
	X	-	-	-	-	-	3.97	-	3.43	-	-	3.44
Methyl	**D**	2.94	-	-	3.19	2.88	2.61	2.65, 2.57	2.81	-	2.81	2.82
Ethyl	**Y**	-	-	-	-	-	1.00	-	0.97	-	-	0.97
Alcohol	**A**	1.65	-	-	-	-	-	-	-	-	-	-

Key: *Me* = Methyl NLO Surrogate; *Et* = Ethyl NLO Surrogate

4. DISCUSSION

4.1 Mellitic Acid Dianhydride - MADA

MADA was synthesized to serve as one of the three components in the polyimide due to its unique dianhydride structure with two carboxylic acid groups per molecule. Because the other two polymer components have phenol groups, selective pendent attachment could take place due to the difference in reactivity of the respective groups. MADA is synthesized through careful heating at 190-195 °C, in which mellitic acid goes to dianhydride, yielding two isomers shown in *Figure 4.1*.

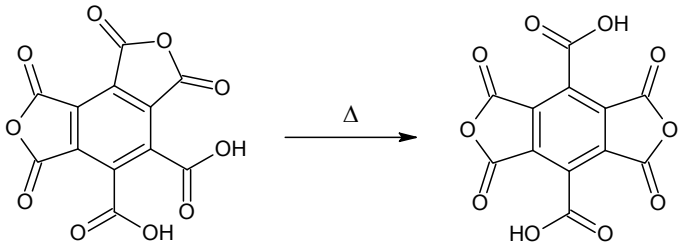

Figure 4.1 – MADA Isomers Resulting from Cyclodehydration of Mellitic Acid

It has been previously established that the initially formed 1,2,3,4-MADA isomerizes to the more stable 1,2,4,5-MADA which has *para* carboxylic acid groups.[17] Mellitic acid monoanhydride (MAMA) and trianhydride (MATA) are both potential results of insufficient heating or overheating, respectively. MAMA would be insufficient as a polyimide building block because polyimide formation could only take place at the one anhydride, resulting in early chain termination and low molecular weight. MATA would make a linear polymer structure impossible. When pure MADA is formed, the lowest temperature weight loss seen with mellitic acid completely disappears from its TGA thermogram, and the remaining weight loss corresponds to 5.88% of the sample mass. The absence of the first weight loss seen with mellitic acid indicates that all MAMA has been converted to MADA, and a weight loss corresponding to ~5.9% indicates that one molecule of H_2O is lost per MADA and that no MATA was present, as shown in *Figures 3.1 & 3.2*.[17]

4.2 UV-Crosslinker

It was the original objective to synthesize the UV-Crosslinker to attach to the carboxylic acid groups on the MADA mers of the 3-Component Polyimide in order to provide crosslinking on both sides of each polymer chain. This approach was meant to immobilize the polyimide chains and NLO-phores by exposure to UV light once the NLO pendents were attached to the phenol groups on both polyimide mers and poling had taken place. The dual crosslinking approach not previously seen in the literature would retain NLO orientation over an extended operational lifetime of the NLO pendent polyimide.

While the original synthesis of the UV-Crosslinker was taken from the literature, no isolation or characterization information was provided.[20] Duplication of the original synthetic procedure resulted in a mix of starting material and product, most likely due to the catalytic amount of potassium iodide (KI) used. Although longer reaction times and KOEt were used, no significant increase in product was observed. It was later discovered that KI catalyzes the S_N2 reaction by first replacing the chlorine on the alkyl halide, which then undergoes the S_N2 reaction with 4-hydroxychalcone. The reaction is catalyzed due to the fact that iodide is a more reactive halide than chlorine, thus more readily undergoing the desired S_N2 reaction. This is outlined in *Figure 4.2*.

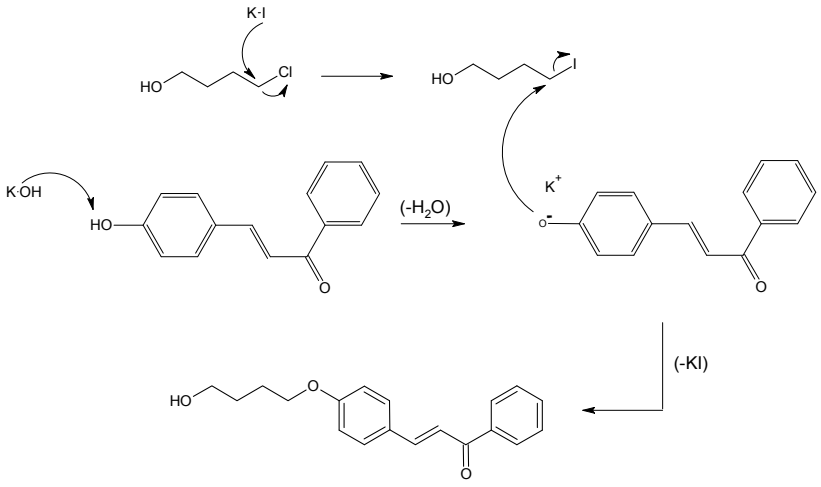

Figure 4.2 – UV-Crosslinker Synthesis Mechanism

Once the amount of KI was increased, a significantly larger product spot was observed via TLC relative to the other spots, both with 4-chloro-1-butanol and 2-chloroethanol. The appearance of a third spot was noted with both alkyl halides however that did not correspond to either starting material or the desired product. A side reaction is made possible by two factors: the resonance stabilization seen with deprotonated 4-hydroxychalcone making it less reactive than a non-resonance stabilized nucleophile, and the prospect of THF and epoxide formation. For this reason, 6-chlorohexanol was then selected as the alkyl halide since any intramolecular ring closing would result in a less favored 7-membered ring. Subsequent work carried out by L. Hawver has shown a larger product formation relative to the other spots in the TLC and no indication of a third spot corresponding to any side product. Further experimentation, however, is required at this time.[21]

4.3 2-[N-methyl-N-[4-[2-(2-thien)ethenyl]phenyl]amino]ethanol (NLO Pendent)

The NLO pendent chosen for this research was found in a study of properties of chiral helical chromophore-functionalized polybinapthalenes.[22] Synthesis was carried out by reacting 2-thiophenylmethanol with triphenylphosphine hydrobromide to yield the protonated ylide, which was then used in a Wittig Olefination with N-methyl-N-(2-hydroxyethyl)-4-aminobenzaldehyde to yield the desired NLO pendent. This is shown in *Figure 4.3*.

Successful isolation of the *trans*-NLO product by column chromatography and subsequent recrystallization from hot toluene was confirmed by melting point, TLC, and NMR. These results were compared to the published literature results [22] and also those of two former undergraduate research students (Brad Loesch and Robert Pasquarelli) and found to be in good agreement. The use of the Methyl and Ethyl NLO Surrogates gives simpler spectra compared to that of the NLO-phore, so the latter hasn't been used yet.

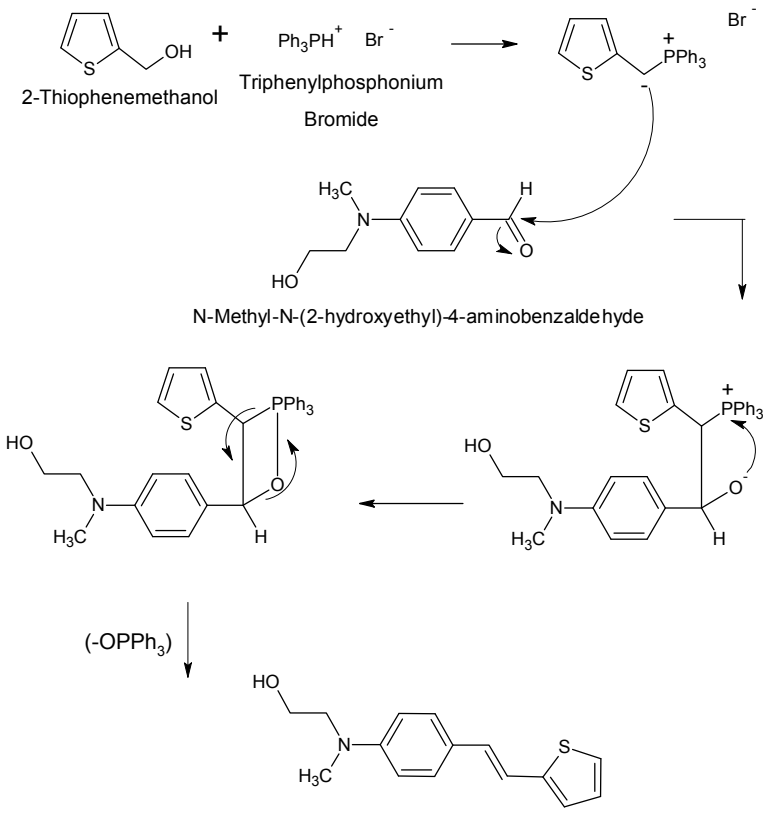

Figure 4.3 – NLO Pendent Synthesis Mechanism
(All Arrows are Double Headed)

4.4 (2-AP)$_2$MADA Diimide

The (2-AP)$_2$MADA diimide was originally designed to establish the degree of selectivity shown for pendent attachment at specific functional groups, in this case a carboxylic acid versus a phenol. Its structure is a simplification of the MADA mers in the 3-Component Polyimide and was meant to provide a simplified system to examine where pendent attachment was taking place. Previous research by R. Pasquarelli had identified DMAc and NMP as the two best solvents to carry out the imidization, due to their polar nature which allowed for good solubility, and their high boiling points which were in the temperature range that imidization occurred in.

Both NMP and DMAc were used for (2-AP)$_2$MADA diimide synthesis and yielded identical results. TLC showed that NMP yielded the imide product slightly faster than DMAc due to the higher imidization temperature. Both NMR and FTIR results indicated successful synthesis

of the (2-AP)$_2$MADA diimide and that complete imidization had taken place, leaving no polyamic acid intermediate and no intermolecular anhydride formation. The aromatic protons *ortho* and *para* to the imide were assigned as the downfield set, due to the electron withdrawing nature of the imide, while the *meta* protons were assigned as the upfield set. Product isolation from NMP followed the method described in two different articles that dealt with polyimide synthesis and isolation from NMP.[6,7] After isolation and vacuum oven drying, no NMP peaks were observed in the NMR, indicating successful removal. Product isolation in DMAc was possible with rotaryevaporation and recrystallization, due to the lower boiling point of DMAc. NMR also indicated that no residual DMAc was observed in the final product.

NMR indicated, however, that the carboxylic acid protons signals had shifted upfield and were now present at either 9.88 ppm or 8.32 ppm, in proximity to the proton signals from each phenol group. Assignment of these two peaks to either functional group was hindered by the fact that each group showed identical splitting and was present in the same ratio, meaning both peaks integrated for two protons each. This shift is most likely due to strong hydrogen bonding or the presence of a zwitterion, shown in *Figure 4.4*.

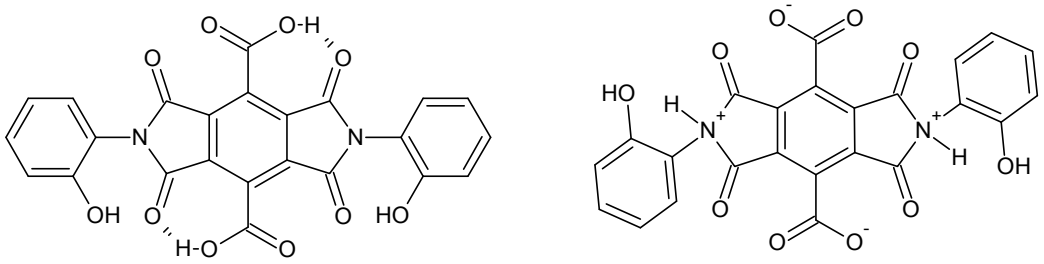

Figure 4.4 – (2-AP)$_2$MADA Diimide in its Nominal H-Bonded (a) and Zwitterionic (b) Form

There is significant evidence for this hypothesis in the literature which helps to explain this occurrence. Similar behavior is observed with most amino acids, where the carboxylic acid proton resides on the amine in favored conditions.[25] Several articles investigating guanidiniocarbonyl pyrrole carboxylate zwitterions cite polar solvents as being a driving force

behind formation.[26,27] Both imidization solvents used are highly polar, possibly promoting the zwitterionic form of the $(2\text{-AP})_2$MADA diimide. The electron pair on the imide nitrogen coupled with the acidity of the carboxylic acid protons (pKa ≈ 11.1[28]) favor the formation of the zwitterion. NMR chemical shift data presented in both articles (also in d^6- DMSO) support the singlet seen at 8.32 ppm as being consistent with a strongly hydrogen bonded or zwitterionic proton; this is also supported by pendent attachment to the $(2\text{-AP})_2$MADA diimide, discussed in section *4.6*.

4.5 Simplified Model Compound

Due to the initial difficulty in synthesizing large amounts of MADA for Model Compound synthesis, the Simplified Model Compound was designed in order to evaluate pendent attachment using the Mitsunobu reaction. Synthesis was identical to that of the $(2\text{-AP})_2$MADA diimide, only phthalic anhydride (commercially available) was used instead of MADA. All results including NMR, FTIR, and MS indicated successful synthesis. Incomplete removal of water could have resulted in some residual PAA in equilibrium with the imide, resulting in an amic acid C=O stretch at 1681 cm^{-1}. As with the $(2\text{-AP})_2$MADA diimide, the aromatic protons *ortho* and *para* to the imide were assigned to the downfield multiplet in the NMR spectrum, and the *meta* protons were assigned to the upfield multiplet. The phenol protons showed an expected chemical shift of 9.76 ppm, consistent with the phenol protons being at 9.88 ppm in the $(2\text{-AP})_2$MADA diimide.

4.6 Pendent Attachment to Model Compounds

The Mitsunobu reaction was chosen as the method of pendent attachment due to the selectivity it showed in being able to perform attachment at a carboxylic acid over a phenol, shown in section *3.7*. This selectivity was important because it meant that selective pendent attachment should be possible with the incorporation of these functional groups into a model compound system and the 3-Component Polyimide. This reaction involves the conversion of an

alcohol (in this case the alcohol of one of the NLO Surrogates) into a good leaving group, which is then displaced by a nucleophile, in this case the oxygen of a carboxylate ion. The product of this reaction is an ester or ether, depending on whether a carboxylate or phenol serves as the nucleophile.[29] This is shown in *Figure 4.5*.

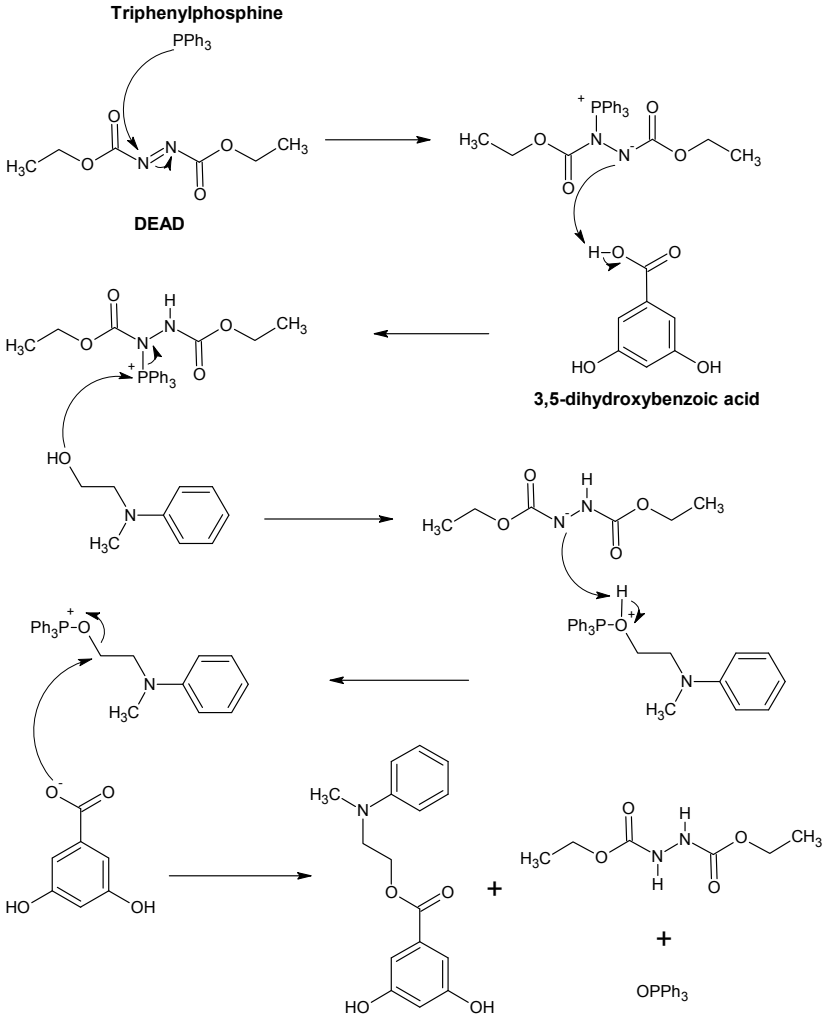

Figure 4.5 – Mitsunobu Reaction Mechanism w/ 3,5-Dihydroxybenzoic Acid & Methyl NLO Surrogate (All Arrows are Double Headed)

4.6.1 Pendent Attachment to Simplified Model Compound

The Mitsunobu reaction was first attempted using the Simplified Model Compound and the Methyl NLO Surrogate in order to evaluate optimal reaction conditions. Although some pendent attachment took place, a significant amount of starting material remained when using a

stoichiometric amount of DEAD that was over a year old – hence stressing the importance of using fresh DEAD. This was also the only reaction product that was isolated with some success using column chromatography as a means to remove the Mitsunobu byproducts, "spent" DEAD and $OPPh_3$. Although the $OPPh_3$ impurity was successfully removed, "spent" DEAD still remained, as shown in section *3.6.2*.

4.6.2 Pendent Attachment to 3,5-Dihydroxybenzoic Acid

Pendent attachment was next attempted using 3,5-Dihydroxybenzoic acid in order to elucidate functional group selectivity in a nominal environment. Complete Methyl NLO Surrogate attachment at the carboxylic acid was confirmed though NMR using a stoichiometric amount of fresh DEAD, shown in *Figure 4*.6 and section *3.7.1.2*. The consistency of the **W** and **V** chemical shifts indicate that no pendent attachment occurred at the phenols, meaning that in a non H-bonded environment this process was completely selective. This is explained based on the pKa difference between a carboxylic acid ($pKa \approx 11.1$[28]) and a phenol ($pKa \approx 18.0$[28]) in DMSO, making the carboxylic acid the more reactive nucleophile. Product isolation was achieved through blending with H_2O which successfully removed the "spent" DEAD, but failed to remove the $OPPh_3$ byproduct.

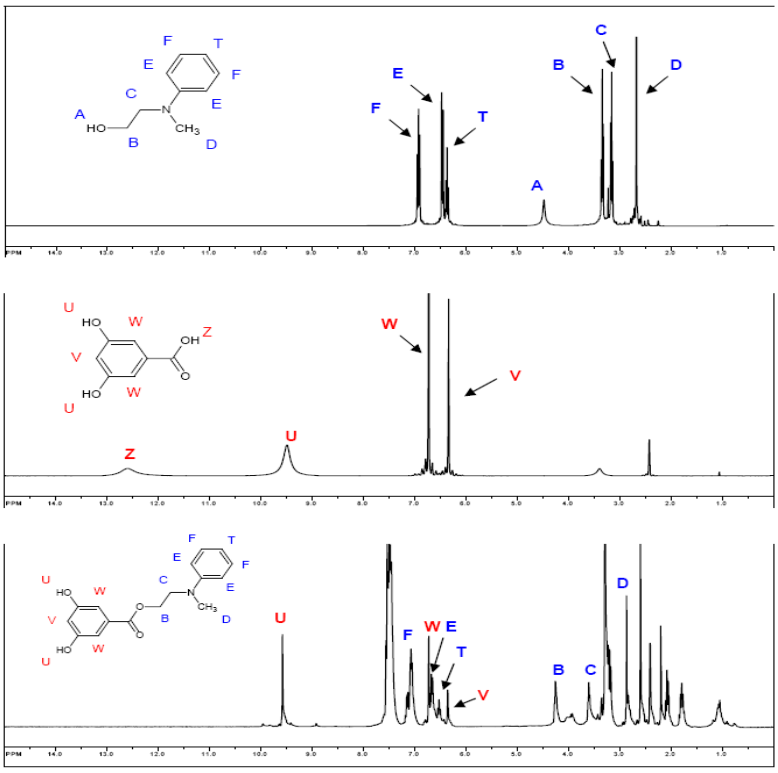

Figure 4.6 – 3,5-Dihydroxybenzoic Acid Methyl NLO Surrogate Attachment ^{1}H NMR Overlay: Methyl NLO Surrogate (top), 3,5-Dihydroxybenzoic Acid (middle), and Pendent Product (bottom).

Pendent attachment at the phenol locations was then attempted using the Ethyl NLO Surrogate and a slight excess of DEAD. TLC indicated both longer reaction times and the need for an excess of DEAD in order to achieve pendent attachment, presumably due to the difference in pKa of the functional groups. Since this was a one pot reaction, however, the effect of Mitsunobu byproducts on the rate of reaction of new pendent attachment is not known. NMR indicated a high degree of pendent attachment at the phenol locations, shown in *Figure 4.7* and in section *3.7.2.2*. Due to the fact that this model compound system was being used primarily for elucidating functional group selectivity, no further attempt was made to remove the $OPPh_3$ impurity.

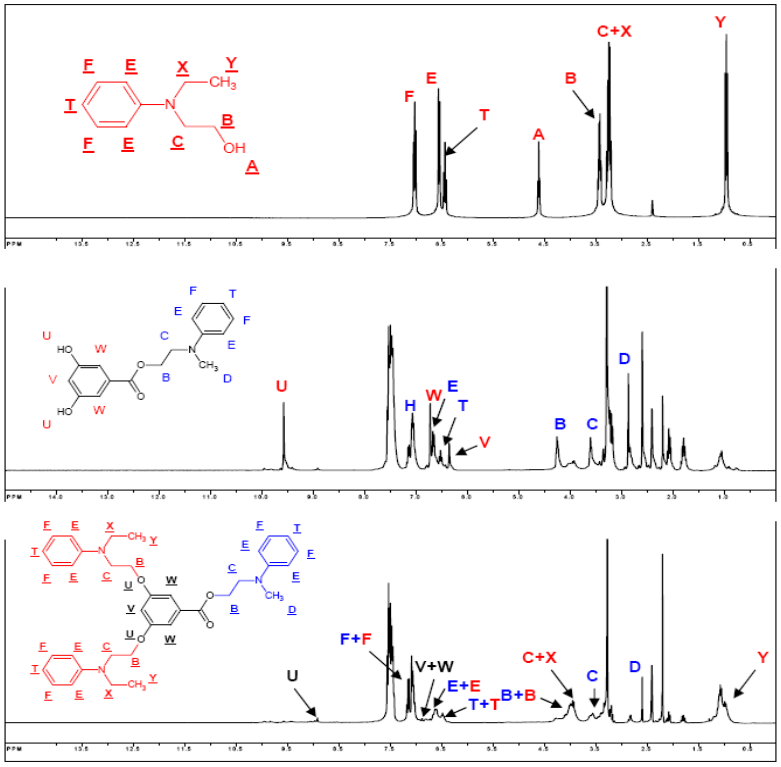

Figure 4.7 – 3,5-Dihydroxybenzoic Acid Ethyl NLO Surrogate Attachment ^{1}H NMR Overlay: Ethyl NLO Surrogate (top), Single Pendent Product (middle), & Dual Pendent Product (bottom).

4.6.3 Pendent Attachment to (2-AP)$_2$MADA Diimide

Finally pendent attachment was carried out using the (2-AP)$_2$MADA diimide in order to evaluate the selectivity that would be seen with the MADA 3-Componnet Polyimide. NMR revealed complete Methyl NLO Surrogate attachment took place at only one functional group using a slight excess of DEAD, seen in *Figure 4.8* and in section *3.8.1.2*. TLC revealed that product formation took place at a slower rate than previously seen with the pendent attachment at the unhindered carboxylic acid group of 3,5-dihydroxybenzoic acid. The virtual absence of the (2-AP)$_2$MADA diimide phenol protons **(L)** and the Methyl NLO Surrogate alcohol protons **(A)** in the NMR of the product also implies that an appending reaction occurred. FTIR revealed several new peaks that indicated that ether linkages were present, consistent with attachment taking place at the phenol locations. The weakening of the broad phenol O-H stretch near 3377 cm^{-1} in the FTIR previously seen with the (2-AP)$_2$MADA diimide (section *3.5.2*) also supports this

hypothesis. Furthermore, if attachment had taken place at the carboxylic acid locations, a new strong peak between 645-575 cm^{-1} (O-C-O bend) should have appeared in the FTIR of the product corresponding to the formation of an ester; this is clearly not present. These facts are consistent with the $(2\text{-AP})_2$MADA diimide existing in a strongly H-bonded or zwitterionic form, along with the peak seen in the FTIR at 3061 cm^{-1}. One fact that leads to functional group selectivity ambiguity is the difference in pKa values between a phenol (pKa ≈ 18.0[28]) and a NH_4^+ ammonium salt (pKa = 10.5[28]), which theoretically indicates that the salt should be the more reactive nucleophile. This value however does not take into consideration however the actual structure that would result from a zwitterion, and does not consider a strongly H-bonded scenario.

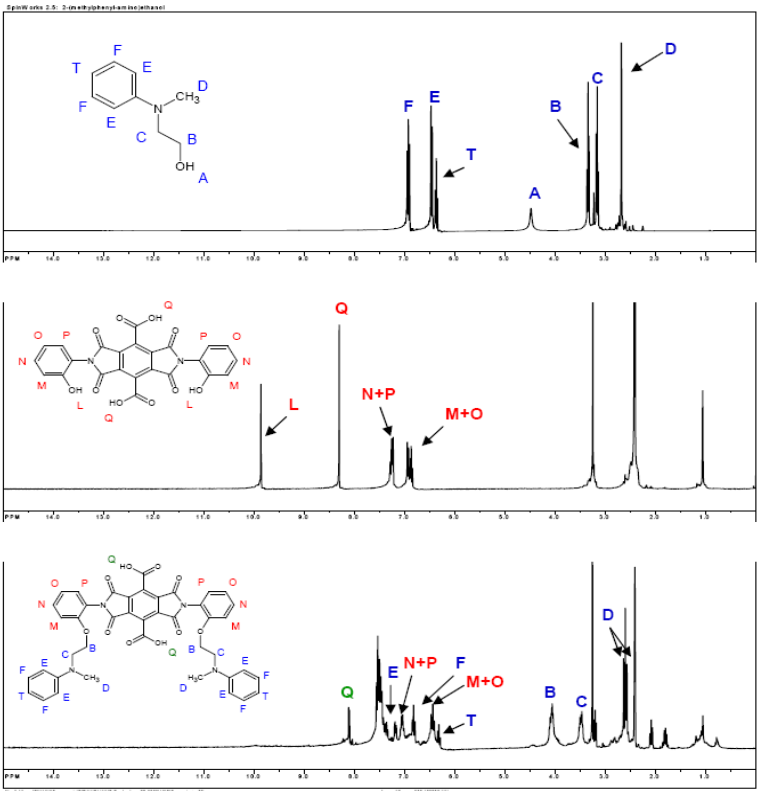

Figure 4.8 – $(2\text{-AP})_2$MADA Diimide Methyl NLO Surrogate Attachment ^{1}H NMR Overlay: Methyl NLO Surrogate (top), $(2\text{-AP})_2$MADA Diimide (middle), and Single Pendent Product (bottom).

Pendent attachment was next attempted at the unreacted functional group of the $(2\text{-AP})_2$MADA diimide using the Methyl NLO Surrogate, with the Ethyl NLO Surrogate already

being attached at the more reactive functional group. TLC revealed that a large excess of DEAD was required to achieve a moderate amount of pendent attachment, consistent with the strongly H-bonded or zwitterionic form of the $(2\text{-AP})_2$MADA Diimide, whose two protons should be much less acidic and therefore much harder to remove. NMR also indicated incomplete pendent attachment at the remaining unreacted functional group, shown in section *3.8.2.2*. Positive identification of all peaks in the NMR spectrum was hindered by the multiple molecule configurations possible, obscuring accurate splitting of some peaks. The presence of several Mitsunobu byproducts also hindered interpretation. Note that if deprotonation of the zwitterionic protons was in fact the rate limiting step of the Mitsunobu reaction, future work could include the addition of a stoichiometric amount of acid in order to catalyze the reaction by activating the DEAD to convert the alcohol into a good leaving group as shown in *Figure 4.5*. Note that this would only work if pendent attachment was occurring at the carboxylic acid location (which has already been deprotonated in the zwitterionic $(2\text{-AP})_2$MADA Diimide) and not the imide. Although only a moderate amount of pendent attachment was achieved, the fact that NMR indicates that it was selective to only one location means that selective pendent attachment in the co-PI[Bis-AP-AF/6FDA$)_{0.9}$(Bis-AP-AF/MADA$)_{0.1}]_n$ should still be possible.

4.7 co-PI[Bis-AP-AF/6FDA$)_{0.9}$(Bis-AP-AF/MADA$)_{0.1}]_n$

The co-PI[Bis-AP-AF/6FDA$)_{0.9}$(Bis-AP-AF/MADA$)_{0.1}]_n$ was designed to facilitate selective attachment of two different pendents using the Mitsunobu reaction. By using two commercially available components, 6FDA and Bis-AP-AF, and the synthesized MADA, a copolymer resulted that has two different mers – the Bis-AP-AF:MADA mer with two carboxylic acid and two phenol groups, and the Bis-AP-AF:6FDA mer with two phenol groups. By controlling the stoichiometric amounts of each component, two different pendents can theoretically be selectively attached: one at only the phenols and one at only the carboxylic acids. Furthermore, by using 6FDA as one of the anhydride components instead of just MADA,

hexafluoroisopropylidene groups were incorporated into the polyimide which shifts absorption outside the near UV-visible region and decreases moisture absorption.

Synthesis of the co-PI[Bis-AP-AF/6FDA$_{0.9}$(Bis-AP-AF/MADA$_{0.1}$]$_n$ was carried out in NMP, as a successful means of synthesis and isolation had previously been identified using the (2-AP)$_2$MADA Diimide in this solvent system. The ratio of the two dianhydrides used was held at 0.1MADA : 0.9 6FDA, due to time limitations and previous reports of gelation with large amounts of MADA.[17,18] Each of the two dianhydrides were dissolved in solution prior to the addition of Bis-AP-AF, the diamine, in order to promote random and not block copolymerization. An important synthetic step was the addition of the diamine all at once in solid form versus drop-wise addition over time in solution; this most likely played a role in determining the average chain length (average molecular weight) and should be investigated further in the future. A 15.50% wt solution was used as this had previously yielded MADA Polyimides with high molecular weights and viscosities amenable to solution casting of films.[1] Imidization was carried out using a Dean Stark Trap charged with sodium metal and dried toluene in order to promote imide formation by removing the H_2O byproduct (as with the (2-AP)$_2$MADA Diimide).

Successful synthesis of the co-PI[Bis-AP-AF/6FDA$_{0.9}$(Bis-AP-AF/MADA$_{0.1}$]$_n$ was confirmed through TLC, NMR, and FTIR, the latter two consistent with the expected structure. TLC indicated incorporation of Bis-AP-AF into the product, along with only one spot corresponding to product. NMR shown in *Figure 4.10* and section *3.9.2* indicated polyimide synthesis with the disappearance of the amine protons previously seen at 4.57 ppm. The presence of NMP is unfortunetly also evident in the spectrum, meaning that vacuum oven drying failed to remove all of the NMP most likely occluded within the polymer chains. One interesting characteristic revealed by NMR is the unexpected splitting corresponding to the aromatic dianhydride signal at 7.13 ppm. While this signal should be seen as a doublet, the splitting seen indicated a multiplet instead. 2-D NMR was utilized to elucidate proton assignment for this peak shown in section *3.9.3*, and indicated spin-spin coupling between the downfield and upfield

doublet that is part of the multiplet. Due to the intensity of these doublets, it was theorized that both correspond to the **GG'** and **FF'** dianhydride protons in the MADA mers, and are shadows of the **GG** and **FF** dianhydride protons in the Bis-AP-AF : 6FDA mers. This could be due to the different electron withdrawing strength of each dianhydride, resulting in slightly different chemical shifts of the dianhydride protons that are *meta* and *para* to each imide. FTIR also indicated successful synthesis, showing the expected imide, phenol, and hexafluoroisopropylidene peaks, and having only a small PAA peak at 1653 cm^{-1}, indicating a high degree of imidization even after only 6 hours at the reaction temperature. Furthermore, there were no indications of anhydride peaks in the FTIR spectrum, indicating that no intra or intermolecular anhydride formation took place during imidization.

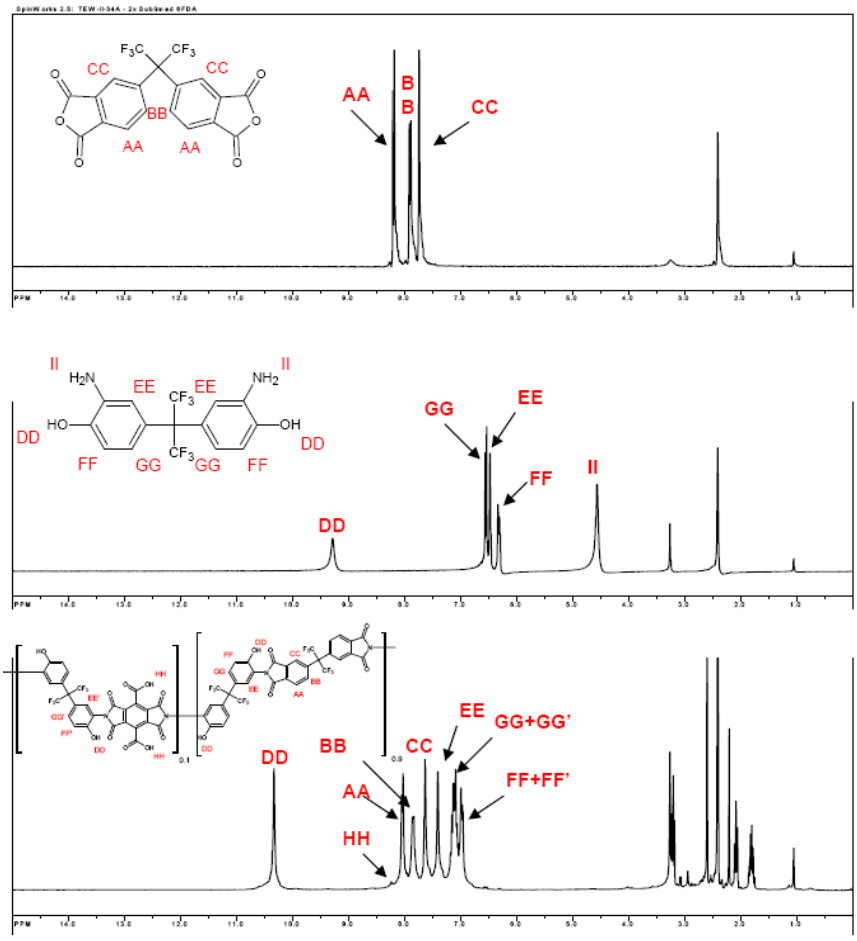

Figure 4.9 – co-PI[Bis-AP-AF/6FDA]$_{0.9}$(Bis-AP-AF/MADA)$_{0.1}$]$_n$ ^{1}H NMR Overlay: 6FDA (top), Bis-AP-AF (middle), and co-PI[Bis-AP-AF/6FDA]$_{0.9}$(Bis-AP-AF/MADA)$_{0.1}$]$_n$ (bottom).

4.8 Pendent Attachment to co-PI[Bis-AP-AF/6FDA)$_{0.9}$(Bis-AP-AF/MADA)$_{0.1}$]$_n$

Pendent attachment to the co-PI[Bis-AP-AF/6FDA)$_{0.9}$(Bis-AP-AF/MADA)$_{0.1}$]$_n$ was carried out in two steps. During the first pendent attachment, a stoichiometric amount of the Methyl NLO Surrogate and DEAD were added proportional to twice the number of carboxylic acid groups present on the copolymer MADA mers. This was done in order to further elucidate where pendent attachment was taking place. TLC, NMR, and FTIR all indicated successful pendent attachment. TLC of the isolated product indicated complete attachment of all Methyl NLO Surrogate; with a 1 spot corresponding to the single pendent polyimide product. NMR also indicated successful attachment by the appearance of Methyl NLO Surrogate peaks in the spectrum, shown in section *3.10.1.2.* Due to the composition of the polyimide, NMR failed to positively identify where attachment took place, as the amount of MADA in the polyimide was too small to decisively recognize a decrease in peak area. FTIR however indicated that pendent attachment had taken place at the phenol locations as several peaks corresponding to the O-H phenol stretch were reduced, and the increase in an existing peak corresponded to new ether linkages being present. Pendent attachment to the polyimide backbone was confirmed by the appearance of a new signal at 540 cm^{-1} (C-N-C bending) previously seen with the first pendent attachment to the (2-AP)$_2$MADA diimide.

The second pendent attachment step involved reacting a stoichiometric amount of the Ethyl NLO Surrogate and DEAD proportional to the complete number of phenol groups present in the polyimide (0.1:0.9 mole ratio MADA:6FDA, 0.4:1.6 mole ratio NLO). Product structural confirmation was again determined by NMR, and FTIR. TLC of the isolated product indicated nearly complete attachment of the Ethyl NLO Surrogate, along with one predominant spot corresponding to the dual pendent polyimide product with small impurities seen from the Mitsunobu byproducts. NMR seen in section *3.10.2.2* indicated approximately 63% pendent attachment at the phenol locations, consistent with the second attachment requiring an excess of DEAD to achieve high yields. NMR also indicated the attempt to remove the $OPPh_3$ impurity

through trituration of the dual pendent polyimide product with chilled pentanes was unsuccessful, but did eliminate the vast majority of the NMP impurity seen with the non-pendent and single pendent polyimides. This is most likely due to the trituration releasing the occluded NMP and not the presence of pentanes, as these two solvents are almost completely immiscible with one another. FTIR was also consistent with the above results, again indicating pendent attachment at the phenol locations, along with the appearance of several new peaks corresponding to the Ethyl NLO Surrogate. One interesting effect of the second Mitsunobu reaction indicated by FTIR was the disappearance of the peak at 1653 cm^{-1}, corresponding to the imidization of any remaining PAA intermediate. The probable cause of this that the Mitsunobu reaction causes dehydration, an effect that also occurs upon imidization.

5. CONCLUSIONS

Significant progress towards the synthesis of a MADA Crosslinkable NLO Pendent Polyimide has been demonstrated. Six novel organic compounds and three novel polymers have been synthesized and characterized in this approach. The procedure for the synthesis of MADA has been refined, as well as the synthesis of a NLO pendent. A novel MADA Model Compound has also been synthesized, with structural confirmation provided by 1-D ^{1}H NMR, FTIR, and MS.

Two separate model compound systems have been presented in order to elucidate functional group selectivity for the attachment of a NLO and UV-Crosslinker pendent using the Mitsunobu reaction. Using 3,5-dihydroxybenzoic acid, it was established that stoichiometric pendent attachment takes place exclusively at the carboxylic acid sites within a host molecule possessing both carboxylic acid and phenol functionality in a nominal state with no steric interferences. Subsequent pendent attachment at the phenol locations without product isolation was possible, but longer reaction times were necessary as well as an excess of Mitsunobu reagents. Next using the $(2\text{-AP})_2$MADA diimide, functional group selectivity was probed in the presence of strong hydrogen-bonding and/or zwitterionic behavior. It was discerned that stoichiometric pendent attachment takes place solely at the phenol locations due to the lowered K_a of the MADA protons. Subsequent pendent attachment at either the imide or carboxylic acid was possible without product isolation, although only moderate attachment was observed and required a large excess of Mitsunobu reagents.

Next the co-PI[Bis-AP-AF/6FDA$)_{0.9}$(Bis-AP-AF/MADA$)_{0.1}]_n$ was synthesized using a one pot approach in NMP. Longer blending yielded a less tacky product. Structural confirmation was provided through 1-D ^{1}H NMR, 2-D ^{1}H NMR, and FTIR. TGA was performed in order verify the thermal stability of the polyimide and revealed that initial dehydration began at approximately 200 °C and major decomposition began at 396 °C, making it sufficiently stable for its intended use. Pendent attachment to the polyimide backbone was then performed using the Mitsunobu reaction, with attachment most likely taking place selectively at the phenol sites only

due to strong H-bonding or zwitterionic behavior in the MADA mers. Subsequent pendent attachment without product isolation was possible. Incomplete attachment however was seen due to the stoichiometric amount of Mitsunobu reagents used. Further investigation is required to positively identify selective pendent attachment at both polyimide functionalities.

6. FUTURE WORK

- Further elucidate $(2\text{-AP})_2$MADA diimide functional group selectivity through the reaction of 2,6-dihydroxyaniline (DHA) with MADA to give $(2,6\text{-DHA})_2$MADA Diimide, in order to positively identify the carboxylic/zwitterionic and phenol functionality by NMR.

- Complete synthesis and purification of a UV-Crosslinker system.

- Vary ratio of MADA-Bis-AP-AF : 6FDA-Bis-AP-AF in 3-Component Polyimide in order to better illuminate the selectivity showed with the MADA mers via NMR and FTIR.

- Increase the amount of time that MADA 3-Component Polyimides are imidized to reduce amount of PAA in product co-PI's.

- Perform molecular weight studies on present and future MADA 3-Component Polyimides to investigate both the effect of the means of diamine introduction on molecular weight, and the effect of an increased concentration of MADA on molecular weight.

- Attach NLO and UV-Crosslinker pendents selectively to polyimide backbone, followed by NLO-phore poling and UV-crosslinking.

- Investigate means to remove the $OPPh_3$ Mitsunobu byproduct from co-PI pendent attachment reactions, possibly through trituration with benzene.

- Purify the two pendant products from the Mitsunobu reactions with 3,5-dihydroxybenzoic acid and $(2\text{-AP})_2$MADA Diimide.

- Investigate the possible acid catalysis of the Mitsunobu reaction for pendent attachment to phenolic and zwitterionic functionalities or alternate chemical means to enhance the difference in reactivities of the two co-PI functional groups (phenol and carboxylic acid).

7. REFERENCES

1. Dalton, Larry R.; Steier, William H.; Robinson, Bruce H.; Zhang, Chang; Ren, Albert; Garner, Sean; Chen, Anto; Londergan, Timothy; Irwin, Lindsey; Carlson, Brenden; Fifield, Leonard; Phelan, Gregory; Kincaid, Clint; Amend, Joseph; Jen, Alex, "From Molecules to Opto-Chips: Organic Electro-Optic Materials", *J. Mater. Chem*, **1999**, 9, 1905-1920.

2. Nalwa, Hari Wingh; Miyata, Seizo, Nonlinear Optics of Organic Molecules and Polymers, CRC Press Inc., 1997.

3. http://moebius.physik.tu-berlin.de/lc/shg/

4. Marder, S.R.; Beratan, D.N.; Cheng, L.T., "Approaches for Optimizing the First Electronic Hyperpolarizability of Conjugated Organic Molecules", *Science*, **1991**, 252, 103-106.

5. Albert, Israel D.L.; Marks, Tobin J.; Ratner, Mark A., "Large Molecular Hyperpolarizabilities. Quantitative Analysis of Aromaticity and Auxiliary Donor – Acceptor Effects", *J. Am. Chem. Soc.*, **1997**, 119, 6575-6582.

6. Hsu, Tzu-Chien; Chen, Chien-Fan; Wu, Shou-Shiun, "Second Order Nonlinear Optical Polyimides Having Benzobisthiazole-Based Pendent Groups, and Preparation of the Same", *US Pat. Appl. Publ.*, **2007**, 20070001154.

7. Leng, W.N.; Zhou, Y.M.; Xu, Q.H.; Liu, J.Z., "Synthesis of Nonlinear Optical Side-Chain Soluble Polyimides for Electro-Optic Applications", *Polymer*, **2001**, 42, 7749-7754.

8. Pan, Jing; Chen, Mingfei; Warner, William; Mingqian He; Dalton, Larry; Hogen-Esch, Thieo E., "Synthesis of Block Copolymers Containing a Main Chain Polymetric NLO Segment", *Macromolecules*, **2000**, 33, 4673-4681.

9. Kim, Tae-Dong; Kang, Jae-Wook; Luo, Jingdong; Chen, Baoquan; Ka, Jae-Won; Jang, Sei-Hun; Tucker, Neil; Shi, Zhengwei; Haller, Marnie; Hau, Steven; Jen, Alex K-Y., "A Novel Approach to Achieve Highly Efficient Nonlinear Optical Polymers from Guest-Host System", *Proc. of SPIE*, **2005**, 593505/1-593505/11.

10. Galperin, Eugene, "Novel Polyimides Based on APAF, 6FDA, and MADA, and their NLO Pendent Polymers", Rochester Institute of Technology Master's Thesis. **2003**, 75.

11. Guenthner, Andrew J.; Wright, Michael E.; Fallis, Stephen; Lindsay, Geoffrey A.; Petteys, Brian J.; Yandek, Gregory R.; Zang, De-Yu; Sanghadasa, Mohan; Ashley, Paul R., "Polyimides with Attached Chromophores for Improved Performance in Electro-Optical Devices", *Proc. of SPIE*, **2006**, 63310M/1-63310M/11.

12. Guenthner, Andrew J.; Wright, Michael E.; Fallis, Stephen; Yandek, Gregory R.; Petteys, Brian J.; Cash, Jessica; Zang, De-Yu; Gaeta, Celestino; Zounes, Maryann, "Multi-Functional Polyimides for Tailorable High-Performance Electro-Optical Devices", *Proc. of SPIE*, **2007**, 66530N/1-66530N/11.

13. Bruma, Maria; Mercer, Frank W,; Schultz, Burkhard.; Dietel, R.; Fitch, J., "Study of the Crosslinking Process in Fluorinated Poly(imide-amide)s Containing Pendent Cyano Groups", *High Perform. Polym.*, **1994**, 6, 183-191.

14. Mercer, Frank W.; McKenzie, Martin T.; Burma, Maria; Schultz, Burkhard, "Synthesis and Properties of Fluorinated Polyimides and Fluorinated Poly(imide amide)s Containing Pendent Cyano Groups", *Polym. Int.*, **1994**, 33, 399-407.

15. Aljoumaa, Khaled; Ishow, Elena; Ding, Jianfu; Qi, Yinghua; Day, Michael; Delaire, Jacques A., "New Side Chain Fluorinated Copolymers for Quadratic Non Linear Optics", *Nonlinear Optics and Quantum Optics*, **2006**, 35, 83-93.

16. Woo, HanYoung; Shim, Hong-Ku; Lee, Kwang-Sup; Jeong, Mi-Yun; Lim, Tong-Kun, "An Alternate Synthetic Approach for Soluble Nonlinear Optical Polyimides", *Chem Mater.*, **1999**, 11, 218-226.

17. Wagner, Shawn; Dai, Huixiong; Stapleton, Russell A.; Illingsworth, Marvin L., "Pendent Polyimides using Mellitic Acid Dianhydride. I. An Atomic Oxygen-resistant, Pendent 4,4'-ODA/PMDA/MADA Co-polyimide Containing Zirconium", *High Perform. Polym.*, **2006**, 18, 399-419.

18. Illingsworth, Marvin L.; Dai, Huixiong; Wang, Wei; Chow, Derek; Siochi, Emilie J.; Yang, Kenwan; Leiston-Belanger, Julie M.; Jankauskas, Jennifer, "Pendent Polyimides Using Mellitic Acid Dianhydride. II. Structure-Property Relationships for Zirconium-Containing Pendent Polymers", *J. Polym. Sci., Part A: Polym. Chem.*, **2007**, 45, 1641-1652.

19. Chen, Tian-An; Jen, Alex K.-Y.; Cai, Yongming, "Facile Approach to Nonlinear Optical Side-Chain Aromatic Polyimides with Large Second-Order Nonlinearity and Thermal Stability", *J. Am. Chem. Soc.*, **1995**, 117, 7295-7296.

20. Hwang, Jeoung-Yeon; Seo, Dae-Shik; Son, Jong-Ho; Suh, Dong Hack, "Generation of Pretilt Angle for Nematic Liquid Crystal Using the Photodimerization Method on Various New Photo-Crosslinkable Polyimide Based Polymers", *Jpn. J. Appl. Phys.* **2001,** 40, L761-L764.

21. Hawver, Lisa, "Private Communication", May 2008.

22. Briers, David; Koeckelberghs, Guy; Picard, Isabel; Verbiest, Thierry; Persoons, Andre; Samyn, Celesta, "Novel Chromophore-Functionalized Poly[2-(trifluoromethyl) adamantyl acrylate-methyl vinyl urethane]s with High Poling Stabilities of the Nonlinear Optical Effect", *Macromol. Rapid Commun.*, **2003**, 24, 841-846.

23. Gottlieb, Hugo E.; Kotlyar, Vadim; Nudelman, Abraham, "NMR Chemical Shifts of Common Laboratory Solvents as Trace Impurities", *J. Org. Chem.* **1997**, 62, 7512-7515.

24. Robert Pasquarelli Research Notebook II, **2007**.

25. http://en.wikipedia.org/wiki/Zwitterion

26. Schmuck, Carsten; Weinand, Wolfgang, "Highly Stable Self-Assembly in Water: Ion Pair Driven Dimerization of a Guanidiniocarbonyl Pyrrole Carboxylate Zwitterion", *J. Am. Chem. Soc.,* **2003**, 125, 452-459.
27. Schmuck, Carsten, "Self-Folding Molecules: A Well Defined, Stable Loop Formed by a Carboxylate-Guanidinium Zwitterion in DMSO", *J. Org. Chem.,* **2000**, 65, 2432-2437.

28. Reich, Hans J., "Bordwell pKa Table (Acidity in DMSO)", http://www.chem.wisc.edu/areas/reich/pkatable/index.htm

29. Zweifel, George S.; Nantz, Michael H., *Modern Organic Synthesis – An Introduction*, 1st edition, Freeman, NY, 2006.